Characterisation of a harvesting step for monoclonal antibodies from mammalian cell culture.

Henry R. Charlton

Doctor of Philosophy

The University of Aston in Birmingham

October 1999

Thesis Summary

The focus of this research was defined by a poorly characterised filtration train employed to clarify culture broth containing monoclonal antibodies secreted by GS-NS0 cells: the filtration train blinded unpredictably and the ability of the positively charged filters to adsorb DNA from process material was unknown.

To direct the development of an assay to quantify the ability of depth filters to adsorb DNA, the molecular weight of DNA from a large-scale, fed-batch, mammalian cell culture vessel was evaluated as process material passed through the initial stages of the purification scheme. High molecular weight DNA was substantially cleared from the broth after passage through a disc stack centrifuge and the remaining low molecular weight DNA was largely unaffected by passage through a series of depth filters and a sterilising grade membrane. Removal of high molecular weight DNA was shown to be coupled with clarification of the process stream. The DNA from cell culture supernatant showed a pattern of internucleosomal cleavage of chromatin when fractionated by electrophoresis but the presence of both necrotic and apoptotic cells throughout the fermentation meant that the origin of the fragmented DNA could not be unequivocally determined.

An intercalating fluorochrome, PicoGreen, was elected for development of a suitable DNA assay because of its ability to respond to low molecular weight DNA. It was assessed for its ability to determine the concentration of DNA in clarified mammalian cell culture broths containing pertinent monoclonal antibodies. Fluorescent signal suppression was ameliorated by sample dilution or by performing the assay above the pI of secreted IgG. The source of fluorescence in clarified culture broth was validated by incubation with RNase A and DNase I. At least 89.0 % of fluorescence was attributable to nucleic acid and pre-digestion with RNase A was shown to be a requirement for successful quantification of DNA in such samples.

Application of the fluorescence based assay resulted in characterisation of the physical parameters governing adsorption of DNA by various positively charged depth filters and membranes in test solutions and the DNA adsorption profile of the manufacturing scale filtration train. Buffers that reduced or neutralised the depth filter or membrane charge, and those that impeded hydrophobic interactions were shown to affect their operational capacity, demonstrating that DNA was adsorbed by a combination of electrostatic and hydrophobic interactions. Production-scale centrifugation of harvest broth containing therapeutic protein resulted in the reduction of total DNA in the process stream from 79.8 $\mu g\ ml^{-1}$ to 9.3 $\mu g\ ml^{-1}$ whereas the concentration of DNA in the supernatant of pre- and post-filtration samples had only marginally reduced DNA content: from 6.3 to 6.0 $\mu g\ ml^{-1}$ respectively. Hence the filtration train was shown to ineffective in DNA removal.

Historically, blinding of the depth filters had been unpredictable with data such as numbers of viable cells, non-viable cells, product titre, or process shape (batch, fed-batch, or draw and fill) failing to inform on the durability of depth filters in the harvest step. To investigate this, key fouling contaminants were identified by challenging depth filters with the same mass of one of the following: viable healthy cells, cells that had died by the process of apoptosis, and cells that had died through the process of necrosis. The pressure increase across a Cuno Zeta Plus 10SP depth filter was 2.8 and 16.5 times more sensitive to debris from apoptotic and necrotic cells respectively, when compared to viable cells. The condition of DNA released into the culture broth was assessed. Necrotic cells released predominantly high molecular weight DNA in contrast to apoptotic cells which released chiefly low molecular weight DNA. The blinding of the filters was found to be largely unaffected by variations in the particle size distribution of material in, and viscosity of, solutions with which they were challenged. The exceptional response of the depth filters to necrotic cells may suggest the cause of previously noted unpredictable filter blinding whereby a number of necrotic cells have a more significant impact on the life of a depth filter than a similar number of

viable or apoptotic cells. In a final set of experiments the pressure drop caused by non-viable necrotic culture broths which had been treated with DNase I or benzonase was found to be smaller when compared to untreated broths: the abilities of the enzyme treated cultures to foul the depth filter were reduced by 70.4% and 75.4% respectively indicating the importance of DNA in the blinding of the depth filter studied.

Acknowledgements

I would like to acknowledge and thank The Biotechnology and Biological Sciences Research Council and GlaxoWellcome for their financial support without which none of this work could have been performed. I would also like to thanks my parents, John and Hilary Charlton, for their financial help towards the end of this work.

I would also like to acknowledge and extend my thanks for the support I received from both of my supervisors. It is impossible to give due credit to two such disparate characters in the same sentence. Therefore I extend my thanks to Professor Nigel K.H. Slater at Aston University for his infectious enthusiasm for the work I performed, and for helping to make the whole process more fun than it ever should have been. And thank you to Dr. Julian M. Relton at GlaxoWellcome for overseeing the day to day issues of my work. I would gladly, and indeed hope to, embark on future projects with both.

Within GlaxoWelcome there were many people who provided me with their time, equipment, expertise, or samples and I would like to acknowledge their input. Particular thanks go to Jonathan Lewis for stimulating and challenging conversations. Also thanks must go to Seema Islam, Sharon White, Gary Millbank, Georgina Carter, Andie Rudzki, Fiona Montague and Tony Sheppard for their various contributions.

There are many other individuals who have helped me enormously in the task of preparing this work but some stand out as deserving a special mention. Notably, Rachel Harrison for bearing the brunt and sharing the joy of my respective lows and highs, taking dictation to expedite the discussion and for being prepared to try and understand a subject which she openly and honestly claimed was of little interest to her, which brings me to the Ph.D. she was always more interested in - Caroline Garaway's - who simultaneously went through the process with me, beat me in the race for submission, Rachel's interest, and general know how of statistics, all of which I will forgive because she still had the patience to explain to me about statistics (not an insignificant number of times), and gave me a sounding board for the emotional side of the postgraduate process. We will recover! I would like to thank Mary Mike who made her points perfectly. Finally, I would like to thank Rachel, Caroline, and my parents (again), along with Julia Andrews who all gave encouragement in the final stages when I needed it most.

Abbreviations

BSA	Bovine serum albumin
C/Co	Dimensionless effluent output
CDR	Complementarity determining regions
CCD	Charge coupled device
ctDNA	Calf thymus DNA
DNA	Deoxyribonucleic acid
dsDNA	Double stranded DNA
DNase I	Deoxyribonuclease I
dN_{x-y}	Oligonucleotides of length between x and y base pairs
ELISA	Enzyme linked immuno-sorbent assay
FDA	Food and Drug Administration (USA)
HPLC	High performance liquid chromatography
HIV	Human immuno-deficiency virus
mAb	Monoclonal antibody
PBS	Phosphate buffered saline
psi	Pounds per square inch
(K)Da	(Kilo)Daltons
RNA	Ribonucleic acid
RNase A	Bovine pancreatic ribonuclease A
SDS	Sodium dodecyl sulphate
TE	Tris(hydroxymethyl)methylamine, 10mM, Ethylene-diamine-tetra-acetic acid, 1mM.
WHO	World Health Organisation

TABLE OF CONTENTS

LIST OF FIGURES

LIST OF TABLES

1. INTRODUCTION

1.1. General

The therapeutic importance of antibodies was first recognised in 1890 when resistance to the diphtheria toxin was transferred from one animal to another by transfer of serum. It was concluded that the serum contained an anti-toxin, later to be named an antibody. For many years thereafter, such anti-sera were used in the treatment of infections, or to counter the effects of toxins. When Kohler and Milstein (1975) demonstrated the continuous production of an antibody with predefined specificity from sub-clones of fused cells, i.e. a monoclonal antibody (mAb), new opportunities for the diagnosis and management of human diseases were created.

Estimates and reports of the commercial value of mAbs vary widely, but all concur that these therapeutic proteins have the potential to create a multi-billion dollar market (Spiers, 1988; Bibila and Robinson, 1995; Frost and Sullivan, 1996). Whilst methods for the large scale production of mAbs have been established for many years, optimisation of manufacturing strategies is ongoing.

Large scale culture of mammalian cells is commonly used for the production of mAbs and primary harvesting steps are generally concerned with configuring such cultured material for initial capture of antibody. The industrial sponsors of this project employ a continuous disc stack centrifuge followed by a series of depth filters and a sterilising grade membrane to produce clarified cell culture material (Figure 1-1) which is concentrated prior to purification, polishing and final formulation.

The depth filters and membranes employed in the initial stages of mAb purification carry a positive electrostatic charge which enhances capture of particles. At the inception of this project there were two problems with the deployment of these depth filters in the mAb purification scheme. First, the ability of depth filters to remove debris appeared to vary from batch to batch and this manifested itself in unpredictable filter blinding at pilot plant scale operations. Second, the capacity of these units for negatively charged solutes, particularly DNA which must be substantially partitioned from the product, was unknown. This lack of knowledge was clearly unsatisfactory, resulting in sub-optimal processing and validation strategies. It was with a view to filling this gap in the knowledge of the characteristics of the harvest step that these studies were undertaken.

This introduction has been compiled to present the research project in the context of established information.

1.2. Therapeutic monoclonal antibodies

That antibodies protect vertebrate animals against harmful foreign materials, such as toxins or microbes, has been recognised for many years. Their success in this role depends on recognition of material as being foreign, followed by removal of these substances from the body. Antibodies are such potent molecules that the means to create them with specified, pre-selected targets has been highly sought after. The major step in the creation of antibodies with pre-defined specificity came when Kohler and Milstein (1975) described a technique to produce cells that could be continuously cultured and which secreted an antibody with specificity to a pre-selected antigen. The ability to produce such "made to order" antibodies meant that biological research, diagnosis and therapy was revolutionised. If disease-specific antigens could be isolated, then monoclonal antibodies which would promptly remove harmful substances from the body could be produced: such was the rationale behind therapeutic monoclonal antibodies.

Kohler and Milstein were able to inoculate a mouse with sheep red blood cells which brought about an immunogenic response in the host animal. Spleen cells were then removed from the mouse and fused with a myeloma cell (myeloma cells are carcinomic and therefore immortal). The resulting cell lines were screened and sub-clones of the fused cells were isolated that could be cultured continuously and secreted a single antibody which aggregated sheep red blood cells. The first antibody of pre-defined specificity was thus made which, interestingly, was not derived from a source that had been highly purified. The researchers immediately recognised the value of being able to produce antibodies to specified antigens for both research, diagnostic and therapeutic purposes and many workers now agree that the technique perfected by Kohler and Milstein has revolutionised almost every area of biology (Liddell and Cryer, 1991; Borrebaeck, 1995; Zola 1995).

The first antibodies with specific applications in mind followed rapidly (Galfre *et al.*, 1977), and mAbs were quickly applied to *ex vivo* diagnostics by use of the ELISA (Enzyme Linked ImmunoSorbent Assay).

The pace of development for therapeutic applications of mAbs was not as rapid. MAbs were derived from murine sources and these provoked immune reactions in humans such that the antibody that was administered for therapeutic purposes was rapidly cleared by the immune response of the human body. The antigen to which it was directed was not bound by mAb, thus murine monoclonal antibodies were unable to perform a therapeutic role (Miller, *et al.*, 1983). Clearly there was a requirement for mAbs that more closely resembled those in humans which could provoke pharmaceutical effects without generating adverse immunogenic reactions.

Ideally, the pre-defined specificity would originate from human mAbs: at the time mAbs were secreted by myeloma cells after fusion with spleen cells from mice that had been immunised with the target antigen. Clearly, to perform the same procedures with humans was unethical. The problem of producing humanised antibodies was addressed by integrating genetic sequences derived from, and coding for, murine complementarity determining regions (CDR's) with sequences of DNA that coded for the human constant antibody domains and using this fused segment of DNA to engineer appropriate mammalian cells. The approach was successfully performed by Reichmann et al (1988) who transfected cells with a gene sequence that coded for the antigen binding domain and some of the surrounding constant region thereby maintaining the orientation of the antigen binding site to the epitopic region of the antigen. More importantly, the work was done using an antibody that had already been selected for therapeutic application. The CDR's did not carry murine sequences that are characteristic of the rodent, and by making the rest of the mAb identical to human antibodies, they were made indistinguishable from human antibodies and antigen binding domains surrounded by human constant regions should not provoke immunogenic effects in humans. Thus, the structure of mAbs that are now employed for human applications have been produced and have succeeded in minimising side effects in the human body.

1.2.1. Production of therapeutic monoclonal antibodies

Whilst research was being conducted to find the optimum antibody structure to elicit safe pharmaceutical effects, considerable effort was also applied to develop methods that could enable efficient production of monoclonal antibodies.

Antibody proteins can be produced from numerous sources including plant cells (Wongsamuth and Doran, 1997), yeast (Horwitz *et al.,* 1988), and bacteria (Better *et al.,* 1988) as well as non-lymphoid mammalian cells (Weidle *et al.,* 1987). Complete antibodies with correct folding have only been assembled by eukaryotic cells. Disulphide bonds in antibodies from *Eschericia coli* are not formed because the intracellular environment is not sufficiently oxidising (Carter *et al.,* 1992) and glycosylation patterns in monoclonal antibodies from non-mammalian sources do not elicit effector functions. For this reason Fab fragments from *E.coli* or monoclonal antibodies from non-mammalian sources may be employed when effector functions are not required or need to be avoided: for site directed delivery of toxins, *ex vivo* diagnostic purposes, or reduced T-cell response, for example.

As outlined above, the use of mAbs generated purely from murine sources can induce adverse immunogenic reactions and for this reason, non-lymphoid genetically engineered mammalian cells

are the chief source of correctly folded and glycosylated monoclonal antibodies for therapeutic applications.

Until the late 1980's many researchers held the view that monoclonal antibodies could not be efficiently produced from mammalian cells because of the additional production costs incurred by using serum containing media, and their sensitivity to denaturing at air-liquid interfaces and hydrodynamic shear. These concerns were progressively shown to be unfounded, (reviewed by Spier, 1988) and alongside the newly developed abilities to engineer humanised antibodies there was a rapid expansion in the culture of animal cells for production of mAbs.

Thus, the large-scale culture of mammalian cells has been pursued as the most common method by which monoclonal antibodies can be manufactured, all with the common aim of maximising productivity and minimising cost. The optimisation of monoclonal antibody production generally addresses a few common issues which typically include cell culture media formulation, mode of cell propagation and reactor configuration or operation, all of which will have various impacts on the rate of antibody production. Researchers tend to focus on growing cells to maximise their output of useful product with minimal accumulation of waste products. This often results in operating in fed-batch mode using a serum free media with supplemental addition of key nutrients to minimise cell death.

1.2.2. Applications and Economics

The exceptional specificity of antibodies for biological substrates means that the number of molecules that can be targeted to promote therapeutic effects is immense. Tumour associated antigens, cell surface markers, cytokines, viral proteins, bacterial proteins, anti-toxins, antibodies and haptens have all been cited as target molecules for humanised antibodies in the development pipeline of both large and small manufacturers (Dick, 1985; Emery and Adair, 1994). More recently, of the 284 biotechnology related products that were registered as under development in 1996, the largest sub-group was that of monoclonal antibodies, accounting for 78 of all the biotechnology based therapeutics in development (Persidis, 1997).

Despite the enormous perceived potential of therapeutic monoclonal antibodies, they failed to realise the market predictions made of them during the 1980's. For the purposes of the following discussion, it is important to point out that estimates of the market size of mAbs can relate either to sales of all antibodies (i.e. those for use in research, diagnostics, and human therapies) or to the sale of therapeutic mAbs only. Spiers (1988) estimated that of all mAb sales, some 20% would be for

therapeutic use. In the following text, where authors have quoted estimated sales for all antibodies, this figure has been divided by 5 to estimate the therapeutic mAb size.

Estimates for sales of therapeutic monoclonal antibodies have been published sporadically since 1986 when Dixon predicted sales of $200 million in 1990 rising to $1000 million in 1995. Ratafia (1987) estimated sales of $340 million in 1991 and Chee (1986) predicted therapeutic mAb sales of $1000 million in 1987. Sales totalled $377 million in 1992, $600 million in 1994 and $576.7 million in 1995 (Bibila and Robertson, 1995; Frost and Sullivan, 1996). Therefore, many predictions in the 1980's were optimistic. More recently, Bibila and Robertson, and Frost and Sullivan estimated the market size for therapeutic mAbs at $4,000 million in 1998 and $3,500 in 2002, respectively. Whether these predictions are also shown to be optimistic remains to be seen, but the progression of mAbs to the clinic has obviously been re-appraised in the past few years.

The failure of therapeutic monoclonal antibodies to reach their anticipated market share was also addressed by the FDA (Stein, 1997) after only 7 such drugs had been approved for human use, despite the successes in producing humanised mAbs. It was argued that production and purification of therapeutic monoclonal antibodies was not problematic, their specificity of action was beyond reproach and the FDA view humanised monoclonal antibodies as safe and potentially potent drugs that should have minimal side effects. Indeed the FDA perceives mAbs as "well characterised proteins" which grants them a regulatory status making product validation a more straightforward exercise. This left the question, why have there been so few successful products?

Three reasons for the failure of mAbs to realise their potential were cited. The most common failing was inadequate characterisation of the specificity of the antibody, its function or intended mechanism of action. This meant that the failure of the antibody to perform was not realised until late on in clinical trials, which may have been poorly or inappropriately designed because the antigenic determinant of the antibody had not been confirmed in the first place.

Second, preclinical development was often inadequate. Preclinical testing often involves the use of animal models to inform of dose and toxicity ranges. Whilst antigenic determinants are not always present in animals when an antibody is intended for use in humans, this should not be an excuse for proceeding immediately to human studies: *in vitro* work can provide valuable data in the estimation of dose and toxicity. Furthermore, every effort should be made to develop animal models to reflect the clinical application. Application of these measures could have prevented numerous antibodies from reaching phase III clinical trials which revealed them to be redundant in their intended therapeutic area. This is an expensive method (in terms of both time and money) by which to

discover such a failing. Resources could have been saved and diverted to the screening of a greater number of antibodies in earlier stages of development.

Finally, expectations of the antibodies were unrealistic, possibly because of the failure to apply adequate preclinical tests or fully characterise the antibody. This in turn would also result in poorly designed clinical trials which would inevitably result in data indicating that the drug was not efficacious. One of the unifying factors in these faults was that many companies had rushed to the market place after the safety of humanised monoclonal antibodies had been confirmed, but neglected to consider these 3 key areas.

So, despite the inability of monoclonal antibodies to match the earlier predictions made of their marketability, their progress to the market place should now be possible if due attention is paid to the errors that have resulted in their disappointing past performance. Indeed, this means that optimum processing and engineering strategies should be considered during the development of manufacturing procedures.

1.3. Project Objectives

The research detailed in this thesis is concerned with the initial stages of a large-scale, generic, process for the manufacture of three distinct therapeutic monoclonal antibodies. After 7 or 9 days of a fed-batch culture, material is transferred to a disc-stack centrifuge which removes whole cells and debris from the process material. The remaining debris is removed from the process stream as it passes through two depth filters of serially decreasing pore size and a sterilising grade 0.2 μm membrane. Following this mAb is concentrated in clarified material by ultrafiltration and is thus correctly configured for capture of mAb by affinity chromatography.

The depth filters and membranes which carry a positive electrostatic charge are theoretically capable of adsorbing DNA by electrostatic interaction with the negatively charged polyphosphate backbone of DNA. Partitioning of DNA from product must be achieved by the process because the FDA state that residual DNA must be reduced to picogram levels per dose in the final preparation. As will be detailed later in this section, the process that the industrial sponsors of this project use has no specific step that adsorbs DNA. Proof that one part of the process can perform such a role would be a valuable addition to the repertoire of robust DNA removal steps. The depth filters and charged membrane offer such an opportunity to demonstrate such partitioning of product and contaminant. However, the mechanism of adsorption to the surface of these modules, and their breakthrough or equilibrium capacity have not been demonstrated for DNA, (this is also true for any other solutes applied to these depth filters and membranes). Furthermore, their ability to do so under processing

conditions in the presence of numerous other species of biomolecule had not been demonstrated. In the first instance it is this lack of characterisation which must be addressed.

The second piece of work must address the unpredictable nature of the fouling of the depth filters in the harvest train. At the inception of this project there was no deployment of a disc stack centrifuge in pilot plant operations and blinding of the initial depth filters was erratic despite cell culture being a closely controlled fed-batch process. The more recent incorporation of a disc stack centrifuge to this process has ameliorated the problem of unpredictable filter blinding and whilst this may deal with the problem of blinding, it does not confront the origin of the problem. Therefore, the second piece of work addresses the ability of the first depth filter in the harvest step to deal with cells and debris originating directly from cell cultures.

The dual function of the depth filters (particle capture and adsorption) means that their sizing cannot be determined without specific details of their capacity for both particles and dissolved contaminants. By determining their DNA capacity, a decision can be made as to whether or not the initial stage of purification represents a clarification step, or if it can also constitute a DNA removal step as well.

A method by which DNA can be determined in the process material must be produced. Since the successful application of DNA quantification methods relies on knowledge of the molecular weight of DNA, the molecular weight of DNA entering the initial stages of mAb purification must be determined and this may give insights into the origin of DNA in mAb cell culture.

The remainder of this introduction deals with DNA as a contaminant and its origin from dying cells; methods for determination of DNA in mammalian cell cultures; details of the process employed by the industrial sponsors for manufacture of mAbs; and the development and application of charged depth filters and membranes in bioprocesses.

A description of the intended areas of therapeutic use for each of the monoclonal antibodies employed in this study is given in Appendix 1.

1.4. DNA as a contaminant in therapeutic proteins

When the therapeutic application of recombinant proteins derived from continuous cell lines was first suggested, DNA was identified as a contaminant of particular concern because the cell lines from which the proteins derived were tumourigenic. The concern being that residual DNA may include active oncogenes that could transfect cells and cause cancer when administered as part of the

therapeutic dose. Study groups and conferences were organised to address the issue and this resulted in a provisional recommendation that total cellular DNA per dose should not exceed 10 picograms and the corresponding probability of transformation would be between 10^{-8} and 10^{-6} (Petriccianni and Regan, 1986). An entire issue of the journal "Developments in Biological Standardization" was devoted to a summary of the arguments and conclusions from these various meetings (Petriccianni and Hennessen, 1986) whilst it was acknowledged that there was little data to guide the debates as to safe levels of DNA in products derived from continuous cell lines.

More recently the deficit in knowledge regarding the risks associated with injection of DNA derived from tumour cells has been addressed enabling a more informed debate of the risks associated with residual DNA in recombinant therapeutic products (Petricciani and Horaud, 1995). A key contribution to the debate was the report that immuno-suppressed monkeys injected with T24 tumour chromatin did not develop tumours, even after many years of observations following inoculation (Wierenga *et al.,* 1995). Also, human blood plasma used for transfusion contains DNA in μg quantities such that a typical transfusion might contain as much as 450 μg of DNA over 800 bp in length. Despite this, carcinoma induction is not a risk associated with transfusion (Duxbury *et al.,* 1995). More recently still, the carcinogenic potential of DNA from tumourigenic cell lines was assesed by injecting mice and rats with 250 μg purified hybridoma DNA: no elevated risk of tumour development was observed (Dortant *et al.*, 1997). Obviously none of these experiments used human subjects, but it was repeatedly concluded that the potential medicinal benefits of using continuous cell lines for the production of therapeutics far outweighed the theoretical risks associated with injection of DNA from tumorigenc cell lines. Thus, the WHO recommended that permissible residual DNA may be as high as 10 ng per dose and could be regarded as a cellular contaminant rather than a significant risk factor (Griffiths, 1997). The simplicity of the WHO recommendation is far from that of the FDA. The FDA state that the analytical goal for determination of DNA in monoclonal antibodies should be 10 picograms per dose and this is widely (but incorrectly) interpreted to mean that DNA levels should be reduced to 10 pg per dose at the end of the purification scheme (Briggs and Panfili, 1991). In fact the FDA state that they will consider each case as it is presented to them but would generally expect DNA to be reduced to 100 pg per dose. Moreover, they have recently conceded that manufacturers who can demonstrate sufficient clearance of DNA from well characterised proteins throughout a process are exempt from continuously having to test the end product of every batch. Thus, their attitude would appear to be relaxing in line with more recent findings, but is certainly not as easy to interpret as the attitude of the WHO. It would appear that the manufacturers who are prepared to risk presenting arguments for quantities of DNA above 100 pg in their product may ease their process validation exercises and production expenses, but it would appear few will endanger the issue of a pharmaceutical product license at the cost of a confrontation with the FDA.

1.4.1. Removal of DNA from therapeutic monoclonal antibodies

Removal of DNA from solutions containing monoclonal antibodies has been demonstrated by the application of numerous downstream operations including, immuno-affinity and anion exchange chromatography (Jiskoot *et al.*, 1991), whilst Ng and Mitra (1994) have also shown clearance of DNA by the same chromatographic techniques as well as by filter aids and size exclusion columns. DNA clearance by immuno-affinity chromatography has been optimised by Tauer *et al.* (1995). Monoclonal antibody production strategies commonly incorporate some or all of these steps. None of these studies reported on the molecular weight of DNA being separated from the antibody. Indeed, information regarding the size of DNA from animal cell fermentations has generally been confined to cell culture studies rather than observations on downstream processes. DNA from NS0 myeloma cells in the decline phase of batch culture consists of a high molecular weight component and oligonucleosomal fragments (Murray *et al.*, 1996). Such fragmentation of DNA is usually associated with apoptosis and the process of programmed cell death (Wyllie, 1980). Rodrigues *et al.*, (1997) have shown that DNA from perfusion cultures of hybridoma cells is generally of low molecular weight and suggested this may have originated by the process of programmed cell death. Since DNA in cell culture systems will almost certainly arise from dead cells, it is worth considering cell death in bioreactors.

1.4.2. DNA and cell death in cell culture systems

Cells die *in vivo* by one of two methods: necrosis or apoptosis. Cell death also occurs in bioreactors resulting in a decline in their operational efficiency. For this reason cell death in bioreactors has been studied intensely over recent years.

The term apoptosis was first applied to describe a series of *in vivo* cellular rearrangements that occurred prior to cell death. The term programmed cell death was introduced to indicate that these morphological changes were mediated by a cells' own metabolism, i.e. cells could commit suicide and actively participated in their own demise. The two phrases are now used interchangeably to describe a process that was initially studied because of its relationship with embryonic development and cancer. Within biotechnology, it has been studied as an engineering issue because it can contribute to loss of bioreactor efficiency. In the following notes it is worth bearing in mind that it is a process that occurs naturally in almost all eukaryotic organisms and serves to benefit the organism as a whole, whereas in bioreactors it is believed to confer no advantages to the efficiency of the industrial process.

The morphological features that define apoptosis include loss of structural attachments to neighbouring cells and cell surface structures such as microvilli followed by membrane blebbing and irreversible condensation of cytoplasm, compaction of cytoplasmic organelles, and condensation of nuclear DNA to form crescent-like structures under the nuclear membrane (Wyllie, 1997). Degradation of nuclear material occurs such that dying cells produce numerous fragments of DNA that have been cleaved between nuclesomes. Since nucleosomes package a constant amount of DNA (approximately 180 base pairs), the size of the oligonucleosomes is a function of that figure (Wyllie, 1980). After these gross changes have occurred, a dying cell will split into a cluster of membrane bound bodies. *In vivo* these cells are then engulfed by neighbouring cells or those in the immune system and effectively cleared from the organism (Devitt *et al.*, 1998; Wu and Horvitz, 1998). This ensures that the material from dead cells is managed carefully thereby minimising adverse reactions in the body whilst recycling cellular material. However, from the bioprocessing point of view, this dead cellular material remains in the bioreactor and DNA, host cell proteins and insoluble material (i.e. debris) will all persist in the bioreactor after cell death has occurred. Furthermore, these contaminants must be partitioned from therapeutic protein at some point in downstream processes. Apoptosis is induced by mild environmental stresses: selection by the immune system during thymic education, normal cell tissue turnover, or exposure to mild doses of ionising radiation and chemotherapy for example. At the metabolic level, apoptosis can be induced via many pathways, and environmental stresses can determine which pathway will elicit programmed cell death. The ubiquitous nature of programmed cell death means that there are also numerous genetic influences in cell death that are common to eukaryotes (see Wyllie, 1997).

Necrosis, by contrast, is a passive process whereby cells take in water as they die, nuclear material remains largely intact, the plasma membrane may rupture to release cytosolic material and *in vivo* this may result in inflammatory reactions. In bioreactors, the problem is the same as for apoptosis in that the dead cell releases materials that must be removed, at some point in the downstream process from the protein of interest. However the nature of this dead material is likely to be different from that released by apoptotic cells.

Apoptosis has been established as a common cause of cell death in bioreactors where T-cell hybridomas (Smith *et al.*, 1989; Shi *et al.*, 1989), B-cell hybridomas (Al-Rubeai *et al.*, 1990; Franěk *et al.*, 1992), insect cell lines (Singh *et al.*, 1994), and myelomas (Mercille and Massie, 1994) have been cultivated. The ubiquity of programmed cell death in cell culture systems led many workers to conclude that the efficiency of bioreactors could be bettered by modulating favourably the frequency of apoptotic cell death, which meant that those factors which triggered apoptosis had to be identified.

Deprivation of glucose, glutamine and cystine was shown to induce apoptosis (Mercille and Massie, 1994) as can the depletion of many other amino acids (Simpson *et al.,* 1998) and accumulation of toxic metabolites such as ammonia and lactic acid can induce necrotic cell death (Mercille and Massie, 1994). Furthermore, conditions of intensive agitation can provoke apoptosis (Al-Rubeai *et al.,* 1994) and hypoxia can also induce programmed cell death (Mercille and Bernard, 1994) although attempts to use an onco-gene (*bcl-2*) which can prevent against apoptosis in conditions of low oxygen (Shimizu *et al.* 1995; Jacobson and Raff 1995) have not succeeded in preventing cell death in NS0 cell lines (Murray *et al.,* 1996). Thus, attempts to modulate apoptosis tend to be addressed by genetic, biochemical or physical parameters. This work has been reviewed recently by Dickson (1998).

Considering downstream processing, the presence of apoptotic cells appears to have attracted very little research attention, although Singh *et al* (1994) recognised that apoptosis will result in the release of lytic products into the product stream and Rodrigues *et al.,* have noted that the DNA from hybridoma perfusion cultures formed a ladder when separated electrophoretically on agarose and suggested that this DNA originated from cells that had died by apoptosis. The presence of apoptotic cells was not confirmed, and such low molecular weight material should not be considered as the sole criteria for identification of apoptosis because low molecular weight DNA can be produced when cells are immobilised on high molecular weight polymers (Collins *et al.*, 1992) or exposed to antibiotics (Kuo and Hsu, 1978). In fact this raises an interesting point in that the origin of DNA that goes on to become residual DNA in the product has not been determined. Whilst arguably the quantity of DNA is related to the amount of cell death that occurred prior to processing, the quantity of DNA that is released by a cell's death, or in its dying by a specified manner has not been established. The work in this thesis should address this at some point because the DNA challenge to the downstream processes is likely to be a function of cell death.

1.4.3. Quantification of DNA.

The accurate quantification of DNA is both important and of general interest within biotechnology and a wide range of biological sciences. It has been the subject of intense work over recent years, and numerous methods of DNA determination are now available. For the purposes of this work there is a requirement for an assay for DNA that will accurately report the quantity of DNA passing through the initial stages of antibody purification. The following serves as a review of the methods that are often used for determination of DNA under various circumstances, and an analysis of their suitability for application to this work. A brief description of the structure of DNA is provided in Appendix 2 which may be used to embellish the following description.

1.4.4. Spectrophotometry

Spectrophotometry is unrivalled in its simplicity for simultaneous confirmation of purity and quantification of DNA. Calculation of the ratio of absorbances at 260 nm and 280 nm gives an indication of the purity of the sample. A ratio of 1.7 to 2.0 indicates that DNA is clean, i.e. free of RNA and protein, whereas an $A_{260/260}$ below 1.7 indicates the presence of protein, and above 2.0 the presence of RNA is implied. Its successful application requires relatively high levels of DNA, typically in the microgram range. Single nucleotides, proteins and aromatic molecules can interfere with accurate determination of DNA (Sambrook, *et al.,* 1989). Spectrophotemtry cannot be used for direct determination of DNA for work detailed in this thesis because samples are protein rich and interference would certainly prohibit its use.

1.4.5. The Threshold Method*

The Threshold Method is a fully automated, kit-based assay which was developed in response to the requirements of the FDA who demanded an assay sensitivity of 10 pg DNA per dose in pharmaceutical proteins derived from myeloma cell lines (see Section 1.4). The method exploits two high affinity DNA binding proteins, one of which is an antibody conjugated to urease. The second protein is a single stranded DNA binding protein which is conjugated to biotin. These two proteins form a complex with single stranded DNA which is captured on a biotinylated membrane via streptavidin which has a high affinity for up to four biotin molecules. After capture of the complex on the membrane, urea is added to the mixture which is converted by urease to CO_2 and NH_3. The pH change accompanying the activity of urease is measured and since the amount of bound urease is proportional to the amount of DNA present, the rate of change of pH in the solution is a direct measure of the quantity of DNA present in the initial sample (Kung *et al.*, 1990). The method is used widely throughout the bioprocess industries because the FDA approves of the method. However, the assay does suffer interference from proteins and despite its automated assay procedure, its successful application normally requires that DNA is purified from samples prior to assay (McKnabb and Tedesco, 1989). Parallel samples have to be spiked with calf thymus DNA, and a recovery of DNA outside 80% to 120% means that the test fails. The manufacturers recognise that DNA must be sufficiently long to accommodate both of the proteins that bind: the assay response from DNA of strand length 603 base pairs or less is reduced. It has been argued that this is not an issue because DNA of such size is not likely to pose a risk of transformation to patients who are administered with the drug (McKnabb and Tedesco, 1989). Therefore, the failure of the assay to detect this low molecular weight DNA is not an issue in assays for residual DNA but is critical for

---

* The Threshold Method is a trademark.

determination of DNA in samples which define the operation of the process. It may be considered for application to this work only if the DNA in mammalian cell culture supernatants is shown to be chiefly high molecular weight DNA.

1.4.6. Hybridisation and Radiolabelling Methods

Hybridisatiom methods were employed prior to the introduction of the Threshold Method for determination of DNA in the picogram range. They involve purification and denaturation of DNA from samples of interest; its immobilisation on nitrocellulose and annealing of complimentary DNA strands (after Southern, 1975). The quantity of residual DNA in the sample is related to the amount of radioactivity detected on the nitrocellulose membrane. Success also depends on a spike recovery, and given the onerous nature of this method, the precautionary measures and costs incurred when working with radioactive materials, the length of time taken to gather valid data for a single sample, it is no longer considered a realistic method for determining residual DNA in therapeutic proteins. It is mentioned here for completeness only.

However, radiolabelled nucleotides are of value for performing mass balances for DNA in scaled down equipment to demonstrate the ability of unit operations to partition DNA from product (Ng and Mitra, 1994).

1.4.7. Fluorescence based assays for DNA

Fluorescence based assays for polymeric nucleic acids have been available since the application of ethidium bromide to such a task (Le-Pecq 1966). The speed and simplicity of DNA or RNA determination using ethidium bromide was such an improvement over previously available methods that fluorescence based determination of DNA or RNA rapidly became a favoured technique. To its credit, ethidium bromide is still widely employed in DNA and RNA studies some 30 years later (Sambrook, 1989), but as a laboratory reagent it is not without its faults (see below) and many compounds have since been developed to improve on its selectivity, safety, and specific fluorescent enhancement. These latter-day compounds, termed fluorochromes, have common structures, namely the inclusion of polycyclic aromatic groups, often including quinoline derivatives, oxazole or thiazole groups. Fluoresence enhancement is greater when dyes bind to DNA as dimeric molecules linked by polyamine bridges and again this is a common structural feature of fluorochromes (Markovitz, 1979; Glazer and Rye, 1992).

Fluorochromes bind within and parallel to the bases that constitute the helical arrangement of RNA or DNA. Such binding induces conformational changes in the intercalater which on exposure to

light of a specific wavelength will cause bound molecules to fluoresce and ideally, unbound molecules to remain unexcited. The resultant fluorescence is proportional to the amount of DNA present and in conjunction with appropriate calibration curves the determination of DNA becomes a straightforward calculation. Fluorochromes typically bind to double stranded nucleic acids at a ratio of one molecule per 4 or 5 base pairs and as such DNA or RNA can be detected even if the polymer is relatively short. Numerous commercial dyes are now available: their relative merits have been reviewed by Glazer and Rye, 1992. A sketch to summarise the proposed method of DNA intercalation by a fluorochrome is shown in Appendix 2 (Figure 2-1).

1.4.7.1. Ethidium Bromide

The first fluorochrome to be applied to quantification of purified nucleic acids (Le-Pecq and Paoletti, 1966), ethidium bromide has since been inextricably linked with routine techniques of molecular biology, with improved methods describing its application to quantification of DNA and RNA in crude tissue homogenates in 1972 (Karsten and Wollenberger); development of micro-assay procedures requiring smaller samples in 1974 (Boer); and optimum dye:base pair ratios for more accurate determinations in 1994 (Dutton *et al.,* 1994). Ethidium bromide has been cited as being a mutagenic substance and also suffers from a high non-specific, or background fluorescence (up to 12% of the total fluorescent signal): its fluorescent enhancement (the ratio of fluorescence intensity emmitted by DNA bound fluorochrome to unbound fluorochrome) is 80 for excitation light of 365 nm (Le-Pecq and Paoletti, 1966; Sambrook *et al.,* 1989). It was claimed that DNA in samples with as little as 100 ng ml^{-1} could be quantified. Although now superseded by more effective, safer dyes it is still used extensively to visualise the distribution of DNA on agarose gels (Sharp *et al.,* 1973, Sambrook *et al.,* 1989). Such electrophoretic separation permits both assessment of DNA molecular weight and quantification of DNA when used in conjunction with any intercalating fluorochromes. However, accurate quantification requires dedicated, costly equipment such as a charge coupled device (CCD) camera or argon laser and the need to purify DNA from samples prior to electrophoresis makes this method onerous. Furthermore, such a method has been criticised in situations where large numbers of samples must be handled quickly (Ahn, *et al.,* 1996) and the optimum dye:base pair ratio for quantification is very narrow, further complicating application of the method (Dutton *et al.,* 1994). Despite this, and because of its shortcomings, ethidium bromide became the basis for the development of many dyes employed to bind and quantify DNA.

1.4.7.2. Hoechst 33258

In the same way that ethidium bromide had been employed for determination of DNA in purified solutions and crude tissue homogenates, Hoescht 33258 has also been applied for the same purposes

with the advantage that it has a specific fluorescence enhancement of 95 and is less susceptible to non-specific fluorescence induced by the presence of protein (Cesarone *et al.*, 1979). The reagent elicits an assay sensitivity of 10 ng DNA ml^{-1}, although dye concentrations must be reduced in relation to the quantity of DNA present (Labarca and Paigen, 1980). Assay conditions can be manipulated to significantly reduce fluorescence from RNA which means that sample preparation can omit RNase steps. However, fluorescence can be impaired at concentrations of 100 µg BSA protein equivalent or above (Moe *et al.*, 1994) and the dye has a preference for binding to A-T rich regions of DNA (Pimpinelli *et al.*, 1975) which means that for accurate DNA determinations calibration curves must be constructed using DNA of the same species or group from which samples have originated. Despite its faults Hoescht 33258 has been employed as the choice fluorescent reagent for quantification of DNA for many years.

1.4.7.3. Cyanine Dyes

As mentioned in section 1.4.7.1, intercalating fluorochromes can also be used to determine DNA that has been separated electrophorectically when used in conjunction with devices that can quantify emissions from a sample. Many dyes such as "YO-YO" and "TO-TO" have been developed on the basis of the structure of ethidium bromide or dimers derived from it. They have enhanced binding affinities for DNA, and specific fluorescence enhancements of more than 1000 fold, making detection of 20 pg DNA possible. One dye, SYBR-Green I, may detect DNA in the femtogram range (Skeidsvoll and Ueland, 1995) but given the expensive nature of equipment required to realise their full potential, they are not considered as a viable method for determining DNA in samples that will be encountered for the generation of data in this thesis.

1.4.7.4. PicoGreen

At the time or writing, PicoGreen is the most recently released intercalating fluorochrome. Its structure has not been publicly stated but presumably it will have structural similarities with fluorochromes that have gone before it. It has been used to quantify DNA in samples of various origin (bacterial and mammalian), sequence complexity (supercoiled, naked and histone bound) with strand length > 150 bp (Ahn *et al.*, 1996). None of these parameters had a significant impact on the specific fluorescent enhancement of the fluorochrome except in the case of supercoiled DNA where a slight reduction in specific fluorescent enhancement was observed. Furthermore, Singer *et al.*, (1997) working on behalf of the manufacturers of PicoGreen, have confirmed the ability of PicoGreen to fluoresce with the same intensity irrespective of the organism from which the DNA originated. They have also quantified nominal DNA levels at 25 pg dsDNA ml^{-1} and demonstrated that the linearity of the assay is maintained in defined solutions containing salts, protein and some

uncharged polymers. Therefore, in conjunction with appropriate calibration curves it is considered to be a valid, accurate, simple and rapid method for quantification of DNA whilst maintaining versatility by its ability to fulfil its pre-defined role under numerous test conditions. Previously published DNA quantification work using PicoGreen has been restricted to defined, relatively pure solutions (Enger, 1996, Ahn *et al.*, 1996, and Seville *et al.*, 1996, Singer *et al.*, 1997). The high specificity and fluorescent enhancement upon binding dsDNA, in conjunction with negligible fluorescence of unbound PicoGreen make it a suitable candidate for quantification of DNA in solutions containing other contaminating species such as surfactants and protein. Also, the speed and simplicity of use of PicoGreen for DNA quantification make it an attractive alternative to other methods. For these reasons it was selected as a potential candidate for determination of DNA in mammalian cell cultures over other fluorochromes that are available.

1.5. Production and purification of monoclonal antibodies employed in this study

The process described in this section was developed to enable manufacture of numerous distinct mAbs, i.e. it is a generic process. By developing a generic process, development, plant capital and manufacturing costs can be rationalised. There are subtle differences in the manufacture of each antibody and these have been described where appropriate. A schematic of the process is shown in Appendix 3.

1.5.1. Fermentation and harvesting

The fermentation step is the method by which monoclonal antibodies are produced. NS0 cells (Bebbington *et al.*, 1992) secrete mAb into the culture broth and can be sustained continuously providing there is a supply of nutrients and removal of waste products. Cells can be grown in a wide range of culture volumes. For large scale work 8000 litre fermenters are employed. Cells are grown under near physiological conditions for seven or nine days, with supplemental nutrient feeds on every second day of culture. At the end of fermentation mAb must be recovered from the supernatant of the broth and the primary step is to remove suspended cells and debris from the cultured materials. Recovery of product from this step is typically in the region of 80 to 100% (*pers. comm.* Julian Relton and Kevin Cownley). The harvest step has been described in greater detail in Section 1.3, see also Figure 1-1.

1.5.2. Viral inactivation and initial antibody capture

Following concentration by ultrafiltration, the culture broth is subjected to a solvent/detergent treatment which is designed specifically for the inactivation of retroviruses, after Horowitz *et al.* (1985) who developed and patented the method in response to concerns regarding HIV in blood products. The concentrated cell culture supernatant is treated with 0.1% (v/v) tri(n-butyl) phosphate and 1.0 % (v/v) polysorbate 80 for at least 6 hours above 18 °C. This treatment is performed early in the process so that there are numerous opportunities elsewhere in downstream processes to remove the solvent and detergent from the product. The treatment will typically reduce the titre of murine leukaemia virus by ≥ 6 $\log_{10}$.

The virus inactivation is essentially an overnight step after which the process material proceeds to an affinity step whereby mAb is captured by immobilised Protein A. Protein A is a *Staphylococcus aureus* cell wall protein which has an exceptionally high affinity for antibodies and acts *in vivo* to

defend this organism against vertebrate immunogenic responses. By immobilising this protein on a gel matrix an extremely potent method for the large scale purification of mAb has been developed (Lee *et al.*, 1986). Not surprisingly Protein A is commonly used in antibody purification schemes, (it is also frequently used in procedures for assay of mAb): it can reduce titres of contaminating DNA (Jiskoot *et al.*, 1989) and host cell protein by as much as 4 logs, whilst recovery of useful product is repeatedly greater than 95%. In the context of this process it also provides a method by which to remove numerous cell culture reagents such as pH indicator, surfactant, salts and minerals. The antibody is eluted from the column in a low pH buffer. The low pH inactivates viruses so the Protein A step constitutes a viral inactivation step and yields a process stream that can be directly loaded onto the subsequent ion exchange column (Ramage and Allen, 1992).

1.5.3. Intermediate purification, polishing and formulation

The SP-Sepharose FF ion exchange column was initially introduced to the purification scheme to remove serum proteins from the culture broth. Since the cell culture media is now serum free, this step is retained to enable removal of host cell protein, DNA, and viruses from the product. The eluate from the Protien A column is configured for immediate capture of mAb on the cation exchange matrix. Most host cell proteins are negatively charged at low pH, whereas antibodies tend to have a higher pI which means they are positively charged at low pH. Therefore, by capturing antibodies on the basis of their charge, this step can elicit exceptional separation of product and host cell protein.

The subsequent ultrafiltration step serves to concentrate the antibody and reduce process volumes which is necessary to maintain efficient flow rates in the two following unit operations. The first of these, the nanofiltration step has very low flow rates because the membrane which has been incorporated for capture of viral particles has nominal pore sizes of 50 nanometres (viral titres can be reduced by as much as 6 logs, but the ability of this step to reduce viral titres will always be a function of viral size) (Oshima *et al.*, 1996; Phillips and DiLeo, 1996,). Consequently, small culture volumes are desirable to expedite processing time, as is the case for the size exclusion column which can only elicit effective separation of mAb and its aggregated forms when the load volume is less than 6.5% of the column volume. The size exclusion column also serves to remove DNA, host cell protein and viruses. The final ultrafiltration step is required only for mAb A and mAb B because the required final administration concentration of these two mAbs is much greater than that for mAb A. The final formulation is a liquid consisting predominantly of mAb but also incorporates small quantities of detergent to prevent shedding (the phenomenon of therapeutic protein drying and remaining insoluble on the surface of the final container).

1.6. Depth filters and membranes as adsorbents

1.6.1. Depth filters

Filtration is the process whereby particles are removed from fluids by means of a porous medium or screen which allows passage of the fluid but retention of particulate matter. Depth filters operate by removing particles along the entire length of their pores and are usually applied as disposable units in bioprocesses. They are characterised by an ability to remove relatively large quantities of solids from fluids whilst maintaining high fluxes before blinding. Such an ability is conferred to the depth filter by the incorporation of materials which posses a high surface area to volume ratio: prelate, carbon, diatomaceous earth and sand for example. The use of such materials was a direct result of the abolition of asbestos containing depth filters from food and drug preparative processes (Meltzer, 1987). However, the ability of these replacement components to remove particulates and clarify colloidal suspensions was poor when compared to asbestos because in contrast to asbestos filters they tend to be negatively charged at typical processing pHs, whereas asbestos is positively charged at typical processing pHs. Thus, a positively charged thermosetting resin was introduced into the manufacture of these devices, resulting in depth filters that more closely resembled those that had been banned. Latex beads, bacteria, endotoxin, and viruses could all be removed from solutions by filters whose pore sizes were at least an order of magnitude larger than the particles they were removing (Hou *et al.,* 1980), and data was also presented indicating their removal was by adsorption rather than by sieving or depth filtration. Such depth filters are available in a wide range of pore sizes and are popular within bioprocesses because they offer a simple, established method by which to remove whole cells and debris from cultured materials at the start of processing, thereby clarifying solutions and making them fit for further processing whilst avoiding premature blinding of downstream sterilising grade microporous membranes. In the system under study in this work two depth filters are employed consecutively in the initial stage of monoclonal antibody production. The first in the filtration train is a Cuno Zeta Plus 10SP depth filter with nominal pore sizes in the range 4.0 to 0.8 μm (see Table 1-1). The second in the depth filter train is a Cuno Zeta Plus 90SP depth filter with nominal pore sizes in the range 0.1 to 0.25 μm. Explicit characterisation of the their ability to adsorb negatively charged solutes from challenge solutions is notably lacking from the scientific and engineering literature.

Filters are generally operated under one of two modes: constant pressure whereby as the filter blinds there is a decline in flux, or constant flow rate where as the filters accumulate particles there is an increase in pressure drop across the filter (Doran 1995; Coulson and Richardson, 1996). The industrial sponsors of this project deploy the depth filters by pressurising the fermenter vessel which

provides the driving force to feed the disc-stack centrifuge. Following centrifugation the remaining debris is removed in the filter train. Since there is no storage of material between centrifugation and filtration, and the volume of particulate matter removed by the centrifuge is negligible, the rate of liquid input to the centrifugation is very close to the liquid input to the filter train. In order to maintain constant centrifugal forces on particles in the disc-stack the filters should be operated at constant flow rate, but in reality pressure drop across the filters may vary: the fermenter is pressurised to 2.0 to 2.5 bar prior to harvesting and in the event that the rate of filtration decreases, the pressure in the fermenter may be increased to 3.0 bar to enable a constant rate of centrifugation and filtration.

1.6.2. Sterilising grade membranes

The use of charged modified surfaces to enhance particle removal was subsequently applied to microporous membranes which are also widely used throughout pharmaceutical processes. They are most commonly used to confer sterility to downstream operations which results in the maintenance of product efficacy and safety. Particles above 0.22 μm in size are removed by a surface sieving mechanism. Incorporation of charge to the surface of the membrane can result in removal of smaller particles or anionic dissolved substrates on internal pore surfaces (Zierdt, 1979). Charged membranes have been manufactured for many years now (Ostreicher *et al.*,, 1983; Gsell *et al.*, 1984),

Unit name	Manufacturer	Unit type	Pore size (μm)	Characteristic materials of construction
Zeta Plus 10SP	CUNO	Depth filter	0.8-4.0	Kieselghur, cellulose, thermosetting charged resin
Zeta Plus 90SP	CUNO	Depth filter	0.01-0.25	As 10SP, ratio of components may change
Posidyne	PALL	Charged sterilising grade membrane	≤0.22	$Nylon_{66}$, quaternary ammonium group
Zetapor	CUNO	Charged sterilising grade membrane	≤0.22	$Nylon_{66}$, quaternary ammonium group
Sartobind Q	SARTORIUS	Advanced membrane adsorbent	≈3.0	Cellulose acetate, quaternary ammonium group

Table 1-1: Key features of membranes and depth filters employed in the initial stages of monoclonal antibody production as described by the manufacturers own literature. Although the Sartobind Q is not employed for antibody production its details are included because the membrane has formed part of the study of DNA adsorption.

and their use in bioprocesses is widespread because of their ability to adsorb endotoxins in addition to particulates (van Doorne, 1993; Brown and Fuller, 1993). In the section of the process studied for the purposes of this thesis they are employed at the end of the depth filtration train prior to concentration of the culture broth by ultrafiltration (see Table 1-1). Thus, they serve to remove any remaining particulate matter and thereby afford protection to the ultrafiltration membrane.

1.6.3. Adsorbent membranes

Membrane adsorbents were initially developed for diagnostic purposes whereby biological substrates were captured and detected on ligands which had been immobilised on the internal surface of microporous membranes. The application of this technique enabled more rapid, sensitive detection of specified molecules such as drugs or microbes (Blankstein and Dohrman, 1985), which conferred advantages to both clinicians and patients alike. The exceptional specificity that could be engineered into such membranes inadvertently produced a method that could be applied to the commercial scale purification of biomolecules. By the mid 1980's it was widely recognised that there was a requirement for more rapid, efficient, commercial-scale biomolecule affinity separations (Hou, *et al.*, 1986): whilst affinity chromatography offered unequalled selectivity for numerous molecules, its application had invariably been in columns where the intrinsic compressibility of beads limited processing speeds and low mass transfer rates of adsorbates to bead surfaces made optimal column use problematic. By placing ligands within the pores of a microporous membrane, thereby ensuring the mass transfer of adsorbate was convective rather than diffusive, the possibility of more efficient affinity separations became an achievable goal (Brandt *et al.*, 1988). Process developers were obviously attracted to the prospect of operations performed with low back pressures, short residence time and high volumetric throughputs as compared to more conventional purification methods and numerous companies developed membrane-based matrices that could be applied for recovery of biomolecules (reviewed by Roper and Lightfoot, 1995).

The first applications of such membranes were reported favourably using well characterised proteins (BSA for example) when compared to various column matrices (Champluvier and Kula, 1991); modelling studies showed the behaviour of the membranes to be predictable (Briefs and Kula, 1992; Suen and Etzel, 1992); and membranes could be used to elicit fractionation of amino acids (Garem *et al.*, 1997). Purification of proteins from complex solutions was also shown to be possible, although the flow characteristics through the membrane module were thought to be sub-optimal under some circumstances (Gebauer, 1997).

Although such membranes are not applied in the initial stages of monoclonal antibody purification, the purification as a whole does not include a specific DNA removal step. Therefore, they were

investigated for their potential to remove DNA from solution as compared with the other membranes employed in the step.

2. Material and Methods

All reagents were analytical grade and purchased from BDH, Lutterworth, Leics, unless otherwise stated.

2.1. Chemicals, Kits and Dyes

Acradine Orange. Obtained from Molecular Probes (Leiden, The Netherlands).

Agarose (Ultra Pure DNA Grade). Obtained from Bio-Rad (Hemel Hampstead, Herts, U.K.).

Deionised Water. Produced by a Millipore (Watford, Herts, U.K.) MilliQ Plus Ultra Pure Water System.

Calf thymus DNA. Obtained from Clontech (Palo Alto, CA, U.S.A.).

Ethidium Bromide. Obtained from Bio-Rad (Hemel Hampstead, Herts, U.K.).

Erythrosin B. Obtained from Sigma (Poole, Dorset, U.K.).

PicoGreen. Obtained from Molecular Probes (Leiden, The Netherlands).

Polyacrylamide Gel Electrophoresis Kits. Obtained from Bio-Rad (Hemel Hampstead, Herts, U.K.).

Poly-L-lysine (28.5 Kda). Obtained from Sigma (Poole, Dorset, U.K.).

Polysorbate 80. Obtained from Croda. (Goole, Korks, U.K.).

Micro BCA Protein Assay Kit. Obtained from Pierce (Rockford, IL, U.S.A.).

Ribonuclease A. Obtained from Sigma (Poole, Dorset, U.K.).

Synthetic oligonucleotides (dN_{5-19}). Obtained from Sigma (Poole, Dorset, UK).

Standard Bovine Serum Albumin. Obtained from Pierce (Rockford, IL, U.S.A.).

ΦX174 Hae III (Daniels., *et al.,* 1983). Obtained from Sigma (Poole, Dorset, UK).

2.1.1. Miscellaneous

All buffers were made up using deionised water from a Millipore MilliQ Plus Ultra Pure Water System.

2.2. Methods

2.2.1. Cell culture

All cell culture work described in this thesis employed a GS-NS0 (glutamine synthase – non secreting) cell line which had been induced to secrete humanised monoclonal antibody by incorporation of a plasmid coding for pertinent MAb. The cell line was initially developed by Bebbington *et al.*, (1992) and was supplied by the European Collection of Animal Cell Cultures.

2.2.1.1. Large scale cell culture

Large scale cell culture was performed and managed by employees of the industrial sponsor. Details of the culture regime are included here because samples were withdrawn from the large scale culture volume and at various points in the downstream process in order to generate data that has been included in this thesis.

The GS-NS0 cell line secreting humanised monoclonal antibody was cultivated in an 8000 litre stirred tank cell culture vessel. Cells were grown in serum-free media. The composition of the media is proprietal and its complete details cannot be included in this thesis. Nevertheless, growth of antibody secreting cells to relatively high antibody titres in the absence of serum has been demonstrated by Bibila *et al.* (1994) and Xie *et al.* (1994). Cells secreting monoclonal antibody A were grown for seven days with bolus feeds on days 2, 4 and 6. Cells secreting monoclonal antibody B were grown for nine days with bolus feeds on days 2, 4, 6, and 8. Samples were taken daily for cell counting purposes, always prior to supplemental feeds.

2.2.1.2. Small scale cell culture

At the laboratory scale GS-NS0 cells secreting monoclonal antibody B were grown at 36 ^{0}C in 250 ml Erlenmeyer Shake Flasks (Corning, New York, U.S.A) (100 ml culture volume) containing the same serum-free medium that had been used to grow cells in the 8000 litre culture vessel. Cells were stored under liquid nitrogen and revived from a master cell bank. After revival procedures had been performed, cells were seeded at approximately 0.3 x 10^{6} viable cells ml^{-1} and sub-cultured every three or four days. Aseptic techniques were employed throughout all procedures as detailed in Freshney, 1983.

2.2.2. Cell type and particle counts

2.2.2.1. Viable/non-viable cell determinations

Viable, non-viable and total cell concentrations were determined using a stock solution of 0.04% (w/v) erythrosin B in phosphate buffered saline (PBS), pH 7.2. The dye is excluded by live cells and taken up by dead cells. Cell suspension samples and erythrosin B were added in equal volume to one another. The resulting solutions were scored in 4 × 1 mm^2 grids of an improved Neubuaer-haemacytometer (BS 748) trans-illuminated by a Zeiss microscope (Oberkochen, Germany) fitted with a 10x objective lens.

2.2.2.2. Healthy, apoptotic and necrotic cell number determinations

For evaluation of the morphological features associated with healthy cells, programmed cell death (apoptosis) and necrosis, fluorescent dye exclusion studies were employed as described below.

Acridine Orange can enter both live and dead cells. When intercalated into double stranded DNA it fluoresces green and when bound to single stranded DNA or RNA it stains orange. Ethidium bromide only enters dead cells and emits light of 254 nm (orange) when bound to DNA or RNA and excited with ultra-violet light (Le Pecq and Paoletti, 1966). Since the emission from ethidium bromide overwhelms that of Acridine Orange, dead cells appear orange whereas live cells are green. Morphological features of the cells were examined and scored according to the descriptions given by Mercille and Massie (1994) which are summarised here: viable non-apoptotic, green with variations in fluorescent intensity; viable apototic, green, highly condensed, uniformly stained nuclei present as one or many bright spherical beads, often smaller than cells; non-viable necrotic, orange, structured nuclei with variations in fluorescent intensity; and non-viable apoptotic, orange with similar morphological features to cells. Mercille and Massie also published fluorescent photomicrographs of each cell type that they described which were extremely useful in embellishing their text. Therefore photomicrographs of each cell type are shown in Figures 2-1 to 2-5 towards the end of this thesis. In the event of any ambiguity in recognising the various cell types, green cells were scored as viable non apoptotic and orange cells were scored as necrotic. Consequently, viable and non-viable apoptotic cell numbers may have been underestimated but at the expense of ensuring that those cells scored as apoptotic were genuinely so.

A stock solution containing 100 µg Acridine Orange ml^{-1} and 100 µg ethidium bromide ml^{-1} (Sigma) was prepared in PBS, and 40 µl of stock solution was added to 1 ml of cell suspension. Cell suspensions were diluted with PBS as necessary. Cells were scored in 4 × 1 mm^2 grids of an improved Neubuaer rubidium-coated haemacytometer (BS 748) using a 40x objective lens. Epi-

illumination induced fluorescence of the bound dyes and a filter set suitable for observation of fluorescein was employed.

2.2.2.3. Particle counts

An automatic particle analyser system (Coulter Channelyzer 256, Coulter Electronics, Hialeah, Fl, U.S.A.) was used to count and size particles in cultured and processed materials. The system operates according to an electronic resistance principle. An electric current is applied between electrodes located on either side of a cylindrical, hollow, glass probe. Current flows through an aperture in the probe courtesy of an appropriate electrolyte. When particles are forced through the aperture the current flowing between the electrodes is impeded. The size of the impedance is related to the size of particle passing through the aperture. This results in particle sizing. Cell culture or process samples were diluted 1:200 with PBS and analysed three times. The average number of counts in each of the 256 channels was used to determine the number and size of particles in each sample. Such a system is claimed to enable sensitive and reproducible size distribution of cell populations (Seewoster and Lehmann, 1997).

2.2.3. Purification of DNA from process supernatants and whole cells.

DNA was extracted from either the supernatant of fermented materials or from whole cells and debris. For extraction of DNA from process supernatants, cells and debris were removed by spinning samples at 7200g for 5 min prior to passage through a Millex GV (Millipore, Watford, herts, U.K.) 0.2 μm membrane. Supernatant was then incubated for four hours at 37 ^{0}C after the addition of $CaCl_2$ to 10 mM with bovine pancreatic Ribonuclease A (approximately 50μg ml^{-1}) (Sigma, Poole, Dorset, U.K.), Proteinase K (approximately 100 μg ml^{-1}) and 0.2% (w/v) SDS (Sigma). DNA was then precipitated with 60% isopropanol, 0.3 M sodium acetate (Sigma), 100 mM $MgCl_2$. Samples were stored at –20 ^{0}C until required. For extraction of DNA from whole cells and debris, fermented samples were spun at 7200g for 5 mins and after decanting the supernatant the pellet was resuspended in 10 mM Tris, 1mM EDTA at pH 7.5 including 100 mM NaCl. The samples were then treated with enzymes in the same way as that detailed for samples of supernatant. Precipitated DNA was purified by centrifugation at 12,000g for 10 min and rinsing the pellet in 70% (v/v) ethanol and 100 % ethanol prior to drying with pressurised N_2. DNA was resuspended in the agarose gel running buffer as detailed in section 2.2.4, below.

2.2.4. Agarose gel electrphoresis

Agarose gel electrophoresis facilitates separation of nucleic acids in an electric field on the basis of their size. DNA moves towards the anode and its location is visualised under ultraviolet light by staining the gel with an intercalator such as ethidium bromide.

1.5% (w.v) agarose (Ultra Pure DNA Grade, Bio-Rad, Hemel Hampstead, Herts, U.K.) gels were prepared using a 90 mM Tris/phosphate buffer (pH 8.2). DNA samples were run on the gel for four hours at 100 V and stained with ethidium bromide. The tank running buffer was the same as that used to prepare the agarose gel.

Both DNA extraction and gel preparation protocols are standard techniques, further details are given in Sambrook *et al.*, 1989.

2.2.5. Determination of fluorescence

For calibration purposes a stock solution of calf thymus DNA was diluted 1:120 with TE, pH7.5. The concentration of DNA in the resulting solution was established by measuring its absorbance at 260 nm against a TE blank in a Shimadzu UV-1201 Spectrophotometer (Tokyo, Japan) using a 1.4 ml quartz cuvette. Appropriate dilutions of this solution were made with the blank challenge material buffer to produce a calibration plot for the determination of DNA levels in pre and post filter fractions samples. A PicoGreen working solution was prepared by diluting the manufacturer's PicoGreen stock solution 1:200 with TE. Fluorescence measurements were carried out by aliquoting 100 µl of sample into a single well of a Nunc Maxisorb 96 well plate (Kamstrup, Denmark), adding 100 µl of PicoGreen working solution, incubating for 2 minutes and reading the fluorescence by excitation at 485nm, emission at 520nm (bandwidth 20nm and 25nm respectively) in a CytoFluor® Multi Well Plate Reader (PerSeptive Biosys, Framingham, MA, USA). All calibration samples were assayed in triplicate and a fresh calibration curve was generated for each 96 well plate. Baseline fluorescence was determined with the challenge material blank, the average of which was subtracted from the averaged fluorescence of other samples.

2.2.6. Protein assay

For determination of protein in samples a Pierce (Rockford, Il, USA) Micro BCA Protein Assay Reagent was employed, which is based on the reduction of Cu^{2+} to Cu^{+} in the presence of peptide bonds followed by complexing of the cuprous ion with bicinchoninic acid (Smith *et al.*, 1985). For calibration purposes a 2 mg ml^{-1} solution of Standard Bovine Serum Albumin was diluted with TE, pH

8.8, 100mM NaCl and assays were performed in a 96 well plate according to the manufacturers protocol.

2.2.7. High Performance Liquid Chromatography

The chromatography system consisted of a Waters (Milford, MA, U.S.A.) 600S controller, 626 pump, 717 plus autosampler, 996 photodiode array and Millennium v2.15 software. Size exclusion chromatography was performed on a BIOSEP SEC S3000 column (7.8mm ID x 300mm; Phenomenex, Torrance, CA, U.S.A.), flow rate 1ml min^{-1}, isocratic elution with TE pH 8.8, 100mM NaCl, injection volume 100µl, absorbance was monitored at 260nm. A fraction collector (Frac-100, Pharmacia, Uppsalla, Sweden) was used to collect 250 or 330 µl fractions. DNA of various strand lengths, monoclonal antibodies A and B, and a Protein Gel Filtration Standard were injected onto the colmun to determine typical retention times.

2.2.8. Application of depth filters and membranes

At the manufacturing scale sampling in between the depth filters and the terminal 0.2 µm membrane was not possible and a scaled-down model, as detailed in Table 2-1, was designed to asses the operation of the products listed when challenged with representative process materials. The flow rate was scaled down on the basis of constant superficial velocity, and the challenge volume was scaled down on the basis of constant volume per unit area of filter or membrane.

	Process scale			Common to both systems		Scaled down model		
Filter or membrane	**Process volume (litres)**	**Flow rate ($l.h^{-1}$)**	**Filter area (m^2)**	**Superficial velocity ($m\ s^{-1}$)**	**Volume per unit area ($l.m^{-2}$)**	**Process volume (ml)**	**Flow rate ($ml\ min^{-1}$)**	**Filter area (mm^2)**
CUNO Zeta Plus 10SP	**8000**	**3000**	**21.6**	**3.858×10^{-5}**	**370**	**2356**	**14.7**	**6362**
CUNO Zeta Plus 90SP	**8000**	**3000**	**10.8**	**7.716×10^{-5}**	**741**	**931**	**5.8**	**1257**
PALL Posidyne	**8000**	**3000**	**4.74**	**1.758×10^{-4}**	**1688**	**430**	**2.7**	**254**

Table 2-1: Operating parameters employed for the study of adsorption of DNA from process streams. Filter areas are the actual area of the membrane through which process fluid could pass (i.e. after O-ring and housing effects had been taken into account).

2.2.8.1. Preparation of depth filters and membranes

The depth filters were held in Cuno In Line 47mm or 90mm Filter Housings, and flushed with 200 ml or 500 ml water respectively, which was expelled from the connecting tubing and filter housing prior to challenge with test materials. The Sartorius Sartobind Q membranes were flushed with 20 ml blank challenge solution which was expelled from the housing prior to challenge with DNA. The Sartobind Q membrane was supplied in pre-formed capsules which were initially used in this study and later, membranes were cut by a 25mm wad punch from an uncut sheet provided by Sartorius and held in a Millipore 25 mm stainless steel housing. The Cuno Zetapor and Pall Posidyne membranes were housed in a 47 mm Pall stainless steel membrane holder. They were flushed with 50 ml water and a bleed valve was employed to expel the water from the housing and to introduce the challenge solution containing DNA. For determination of DNA breakthrough curves, fractions of an appropriate size were collected downstream of the filter, and their DNA content was assayed using the fluorescent DNA quantification reagent PicoGreen.

2.2.8.2. Challenge materials for depth filters and membranes

Test solutions containing calf thymus DNA were prepared by dissolving 10mM Tris and 1mM EDTA (TE) in water and titrating with HCl until the desired pH values (7.5 or 8.8) were reached. Solutions employed to study the membranes were then 0.2 μm filtered (Pall, Portsmouth, U.K.). NaCl or polysorbate 80 was then added to the required concentration, and the pH value of the resultant solution was confirmed as that desired. At this point a portion of the buffer was reserved for use as a blank or preparation of a DNA standard plot. Calf thymus DNA was added to the remaining solution, a portion of the resultant solution was retained to determine the pre-filter DNA concentration.

At the process scale samples were taken from a 8000 litre production volume at the end of a seven (antibody A) or nine (antibody B) day fed batch fermentation or after the appropriate unit operations in the downstream process and used to challenge the depth filters and membranes as described in the scaled down model.

Cells cultured in shakes flasks were also used to determine the filter-ability of various feed streams by the Cuno Zeta Plus 10SP depth filter.

2.2.9. Viscosity measurement

Cell culture viscosity was determined using a Brookfield (Coventry, U.K.) DV-III programmable rheometer fitted with an ultra-low viscosity adapter.

3. Qualitative analysis of DNA in the initial stages of monoclonal antibody purification

3.1. Overview

The purpose of the work detailed in this chapter was to determine the molecular weight of DNA as it passed from the culture vessel to the ultrafiltration step via the disc stack centrifuge and the depth filters. Such information is crucial for successful development of an assay for DNA because many methods of DNA quantification are sensitive to its molecular weight. Furthermore, the partitioning of DNA and useful product is generally achieved either on the basis of their differential adsorption (to ion exchange or immuno-affinity resins, for example) or on the basis of their molecular weight (in size exclusion chromatography, for example). Since the operation of both these processes depend on the molecular weight of material passing through them, data regarding the size of DNA entering the purification scheme will also be of value in considering optimum methods for separation of contaminant and product.

Preliminary experimental work using antibody A (data not shown) had indicated that clarification of the process stream was coupled to removal of high molecular weight DNA from the process stream and the remaining DNA was of predominantly low molecular weight, possibly having undergone internucleosomal cleavage. Such internucleosomal cleavage is commonly, but not exclusively, associated with apoptosis (Wyllie, 1980) and apoptotic cells have been observed in batch cultures of NS0 cells (Mercille and Massie, 1994). Therefore, cells from the culture vessel were examined for the morphological features of apoptosis and necrosis throughout the fermentation prior to processing of the broth. In this way it was hoped that the origin of DNA in cell culture supernatants could be established. If the origin of DNA could be determined, then the quantity of DNA entering the purification scheme and challenging the depth filters could be determined by events in the fermenter preceding the downstream process. Particle analysis of the material in the early stages of purification was also performed to evaluate the clarification of the process material. It should be noted that samples cannot be withdrawn from the process between the filters because this risks contamination of the culture supernatant and hence product efficacy. For this reason a scaled down model was applied and samples were drawn from the resulting filter effluents. Since the adsorption of solutes was being assessed, the scaled-down flow rate was calculated on the basis of superficial velocity which is commonly applied for scale up of adsorptive chromatographic systems and the challenge volume was calculated on the basis of constant volume per unit area of external surface of filter or membrane.

At the full scale, harvest material was passed through a Westfalia CSA-19 disc stack centrifuge and then Cuno Zeta Plus 10SP and 90SP depth filters, and finally through a 0.2 μm Pall Posidyne membrane cartridge. Depth filters and membranes were prepared according to the manufacturers recommendations. Samples were taken prior to and following centrifugation, from a holding tank following passage through the entire filter train, and subsequent to concentration of the antibody by ultrafiltration. DNA was extracted from each sample and the particulate contents of samples prior to and following centrifugation were determined.

At the laboratory scale depth filters were challenged with output material from the full scale disc-stack centrifuge. The depth filter effluent was used to challenge the 0.2 μm membrane, thereby mimicking conditions at the process scale. Depth filters were held in 90mm or 47mm diameter filter housings, and the 0.22 μm membrane was housed in a 25mm diameter stainless steel membrane holder. Prior to challenge the depth filters and membranes were prepared in the same manner as at the large scale: by flushing through with water and expelling water from the housings with air. Solutions were gently agitated on a magnetic stirrer. Samples were withdrawn from the effluent of each filter for extraction of DNA and particle size analysis was performed on effluent from the 10SP depth filter. Whilst particle analysis of material passing through the final depth filter and microfiltration membrane was not feasible because the Coulter Channelyzer did not respond accurately to particles of less than 2.0 μm in size, the 0.22 μm microfiltration membrane was successfully integrity tested at the end of processing, and this served as confirmation that the material entering the ultrafiltration step is free of particles above 0.22 μm.

3.2. Particle counts

For analysis of particles in cell cultures, material of less than 5 μm in diameter was considered to be debris, consisting of broken cell membranes or intracellular organelles but free of whole cells which generally ranged from 8-20 μm in diameter (Seewoster and Lehmann, 1997). Figure 3-1 shows the particle size distribution of material from the culture vessel consisted of both debris and whole cells, whilst the disc stack centrifuge removed whole cells yielding a process stream consisting of only debris with particles sizes of less than 5 μm. At the process scale, output material from the disc-stack centrifuge challenged the depth filters which effected final clarification of the broth: the remaining particles in the broth were removed after passage through the filtration train consisting of Cuno Zeta Plus 10SP, 90SP and Pall Posidyne 0.22 μm membrane.

Particle analysis of the effluent from the 10SP depth filter indicate that very little material is removed by the 10SP depth filters. The number of particles detected in material entering the disc-

stack centrifuge was $4.9x10^6$ particles ml^{-1} which fell to $6.7x10^4$ particles ml^{-1} in the output of the centrifuge. This figure was reduced to $6.0x10^4$ particles ml^{-1} after passage through the 10SP scaled down depth filter. Although the scaled down model was generated on the basis of adsorption of solutes to the surface of the depth filter (i.e. constant superficial velocity) rather than constant flux or pressure, it appeared that the 10SP depth filter failed to remove large quantities of particles from the process stream and this conclusion was supported by two other observations. First, the pressure drop across the depth filter remained constant at 1.6 psi as process material was pumped through it indicating that there was insignificant capture of particles by the depth filter. Second, the 10SP depth filters were originally used to remove whole cells from challenge materials (pore size range 0.8 to 4.0 μm) a task now performed by the disc-stack centrifuge.

Evidently, there is a duplication of roles in this part of the process. As a consequence of this, the 10SP filters are challenged with particles with a size distribution typical of their own effluent. Thus, the challenge particles pass through it largely unaffected. The failure of this part of the process to operate efficiently results from the incorporation of the disc-stack centrifuge into the process after the 10SP depth filters had been designed and commissioned to receive material directly from the production vessel. The 10SP depth filters were not removed from the process after commissioning of the disc stack centrifuge. These findings were reported to the industrial sponsors with a recommendation to reconsider the configuration of the depth filters applied after the disc-stack centrifuge.

3.3. Cell types present

Healthy viable, viable apoptotic, and cells that had died by the process of apoptosis and necrosis were all observed in the fermenter on every day that suspended material was withdrawn for staining with acridine orange and ethidium bromide (Figure 3-2). In this way, apoptotic cell death in a large-scale culture vessel was confirmed as a major mechanism of cell death in bioreactors. This has been previously observed by many workers studying small scale cultures (Mercille and Massie, 1994; Singh *et al.*, 1994) and has been confirmed here at the large scale. The high number of viable apoptotic cells present, reaching a maximum of 2.4×10^6 cells ml^{-1} on day 7 of the fermentation, and cells that had died by the process of apoptosis implied that DNA should be present in the broth as a result of apoptotic cell death. However, numerous cells that had suffered necrosis were also observed, which has not been cited as a major mechanism of cell death in bio-reactors. The accumulation of cells that died by both processes may be explained, as follows, by the depletion of nutrients and accumulation of metabolic by-products.

Aston University

Content has been removed for copyright reasons

Table 3-1: Concentration of glucose and lactate in pre-feed suspended large scale culture of NS0 cells. This data was provided by Julian Relton and Kevin Cownley at GlaxoWellcome, Beckenham. U.K.

Glucose and lactate levels were monitored throughout the fermentation (Table 3-1). Glucose was found to be absent from the culture vessel in pre-feed samples taken on days 7 and 8 and was relatively low at 0.13 g l^{-1} on day 6 of culture (NS0 cells are generally grown in glucose at a concentration of 2.0 to 5.0 g l^{-1}). When Mercille and Massie (1994) studied the cell death of NS0 cells under various circumstances, they observed that cells grown in culture media formulated without glucose suffered both types of cell death and necrotic cell death dominated the decline in viability during the first 24 hrs of glucose deprivation. Thereafter the dominant mode of cell death was apoptotic until all the cells were dead after 56 hours culture.

The concentration of lactate was determined as between 0.0 and 2.0 g l^{-1} for the first 5 days of culture and rose to 7.6 g l^{-1} by day 9 of culture. When Mercille and Massie manipulated the concentration of lactate in fresh cell culture media by increasing it to 3.1 g l^{-1} the dominant mode of cell death was necrotic. Inspection of Figure 3-2 shows that apoptotic cells increased in number from day 5 onwards reaching a peak on day 7 whereas necrotic cell numbers increased from day 6 onwards, reaching a peak on day 8. In the system studied here it would appear that the decline phase of the culture, defined by the overall reduction in viability was associated with the simultaneous decline in nutrient concentration and increase in concentration of metabolic by products that are known to be associated with elevated levels of both apoptotic and necrotic cell death respectively.

The cause of the depleted glucose levels observed in this fermentation has not been addressed, but the increase in lactate levels is unavoidable because it is concomitant with the constitutive metabolism of eukaryotic cells.

3.4. Molecular weight of DNA

Electrophoretic fractionation of DNA from the culture vessel reveals a high molecular weight DNA component consisting of DNA with more than 12, 216 base pairs and a ladder of lower molecular weight DNA (Figure 3-3). This band of high molecular weight DNA is removed from the process material by passage through the disc stack centrifuge. In combination with data from the particle analysis (Figure 3-1) it is evident that intracellular genomic DNA or high molecular weight DNA associated with debris is being removed from the process stream at this point. There is little apparent further change in the molecular weight distribution of the DNA as process material passes through the filter train. Similar removal of high molecular weight DNA can be achieved by laboratory scale centrifugation of the culture vessel material (5 min at 7,200 g) and it is clear that high molecular weight DNA is entrapped within whole cells and possibly on debris but not freely dissolved in the culture broth, whereas low molecular weight DNA is dissolved in the process broth along with monoclonal antibody. This data clearly demonstrates that clearance of high molecular weight DNA from mAb is achieved by, and coupled, to clarification of the fermented materials.

The depth filters and membranes are positively charged and theoretically capable of removing polyanionic species such as DNA. The results of this study qualitatively demonstrate that low molecular weight DNA persists after passing through the filter train. Further work is required to quantify DNA removal by these units, although the fact that DNA persists in sufficient quantity to allow its purification from the culture supernatant after the filtration step indicates that the depth filters do not provide substantial partitioning of nucleic acid and therapeutic protein. Furthermore, changes in the molecular weight profile of DNA as it passes through the filter train are not evident which provides evidence to suggest that DNA of this size is not removed on the basis of depth filtration. DNA appears to be concentrated with monoclonal antibody in the ultrafiltration step following 0.2 μm microfiltration.

Also of note is the ladder effect observed on the agarose gel. Close inspection of this ladder reveals that each band is a multiple of approximately 180 base pairs. For example, counting from the bottom of the gel the third band is just above the 506 base pair marker which is compatible with the third band being 540 base pairs in size. A similar effect is observed with location of the sixth band located just above the 1018 base pair marker, which is compatible with this band being approximately 1080 base pairs in length. In cell culture studies, the appearance of such DNA within

cells is associated with apoptosis (Wyllie, 1980) although morphological examination of cells is generally employed alongside electrophoretic separation of DNA to confirm apoptosis. By staining cells from the fermenter with a combination of acridine orange and ethidium bromide, viable cells undergoing apoptosis and non-viable cells that had suffered either necrosis or apoptosis were observed (Figure 3-2). DNA from necrotic hybridoma cells has been described as having high molecular weight with a random size distribution but may also produce small quantities of fragmented DNA, presumably because the endogenous nucleases are released into the cell cytoplasm as the integrity of the cell declines when it dies (Franěk *et al.*, 1992). Therefore, DNA passing into the downstream process may have been released from apoptotic cells since the profile of DNA on the gel indicated that internucleosomal cleavage of DNA had occurred. However, for the NS0 myeloma cell line under large scale processing conditions it cannot be discounted that high molecular weight DNA has been released into the broth by necrotic cells and then subjected to internucleosomal cleavage by nucleases from lysed cells, or it is present in such low concentrations that it has not appeared on the agarose gel. Furthermore, it is unclear whether DNA is released by rupture of the dead cell membrane, or in the same way that lactate dehydrogenase is released by leakage from intact non-viable cells (Goergen *et al.*, 1993).

The data presented here indicate that DNA remaining in the final therapeutic preparation could consist of material with as few base pairs as 180. This has two important implications for the safety and determination of residual DNA in biotherapeutics. First, concerns over residual DNA in therapeutic proteins were based on an assumption that the shortest observed oncogene was 1 kilobase long and the risk analysis for injection of oncogenic DNA in final therapeutic protein preparations was based on DNA being at least 1 kilobase long (Pettricianni and Regan, 1986). This data shows qualitatively that residual DNA in therapeutic proteins is likely to contain DNA with fewer than 1 kilobase pairs, and therefore unlikely to contain any active oncogenes. Whilst the WHO have responded to calls for a relaxation of permissible residual DNA levels by allowing the contaminant to be present at concentrations as high as 10ng per dose (Griffiths, 1997), the FDA have not. Data presented here may contribute further to the regulations relating to the safe levels of residual DNA in biotherapeutics: because the majority of DNA appears to be of less than one kilobase, it could be argued that the regulatory authorities should explicitly state the molecular weight of DNA below which they do not consider DNA to be of concern.

Irrespective of further downstream purification, the DNA in crude monoclonal antibody preparations is predominantly less than 1 kilobase pairs in length although DNA of over 6 kilobases was observed when the process supernatant was concentrated following ultrafiltration. The ability of assay procedures to determine DNA of this molecular weight is critical where quantification is required for evaluation of the process to partition DNA from protein. For example, the Threshold Method

exploits two high affinity DNA binding proteins, one of which is an anti-DNA antibody conjugated to urease which is captured on a biotinylated membrane via streptavidin which binds to the second protein: a biotinylated single stranded DNA binding protein. The amount of DNA determined is proportional to the detected urease activity. An assay sensitivity of 10 pg DNA is claimed by the manufacturers (Kung, *et al.*, 1990). The affinity and specificity of the binding proteins make this method preferable for determination of residual DNA in therapeutic proteins over intercalating fluorescent dye assays. However, DNA of <600 base pairs are too short to accommodate both proteins (Kung, *et al.*, 1990). The manufacturers recognise that DNA must be sufficiently long to accommodate both the conjugated antibody and the biotinylated single stranded DNA binding protein and the assay response from DNA of strand length 603 base pairs or less is reduced. Since, in this case, the majority of residual DNA has a strand length of between 1000 and 180 base pairs, the Threshold Method will require careful calibration, without which it may be unsuitable for determination of residual DNA.

McKnabb and Tedesco (1989) have argued that the Threshold Method is ideally suited for determination of DNA in therapeutic proteins because it does not efficiently detect low molecular weight DNA which cannot contain entire oncogenic sequences. Their argument was formulated to address criticisms of the assay when applied to detection of residual DNA in therapeutic proteins at the end of processing, but does not address the need to appraise the ability of unit operations within an entire process to partition DNA from product .

For the reasons detailed above the Threshold Method was not considered further for determination of DNA in the initial stages of monoclonal antibody purification.

In conclusion, for the purposes of this thesis, an accurate method of determining the DNA removal capacity of the depth filters at the process scale is required. Evidently DNA persists in process material after the harvest step, but a mass balance for DNA through this step has not been effected by this work and it is not clear whether or not the filtration train is capable of eliciting a $\log_{10}$ reduction of DNA in the process supernatant. The ideal candidate method for determination of DNA with low molecular weight is an intercalating molecule because this can elicit a signal response from relatively small fragments of DNA. In the next chapter arguments will be presented for the use of an intercalating dye, PicoGreen, to quantify DNA levels throughout the harvest step.

The data presented in this chapter was published in *Biotechnology Letters* in September 1998, (Charlton *et al.*, 1998).

4. Quantification of DNA in mammalian cell cultures

4.1. Overview

This chapter includes the details of work performed to develop an effective assay for DNA in cell cultured materials, and consequently a method for determining the concentration of DNA in material passing through the initial stages of monoclonal antibody purification. In the Methods section it was proposed that one of the most promising candidates for use in determining DNA in solution of unknown composition was PicoGreen, although it had not been tested in the presence of the multitude of ill-defined contaminating species present at the end of fed-batch fermentations. It is to perform such tests that this work has been undertaken and reported here. In the light of information detailed in the preceding chapter relating to the molecular weight of material in the initial stages of monoclonal antibody purification, PicoGreen remains a good candidate because it can detect relatively short strands of DNA: its fluorescent signal is dependant on its intercalation with DNA, which only requires the DNA to consist of a few base pairs. A sketch to summarise the proposed method of DNA intercalation by a fluorochrome is shown in Appendix 2 (Figure 2-1).

The observed fluorescence from any sample will be the sum of numerous factors, and these can be detailed as follows:

- fluorescence emitted from PicoGreen intercalated with DNA,
- fluorescence emitted from unbound PicoGreen (i.e. background),
- fluorescence emitted from PicoGreen intercalated with other nucleic acids (i.e. RNA),
- fluorescence emitted from unspecified sources (protein, media components, etc.),
- reductions in fluorescence caused by unspecified sources.

Experiments were designed to quantify, as far as possible, each of the above. Initially, this involved determining the effect of fresh culture media and purified monoclonal antibodies A, B, and C on the fluorescence of PicoGreen in the presence of calf thymus DNA* and the background levels of fluorescence under these conditions in the presence of PicoGreen only. Spent culture media (containing secreted mAbs, DNA, RNA, and host cell protein) that would be typical of material entering the harvest step was assessed for its ability to interfere with fluorescent emissions from

---

* Calf thymus DNA is commonly applied as a standard in DNA studies concerning DNA quantification. It is readily purchased in highly purified form from a number of suppliers and is usefully applied in this situation because its molecular weight distribution is from 23,000 to 100 base pairs, although it has not undergone internucleosomal cleavage.

DNA. Finally the extent to which the fluorescent response in such samples was attributable to DNA was also addressed. To prepare clarified materials for these experiments Millipore Millex GV 0.2 μm sterilising grade membranes were employed. It is essential to the success of the method that these membranes do not adsorb DNA from solution, and this was checked prior to application of the method. Experimental details are given in Appendix 4.

4.1.1. Generation and presentation of study results

PicoGreen was studied for its ability to quantify DNA in two types of sample. For the first type of sample, cells and/or debris from fed-batch fermentations were lysed by the addition of SDS to a final concentration of 0.2% (w/v) and diluted with TE, pH 8.8, 100 mM NaCl. Hereafter, this type of sample is termed "diluted cell lysate". For the second sample type, cultured cell materials were centrifuged at 7200 g for 5 minutes prior to passage through a Millex GV 0.2 μm microporous membrane. Hereafter, this sample type is termed "clarified culture broth". It is this second type of sample which most closely represents the material that is passing through the initial stages of monoclonal antibody purification.

Spiking experiments were performed on five occasions, whereby samples were supplemented with exogenous nucleic acids (calf thymus DNA or baker's yeast RNA), to elicit the ability of PicoGreen to recover or detect the quantity of extra material added in the presence of potential sources of interference. Calf thymus DNA was added to unused culture broth, purified monoclonal antibodies, clarified culture broth and diluted cell lysate, or clarified culture broth and diluted cell lysate following sequential fractionation by size exclusion HPLC. Results involving such work are described as the percentage spike recovery which is:

$$\text{Percentage Spike Recovery} = \frac{(\text{Spiked sample fluorescence} - \text{Unspiked sample fluorescence}) \times 100}{\text{Fluorescence from calf thymus DNA spike in TE blank}}$$

On a final occasion RNA was spiked into clarified culture broth and diluted cell lysate and subsequently digested with RNase. The results of this work have been described as the percentage reduction in fluorescence of the spike after enzymatic treatment. For the purposes of this work, the reagent has been deemed to have performed satisfactorily if the spike recovery is between 80% and 120%, which is slightly more stringent than anticipated spike recoveries cited by other workers in this field (McKnabb and Tedesco, 1989).

Where experiments have involved fluorescence determination on three or more samples the standard error has been quoted alongside the mean result, or as error bars on plotted data. However, error bars

were often smaller than the points that were used to plot the graphs and for this reason they may not appear to be present on every plot.

4.2. Potential sources of interference

4.2.1. Culture broth

The effect of fresh serum-free culture media on fluorescence was determined by diluting calf thymus DNA in unused culture broth and comparing this to the same series of dilutions performed with TE, pH 7.5. The concentration of DNA in a solution of calf thymus DNA was determined spectrophotometrically as 13.0 μg ml^{-1}. This was diluted with either TE at pH 7.5 or fresh culture media (Figure 4-1) to produce solutions of nominal DNA concentrations ranging from 0.004 μg ml^{-1} to 1.95 μg ml^{-1}, .

Fluorescence of DNA in the presence of PicoGreen was insensitive to the presence of culture media up to a concentration of 40% (v/v) culture broth. Above this point the spike recovery declined such that the 100% stock solution containing culture broth had a spike recovery of 76%. The average spike recovery in the range 0.2% to 40% (v/v) culture broth was 104% ± 4.1. One explanation for the decline in spike recovery at high concentrations of culture broth and DNA is that the PicoGreen has bound to charged species in the culture media that would otherwise allow it to intercalate with DNA. This results in a decline in observed fluorescence at increased culture broth concentrations as the quantity of PicoGreen available for intercalation declines.

The influence of culture broth on background fluorescence was negligible (i.e. baseline fluorescence was not more than double that of TE, pH 7.5) up to a concentration of 10% (v/v) culture broth. Therefore, components in the culture broth which are not consumed by the growth of cells such as pH indicators, surfactants and various ions do not impair or add to the fluorescence of DNA at concentrations of less than 10% (v/v) culture broth in TE, pH 7.5. Henceforth, all experiments involving the determination of fluorescence in samples that contained culture broth were performed only after they had been diluted into the range 0.5% to 10% (v/v).

4.2.2. Monoclonal antibodies

The ability of three monoclonal antibodies to interfere with the fluorescence assay was determined by spiking a constant, known quantity of calf thymus DNA into solutions of various monoclonal antibody concentrations alongside appropriate controls (i.e. monoclonal antibodies without calf thymus DNA) (Figure 4-2). In all cases, the baseline fluorescence of controls were similar to a TE

blank at antibody concentrations of up to 1000 μg ml^{-1}. For antibodies A and C spiked with calf thymus DNA, the recovery of the calf thymus DNA was 101.5% ±1.2 (minimum recovery = 93.2%, maximum recovery = 107.8%) and 101.0% ±1.2 (minimum recovery = 96.2%, maximum recovery = 108.6%) respectively, thereby indicating that the interference from these two antibodies in the determination of DNA by PicoGreen was minimal. However, antibody B reduced fluorescence attributable to DNA to 45.7% of the spiked control at an antibody concentration of 500 μg ml^{-1} . This reduction in fluorescence was largely reversed by increasing the pH of the Tris-HCl buffer to 8.8 and incorporating 100 mM NaCl (mean spike recovery = 94.7% ±1.6). The pI of antibody B is in the range 8.5 to 8.9 (J. M. Relton, *pers. comm.*). Therefore at pH 7.5, electrostatic binding of the negatively charged backbone of DNA to the positively charged surface of the antibody is possible. Such binding of oppositely charged species to DNA is known to cause collapse of the DNA helix because there is no charge repulsion along the poly-phosphate backbone of the DNA. Indeed it is the charge repulsion that maintains the integrity of the DNA structure and one of the effects of such conformational changes is prevention of fluorochromes intercalating with DNA (Wolfert and Seymour, 1996). Therefore, to minimise binding of DNA to proteins in the culture broth, all assays involving material from cell culture sources were performed with TE at pH 8.8 including 100 mM NaCl.

After this point in the experimental procedures material containing monoclonal antibody C was no longer available for study and the rest of this chapter (indeed, the rest of the thesis) concerns itself with materials containing mAbs A or B.

4.3. Linear fluorescence range of cell culture derived samples

Clarified culture broth and diluted cell lysate containing mAbs A and B were diluted with TE, pH 8.8, 100mM NaCl to determine the concentration range where fluorescence was linear. The linear fluorescence ranges for clarified culture broths containing mAbs A and B were 0.5% to 4% v/v and 0.2% to 1.0 % v/v respectively. The fluorescence of diluted cell lysates containing antibodies A and B increased in a linear fashion up to a concentration of 0.5% (v/v). This data was used to indicate the point to which samples had to be diluted for future quantitative development of the method to determine DNA levels in respective samples. Protein concentration was determined on the same samples, (Figure 4-3) in order to enable a comparison with Hoecsht 33258 which suffers interference from protein at a concentration of 100 μg ml^{-1} BSA equivalent. The comparison was made valid by using a BSA as a standard in the experiment. In this example the response of PicoGreen to increasing concentration of culture media remained linear up to a concentration of 300 μg ml^{-1} BSA equivalent protein.

4.4. Spiking calf thymus DNA in unused culture broth

Initial experiments were designed to quantify the impact on fluorescence of culture broth or purified monoclonal antibody. To determine if the fluorescence of the PicoGreen:DNA complex was predictable at culture broth concentrations employed under assay conditions a spiking experiment was performed. The results are shown in Table 4-1. For both antibodies A and B the recovery of the calf thymus DNA spike in both clarified culture broth and diluted cell lysate, was repeatedly close to 100%.

Material and dilution		Protein concentration ($\mu g\ ml^{-1}$)	% DNA spike recovery
Antibody A:			
Clarified culture broth	**1.0%**	44.3	100.5
	3.0%	102.6	99.0
	5.0%	156.3	101.9
Diluted cell lysate	**0.1%**	b.d.	99.3
	0.2%	b.d.	98.2
	0.5%	b.d.	96.1
Antibody B:			
Clarified culture broth	**0.6%**	40.4	98.3
	1.0%	60.5	97.7
	5.0%	199.0	102.3
Diluted cell lysate	**0.1%**	b.d.	105.3
	0.2%	b.d.	100.6
	0.5%	b.d.	96.8

Table 4-1: The effect of spiking calf thymus DNA into culture broth of various concentrations. Solutions were prepared as for Figure 4-3 prior to combining 50 µl of each solution with 50 µl of a calf thymus DNA stock solution. The concentration of DNA in the stock solutions were 660 and 811 ng ml^{-1} for solutions containing antibodies A and B, the difference in these concentrations approximately mimics the difference in protein concentration of the two samples. The concentration of protein was below the limit of detection (b.d.) for diluted cell lysate samples. The fluorescence of the resultant solution was determined and the percentage recovery was calculated by the addition of half the fluorescence above baseline observed in the unspiked sample to that observed when the calf thymus DNA stock was combined with 50 µl TE pH 8.8, 100 mM NaCl.

4.5. HPLC size exclusion chromatography of culture broth and cell lysate

The purpose of HPLC was to separate the nucleic acid component of the culture broth from the protein component, and determine if such partitioning induced significant changes in the total fluorescence recovered downstream of the HPLC column. The HPLC size exclusion separation was

characterised with respect to the retention time of monoclonal antibodies A and B, various nucleic acids, and a combination of proteins. From this data monoclonal antibodies behaved predictably in terms of their elution time from the HPLC column. The results are shown in Figure 4-4. Their retention time across the column was 8.0 mins. Since all other proteins in the supernatant are understood to be of lower molecular weight than the monoclonal antibodies, they would be expected to have a retention time greater than that of the monoclonal antibodies. Following characterisation of the HPLC size exclusion column, DNA of 159 base pairs or greater should elute prior to monoclonal antibodies. Since NS0 DNA in clarified culture broth has strand length of at least 6,000 base pairs to approximately 180 base pairs (see Chapter 3) the system should provide substantial separation of the protein and nucleic acid components of the broth.

Inspection of the chromatograms reveal that fluorescence and proteinaceous materials were largely separated from one another by the HPLC system (Figures 4-5 and 4-7).

By determining fluorescence and assaying for protein prior to injection of materials onto the column and in the fractions collected after size exclusion chromatography, a mass balance was performed for fluorescent components and protein across the column (Figures 4-5 and 4-7). In the case of clarified culture broth containing monoclonal antibody A the mass balance for total protein was 103.6% and by considering fluorescence as the equivalent mass of calf thymus DNA, the mass balance for DNA equivalent fluorescence was 97.2%. In the case of clarified culture broth containing monoclonal antibody B the mass balances were 104.1% and 89.4% for protein and calf thymus DNA equivalent fluorescence respectively. For material containing antibody B there was a slight drop in the observed fluorescence following HPLC and this may be attributable to the fact that fluorescence in some of the collected fractions was above the determined linear range of the calibration plot (see Figure 4-17). Whilst a substantial increase in fluorescence following size exclusion chromatography would have indicated that the protein in the broth, or other factors, were acting to diminish fluorescence prior to separation by size exclusion chromatography, these figures are compatible with negligible interference from protein in the broth.

The absence of interfering species was further confirmed by spiking a known quantity of calf thymus DNA into the sequential HPLC fractions that were shown to contain protein at concentrations as high as 135 and 204 $\mu g\ ml^{-1}$ from broth containing antibodies A and B respectively, the recovery of the spike was quantitative and consistently close to the predicted values (Figures 4-6 and 4-8). Furthermore, the ability of PicoGreen to avoid interference moreso than Hoechst 33258 is further confirmed by this experimental data.

For both antibodies A and B the protein concentration in fractions collected following injection of the diluted cell lysate, was below the limit of detection of the assay and the mass balances were not determined.

Therefore, the data presented thus far demonstrate that interference from fresh culture media and mAbs can be minimised by sample manipulation, indicating that detection of DNA by fluorimetry can be successfully performed under the assay conditions employed without interference from common contaminants. However, the origin of fluorescence in cultured materials has yet to be established, and it is this end that the next section of the work in this chapter concerns itself.

4.6. Origins of fluorescence

One of the most effective ways of validating responses in biological assays is to treat samples with enzymes whose substrate is thought to be the source of the signal. The work described in this chapter, so far, has eliminated fresh culture media, mAbs, and host cell protein as a source of fluorescence or any other type of interference, and there are two prime candidates remaining for the source of fluorescence: RNA (which has been shown to induce fluorescence in the presence of PicoGreen, albeit with reduced specific fluorescence enhancement over DNA, Singer *et al.,* 1997), and obviously, DNA. In the first series of experiments, samples were treated with bovine pancreatic ribonuclease A which cleaves phosphodiester bonds between the ribose groups of nucleotides in the RNA sequence. In doing so RNA is converted to individual nucleotides or very short strands of polynucleotides. In each case this should elicit substantial reduction in the ability of RNA to intercalate any fluorochrome, which will bring about a reduction in any fluorescence associated with RNA. RNase is found in greatest quantities in ruminant pancreas, (hence the bovine source). DNA inhibits RNase A activity and for this reason RNase A was added to relatively high concentrations (50 $\mu g\ ml^{-1}$) in the digestion experiments. In this way, competition for binding sites between DNA and RNA on the surface of the enzyme should be ameliorated.

Deoxyribonulcease I (DNase I) also cleaves phosphodiester bonds in the same way that RNase A does, and the same rational was applied for concomitant reduction in fluorescence brought about by digestion of cultured materials with DNase I.

4.6.1. Treatment of samples with ribonuclease A

The significance of RNA for assay of DNA in the clarified culture broth and diluted cell lysate samples was determined by their incubation with RNase, see Figures 4-9 and 4-10. Incubation of clarified culture broth and diluted cell lysate containing antibody B for one hour at 37 ^{o}C had no

significant impact on fluorescence. This was also found to be the case for clarified culture broth spiked with RNA. A reduction in fluorescence of the diluted cell lysate incorporating an RNA spike was observed, although 81±0.7 % of the RNA spike was recovered. This data indicated that endogenous ribonucleases may have been a factor in this experiment. Nevertheless, after addition of RNase to the culture broth and diluted cell lysate there was a 11% and 16% reduction in fluorescence respectively and the RNA spike was completely digested by the addition of enzyme indicating that RNase was functional in the culture broth. Indeed fluorescence of the enzyme treated, spiked samples fell to less than that of the unspiked samples since the addition of the spike led to a dilution of the DNA in the culture broth. Therefore, any reduction in fluorescence following the addition of RNase was attributable to the presence of RNA. Thus pre-digestion of culture broth and diluted cell lysate samples with a ribonuclease enabled the unambiguous determination of DNA in samples containing RNA.

Results for clarified culture broth and diluted cell lysate containing antibody A were ambiguous, possibly because of the presence of greater quantities of RNA. For example, fluorescence of control samples fell by 9% for the clarified culture broth and increased by 10% for the cell lysate samples, but this data could be ascribed to plate to plate variation within the assay but still satisfies the criteria for sussesful performance of PicoGreen because the data did fall outside the 80% to 120% spike recovery limits. Furthermore, the reduction in fluorescence of material that was spiked with RNA but without enzyme seemed to indicate that endogenous ribonucleases were present, but again, the spike recovery was 81%, just inside the prescibed limits which could mean that PicoGreen has performed satisfactorily. Nevertheless, the fluorescence of the spiked material fell to 91% and 96% of expected values for the clarified culture broth and diluted cell lysate respectively indicating that bovine pancreatic RNase was still functional under these conditions. Since the fluorescence of digests performed without a RNA spike also fell, for accurate quantitation of DNA in the respective samples pre-digestion with RNase is a necessity.

4.6.2. Treatment of culture broth with DNase I

The validity of the DNA assay method using PicoGreen was assessed by enzymatic treatment of samples with deoxyribonuclease 1 (DNase I) which, when performed alongside appropriate controls, unequivocally determines the proportion of the assay response attributable to the presence of DNA. The fluorescence of samples after digestion with DNase I was assessed by comparison with the same samples that were incubated with 10 mM $MgCl_2$ only (DNase I has an absolute requirement for bivalent metal ions, Junowicz and Spencer, 1973).

To gain an insight into the behaviour of a sample of highly purified DNA under the experimental conditions, the response of calf thymus DNA to digestion with DNase I was determined. The results are shown in Figure 4-11. Incubation of calf thymus DNA with only 10 mM $MgCl_2$ did not impact on fluorescence of the sample. Addition of DNase I to the sample reduced fluorescence by 93.1% ± 0.17. The residual fluorescence was likely to originate from a population of short oligonucleotides because DNase I does not systematically digest DNA to single nucleotides (Prunnel *et al.*, 1979) and PicoGreen can intercalate and fluoresce in the presence of short strands of DNA. Reduction of fluorescence of the same magnitude following incubation with DNase I in other samples would indicate that fluorescence originated from DNA.

All cell culture derived samples were incubated with RNase prior to incubation with DNase I. The pH of diluted cell lysate samples was reduced to 7.5 prior to incubation with DNase I by titration with 2M HCl. For clarified culture broth samples the reduction in fluorescence after incubation with DNase I and Mg^{2+} (as compared with samples that were incubated with Mg^{2+} only) was 93.4% ±0.2 and 90.8% ±0.5 for solutions containing mAbs A and B respectively (Figures 4-12, and 4-13). For the same experiments performed with the diluted cell lysate the reduction in fluorescence following incubation with DNase I was 89.4% ±0.4 and 86.5% ±1.0 for solutions containing mAbs A and B respectively. These data indicate that fluorescence above baseline in the clarified culture broth and diluted cell lysate was attributable to the presence of DNA. The reduction in fluorescence of the diluted cell lysate samples was not as great as that for the clarified culture broth and the failure of DNase I to reduce fluorescence to the same extent on these samples may have been due to the presence of SDS in the incubation buffer. Alternatively, because the DNA originated from whole cells: it was likely to be present as chromatin, and DNase I does not act as rapidly or effectively on DNA that is histone bound (Mirsky and Silverman, 1972).

Of note is the extension of the linear fluorescence range (as determined when RNA would have been present in the culture broth, (Figure 4-3) to 5% (v/v) for both clarified cell culture broths after their incubation with RNase. This data is indicative that RNA competes with DNA to intercalate PicoGreen, but since RNA had a lower specific fluorescence enhancement than DNA this manifests itself as a plateau in the fluorescence against concentration of clarified cell culture broth plot.

4.6.3. Treatment of samples with poly-L-lysine

Poly-L-Lysine is known to reduce fluorescence of intercalators in the presence of DNA by binding to the negatively charged poly-phosphate backbone of the molecule (Wolfert and Seymour, 1996). Charge repulsion along the backbone of the molecule is neutralised causing a collapse of the linear molecule. The conformational changes in the DNA molecule result in the exclusion of intercalators

such as PicoGreen hence reducing fluorescence. In a series of experiments to determine the total contribution of nucleic acids to fluorescence without resorting to the use of enzymes, a stock solution of poly-L-lysine was added to calf thymus DNA, clarified culture broth, or diluted cell lysate, and the fluorescence in the presence of PicoGreen was determined prior to and following the addition of the poly-cationic peptide. The results are shown in Figures 4-14 and 4-15 and a comparison of the total effect of incubations with RNase and DNase I against that of treatment with poly-L-lysine is shown in Figure 4-16.

The fluorescence of calf thymus DNA was reduced by 97.8% ±0.03 by the addition of poly-L-lysine. The fluorescence of clarified culture broth containing antibodies A and B was reduced by 92.1% ±0.5 and 94.2% ±0.7 respectively after the addition of ploy-L-lysine. For samples derived from diluted cell lysate, the reduction in fluorescence was 94.5% ±0.4 and 98.0% ±0.9 for material containing antibodies A and B respectively. Therefore, in this experiment, the fluorescent signal behaved in the same way as calf thymus DNA. Whilst enzymatic means are the ultimate method for validation of DNA or RNA quantification methods, this is proposed as a more rapid, simple method by which to determine the validity of fluorescent signals from DNA or nucleic acids in undefined samples prior to embarking on more onerous enzymatic studies. This method may also have a role in the determination of background levels of fluorescence for problematic samples where background levels are unusually high.

4.7. Variability, sample stability and calibration stability

4.7.1. Variability

All fluorescence determinations in this study were performed in triplicate and the data concurred with that of Singer *et al.*,(1997) i.e. signal variation was so small that error bars (equal to the standard error) calculated from triplicate data points of the same sample lay within the symbols used to plot mean fluorescence. Typically, a sample assayed with an average fluorescence of 100 units would have a standard error of 0.4 to 1.0 fluorescence units.

The day to day variability of the assay was evaluated by performing the same experimental procedure 9 times over a period 9 days on a sample of clarified culture broth containing antibody B. The average concentration of DNA was determined as 13.6 μg ml^{-1}. For a 95% tolerance interval and p=0.95 the concentration of DNA was between 10.3 and 16.9 μg ml^{-1}. The coefficient of variance was 0.07. The coefficient of variance for PicoGreen determination of DNA has not been cited elsewhere, but this data compares well with that published regarding the Threshold Method. Kung *et al* (1990) cited coefficient of variances in the range 0.02 to 0.04 for determination of DNA

only, and McKnabb and Tedesco (1989) cited coefficient of variances in the range 0.05 to 0.19 for assay of DNA in various solutions containing mAbs.

The variability of DNA determined on 12 samples on the same day and the same 96 well plate was also evaluated. For a 95% tolerance interval and p=0.95 the concentration of DNA was between 11.1 and 13.0 μg ml^{-1}. The coefficient of variance was 0.02. These two pieces of data taken together mean that to maximise the significance of comparing two or more samples, DNA determinations should be carried out on the same 96 well plate.

4.7.2. Calibration plot

Figure 4-17 shows a typical calibration plot used to quantify the concentration of DNA in unknown samples. The fluorescent response of various DNA concentrations was linear for all concentrations of DNA between 0.32 and 1.29 μg ml^{-1} DNA. Ordinarily this would indicate the fluorescent range that samples must be diluted into for the calibration to be valid. However, data published by the manufacturers (Singer *et al.*, 1997) demonstrated that the fluorescent response to DNA concentration was linear over 4 orders of magnitude and the range was determined by the concentration of PicoGreen in the working solution. The plot could remain linear up to 5 μg ml^{-1} DNA but this exceptional linear range was to the detriment of sensitivity to DNA in the pg ml^{-1} range and greater consumption of the relatively expensive reagent. Therefore, samples were always diluted to 2% (v/v) with TE, pH 8.8, 100 mM NaCl after digestion with RNase A because it was understood that the fluorescent response would be linear in relation to DNA even when the concentration of DNA in the diluted sample was below that of the lowest concentration of DNA. The working solution of PicoGreen was diluted so that the linearity of the fluorescence range would fail above 1.5 μg ml^{-1}. In this way, predetermination of the linear fluorescent range of numerous samples was avoided. The r^2 indicates the likelihood that the plot is attributable to the experimental conditions, and serves as a guide to the accuracy of the work performed. Throughout this work r^2 of greater than 0.98 was typical, which was in close agreement with data published by Singer *et al.* (1997) who regularly observed r^2 between 0.997 and 0.999 for such calibration plots.

4.7.3. Calibration and sample stability

Figure 4-18 shows a plot of the fluorescence from a single DNA concentration (1.0 μg ml^{-1}) used in calibration plots generated over a period of 118 days plotted against the length of time for which the stock solution had been stored and used for production of these calibration plots. This data was collated to ensure that the calibration DNA was stable (DNA can undergo autolysis: Sambrook *et al.* 1989) and that there was no drift in the assay. Only one of the samples deviated by more than 2

standard deviations from the mean, and in a sample of 71 data points this would be expected. From this it was understood that the calibration material was stable and the assay was not undergoing drift.

In a final experiment clarified culture broth containing monoclonal B was filtered through a sterile Millex GV 0.2 μm membrane in a laminar flow hood. A portion of the sterilised material was immediately assayed for DNA whilst a second portion stored at 37 °C for nine days. The concentration of DNA prior to storage was 12.2 ± 0.1 μg ml^{-1} and after incubation it remained apparently unchanged at 12.4 ± 0.1 μg ml^{-1}. This data indicates that DNA in the culture broth does not appear to degrade. Since DNA is released as a result of cell death, the application of an assay for DNA may be an indicator of the cumulative quantity of cell death that had occurred. If the DNA ladder pattern is shown to be exclusively the product of apoptosis, this may also mean that an assay for determination of the cumulative number of apoptotic events may have been developed.

4.8. Summary

Experiments were designed to validate a fluorescence based assay employing PicoGreen, for the quantification of DNA in materials derived from mammalian cell cultures secreting humanised mAbs. The effect on PicoGreen:DNA fluorescence of components in unused culture broth (such as surfactants, pH indicators, salts and nutrients) was negligible: background levels of fluorescence did not increase appreciably when the culture broth concentration was below 10%. The influence of three mAbs on fluorescence was quantified and showed that there was no significant effect on background levels of fluorescence, but one of the mAbs was able to impair the fluorescent signal in the presence of DNA. This interference was avoided by increasing the pH of the assay to 8.8, above the pI of the antibody in question. This information was useful in highlighting a possible source of error in the assay: that positively charged proteins are capable of binding to DNA. Therefore, all future assays were performed at pH 8.8. This is considered to be a general disadvantage in the use of fluorochromes for assay of nucleic acids, but steps can be taken to protect fluorescent signals from interference with cationic substances.

In a series of studies in which calf thymus DNA was added to materials derived from cell cultures, the fluorescent signal of the added DNA was undiminished in clarified culture broth or cell lysate after dilution with TE at pH 8.8 including 100 mM NaCl. This indicates that typical constituents of the culture broth do not impair fluorescent signals generated by samples under such conditions. Furthermore, HPLC separation of the nucleic acid and proteinaceous components of the broth did not have an impact on the total protein or fluorescence recovered following such partitioning thereby indicating that interference from host cell protein was negligible. DNA added to the fractions

containing protein was reproducibly recovered at high yield, further confirming the applicability of the assay for the detection of DNA in the presence of NS0 proteins.

To determine the identity of fluorescence signals in cultured materials, samples were treated with RNase A and DNase I. In this way, it was demonstrated that 97% and 89% of fluorescence from clarified culture broth and cell lysate containing mAb A respectively in the presence of PicoGreen was attributable to either RNA or DNA. The fluorescence of cultured materials containing mAb B, exposed to the same procedures reduced fluorescence by 93% and 89% in clarified culture broth and diluted cell lysate, respectively. Throughout this work, factors have never been observed, other than RNA or DNA, in the cultured materials that fluoresce in the presence of PicoGreen, and the residual fluorescence following incubation with RNase A and DNase I is ascribed to short oligonucleotides that remain after incubations. This is exemplified by the same digestion of calf thymus DNA with DNase I which produced a 93% reduction in fluorescence (i.e. even a sample that is recognised as being free of contaminants has a residual fluorescence above background after DNase I digestion.).

In a final body of work poly-L-lysine, although lacking the specificity of DNase I and Rnase, was shown able to perform the same function as RNase and DNase I together in destroying the fluorescent signal from nucleotides in cell culture derived materials.

The ability of PicoGreen to fluoresce and determine the quantity of DNA in cell culture supernatants containing mAbs and numerous other unidentified proteins or cellular contaminants was demonstrated. Singer *et al.*, (1997) have shown that the specific fluorescent enhancement of PicoGreen in the presence of linear dsDNA is constant and independent of source organism. In addition, Ahn *et al.*, (1996) demonstrated that PicoGreen can bind DNA of 150 base pairs with the same sensitivity and efficiency as larger strands of DNA. The combined data provide explicit evidence endorsing the use of PicoGreen for the unequivocal quantification of DNA in crude mammalian cell cultures. This work will have application in characterisation of the early stages of mAb purification for evaluating DNA adsorption from process streams.

5. ADSORPTION OF DNA BY DEPTH FILTERS AND MEMBRANES

5.1. Overview

In the previous chapter the development of a method that could effectively determine the concentration of DNA in material passing through the initial stages of monoclonal antibody purification was established. The gathering of this data took many months: time during which the physical parameters influencing DNA adsorption to the surface of the depth filters and membranes was also assessed, and their typical capacities for DNA when challenged with purified DNA in buffers of various ionic strength and hydrophobicities. In this way breakthrough curves for DNA have been determined without the complications of competitive adsorption of contaminants that are present following harvest or during processing of the broth. This data is included in this chapter because it consists of useful, interesting and pertinent information relating to the depth filters and membranes. It may also be of use for researchers who are interested in the capture of DNA for the purposes of its purification.

5.2. Membrane housings

The research in this chapter starts with a report on the ability of membrane housings to effect the replication of DNA breakthrough curves. The work was carried out because breakthrough curves for one of the membranes employed in the study could not be replicated and a serendipitous discovery hinted at problems with the housing of the membranes in question. The data that indicated a failure in the reproducibility of this work, and that the membrane housings may be at fault are shown in Appendix 5.

From the data shown in Figure A2-1 it can be seen that the breakthrough curves generated using the Sartobind Q membranes held in the manufacturers' own pre-formed housings were variable for the same set of conditions and the curves themselves did not appear in the format of a conventional breakthrough curve from adsorbents containing ligands with constant affinity for adsorbate which are equally dispersed throughout the matrix. Since these membranes are sold as having constant ligand density and affinity, other explanations for the failure in reproducibility of the breakthrough curves had to be found.

One hypothesis to explain the erratic breakthrough curves was that the challenge material was not being distributed evenly across the membrane surface. To test this theory the Sartorius Sartobind Q membranes were challenged with a negatively charged blue dye (bromophenol blue). Thus, the

distribution of challenge material under the test conditions on the surface of the membrane could be readily visualised. This experimental approach yielded useful information, and was applied to all the membranes and membrane housings that were to be employed in the breakthrough experiments. Experimental parameters and data generated by this work are shown in Appendix 5. It should be stressed that this work can only offer a qualitative description of the distribution of challenge material across the surface of the membrane.

For the 0.2 μm microporous membranes (Pall Posidyne and Cuno Zetapor) that were challenged with bromophenol blue in any of the three housings considered, there was an apparently equal distribution of challenge material across the available surface area of the membrane. Such data would indicate that the breakthrough curves resulting from placing these membranes in any of the housings tested are valid and reproducible. On the basis of this data, the 47 mm Pall membrane housing was used for production of breakthrough curves when purified DNA was employed as a challenge material.

The membranes used for visualisation of fluid dispersal across the Sartobind Q material were cut from a sheet that was provided by Sartorius (Epsom, U.K.). There was insufficient of this material for application of the 47 mm housing in numerous tests. The dispersal of fluid across the surface of the Sartobind Q membrane was shown to be problematic. The dispersal of dye across the Sartobind Q membrane housed in the Millipore 30 mm diameter polyethylene unit was uneven resulting in a large patch of membrane that remained uncoloured. It is likely that such a dispersal of fluid across the membrane would explain the breakthrough curve in Figure A2-2 whereby disturbance of the membrane during the experimental procedure resulted in fluid passing onto an part of unused membrane therefore enhancing the adsorption of challenge material. For the 25 mm stainless steel Millipore membrane housing there was a more even distribution of challenge material across the membrane and this housing was used in the subsequent DNA challenge experiments.

For the Sartobind Q membrane that was challenged with bromophenol blue in the pre-packaged housing as supplied, there was very poor dispersal of dye at flow rates of 6.0 and 50.0 ml min^{-1}. The upper of these values is reported by the manufacturers as the maximum flow rate at which the membrane should be operated. However, it was at 430.0 ml min^{-1} that satisfactory dispersal of fluid was observed (and the effluent material was also largely colourless indicating that dye was still adsorbed from the challenge fluid at this exceptionally high flow rate). This data indicate a significant failure of the pre-assembled membrane housing to distribute fluid evenly across the membrane surface under the recommended operating parameters and on the basis of data generated from these units, no further data was used that had originated from these units. It is interesting to note that other workers have observed sub-optimal flow characteristics at the inlet and outlet of the Sartobind membranes and cited this as the major problem to be addressed to ensure successful

transition of these modules from lab-scale to pilot plant and beyond (Gebauer *et al.*, 1997). Where a failure to scale up was observed the group cited low Peclet numbers and a need to address the configuration of the of the membrane module with respect to the liquid flow distribution.

As a final note on this discussion, sketches are provided (Figure A2-3) showing ideal and non-ideal fluid distribution across the surface of the membrane. In these hypothetical situations fluid is shown as behaving ideally in the membrane housing when it is distributed evenly across the membrane surface and passes through the membrane in equal measure. Non-ideal flow occurs when fluid passes through a portion of the membrane surface resulting in a small part of the total membrane area being handled by challenge solutions.

5.3. Breakthrough curves using calf thymus DNA

5.3.1. Depth filters

Throughout this work DNA has been viewed as a contaminant of the product and consequently its persistence throughout the monoclonal antibody purification process is undesirable. Therefore, for the purposes of this work, breakthrough is taken to mean the point at which the exit concentration of DNA is 10% that of the challenge concentration. This point represents the operational capacity of the filter or membrane, i.e. the operational capacity of the filter is cited as total amount of DNA bound to it at breakthrough per square millimeter of external filter surface area. The equilibrium capacity (100% breakthrough) is usually sought in experimental procedures involving adsorptive processes where useful product is being studied and as such, in this body of work, the equilibrium capacity of the depth filters and membranes with respect to DNA has not been determined. The operational capacity of all the units tested have been summarised in Table 5-1 which is located at the end of this chapter.

Figure 5-1 shows calf thymus DNA breakthrough curves for 47mm Cuno Zeta Plus 10SP depth filters under various conditions of ionic strength and hydrophobicity. For this unit 241.2 μg DNA was bound to the filter at breakthrough, corresponding to a capacity of 0.192 μg DNA mm^{-2} in salt free TE, pH 7.5. DNA binding increased to 433.9 μg (0.345 μg DNA mm^{-2}) in the presence of 50 mM NaCl. Had the depth filter behaved as a true anion exchanger then increasing the ionic strength of the buffer should have reduced the adsorption of DNA because when species are adsorbed by electrostatic interactions there should be competition between similarly charged ions for adsorption to the anion exchange matrix, resulting in progressively reduced capacity for adsobates on the adsorptive surface. The opposite effect was observed at low ionic strength and such data is

compatible with hydrophobic interactions playing a role in adsorption. Indeed, successful adsorption by hydrophobic interaction relies on operating at high salinity, and elution from the hydrophobic surface occurs at low salinity. To determine if the change in capacity for DNA was attributable to hydrophobic interactions between the filter surface and DNA, the influence of adding a non-ionic surfactant (polysorbate 80) to the challenge solutions was examined for the 10SP depth filter. A non-ionic surfactant should be able to impede hydrophobic interactions without affecting ionic interactions, thus if hydrophobic interactions were playing a role in adsorption of DNA, then there should be a reduced capacity for DNA in its presence. It is worth noting that adsorption of DNA to diatomaceous earth, a chief component of the depth filters employed in this study, has been recognised as a method by which to purify nucleic acids, and the adsorptive step exploits high ionic strength (4 M sodium perchlorate) (Koo, *et al.,* 1998). From this it is inferred that DNA is adsorbed to the surface of diatomaceous earth by hydrophobic interactions. Similar effects of DNA binding to other substances via hydrophobic interactions have also been observed specifically between surfactants (Bhattacharya and Mandal, 1997); nitrocellulose membranes (Tsukakoshi and Yamazuki, 1996); and steroidal polyamines (Muller *et al.,* 1997).

The addition of polysorbate 80 to the 50 mM NaCl TE buffer at pH 7.5 brought about a reversal in the quantity of DNA adsorbed when compared to the same solution without 0.1% (v/v) polysorbate 80: the operational capacity of the depth filter was 0.151 μg DNA mm^{-2} compared with 0.345 μg DNA mm^{-2} respectively. This data further supports the theory that at low ionic strength adsorption of DNA to the depth filter surface is promoted by hydrophobic interactions. As a further control, a depth filter was challenged with a salt free TE buffer at pH 7.5 including 0.1% (v/v) polysorbate 80. The operational capacity under these circumstances was 0.144 μg DNA mm^{-2} which is very close to that observed when the depth filter was challenged with 50 mM NaCl in TE buffer at pH 7.5 including 0.1% (v/v) polysorbate 80, possibly indicating that 0.1 % (v/v) polysorbate 80 had impeded hydrophobic interactions to the same extent that 50 mM NaCl had promoted the adsorption of DNA.

In a final series of tests involving 10SP depth filter, TE buffers at pH 7.5 including 100 mM or 150 mM NaCl were used as challenge materials. In both cases the operational capacity fell when compared to the salt free equivalent buffer to 0.126 and 0.097 μg DNA mm^{-2} respectively. This reduction in capacity at elevated concentrations of NaCl is indicative of electrostatic effects playing a role in adsorption of DNA. This is supported by the fact that adsorption of DNA was still observed in the salt free buffer at pH 7.5 that contained 0.1 % (v/v) polysorbate 80 i.e. despite hydrophobic interaction being overcome, some adsorption of DNA was still possible. Furthermore, when a range of depth filters consisting of the same materials as the 10SP depth filter were tested by the manufacturer, reduced adsorption of particles was observed at 140 mM NaCl as compared with the

salt free situation (Hou *et al* 1980). It is interesting to note that had this work been performed at lower salt concentrations, then the researchers may have realised a secondary adsorptive process at work and for many years it has been assumed that the dominant method by which these units adsorb or capture particles is by electrostatic interactions. In this work it has been shown that adsorption of solutes to the surface of the Cuno Zeta Plus 10SP depth filter occurs by both ionic and hydrophobic interactions.

The operational capacity of the Cuno Zeta Plus 90SP depth filter for DNA was shown to be approximately six times that of the 10SP, based on a comparison of the operational capacities of each type of depth filter in salt free TE at pH 7.5. Clearly the components in the 90SP depth filter have changed when compared to that of the 10SP depth filter. The change will have occurred to enable capture of particles smaller than those which the 10SP depth filter would ordinarily capture, and this alteration in the composition of the depth filter has favoured the adsorption of DNA to the surface of depth filter. The capacity for DNA adsorption from salt free TE for the 90SP filter was 1.06 μg DNA mm^{-2}, which increased to 1.84 μg DNA mm^{-2} for TE containing 50 mM NaCl. As with the 10SP depth filter, this was compatible with hydrophobic interactions playing a role in adsorption of DNA. This was further confirmed as the operational capacity fell to 1.53 μg DNA mm^{-2} when 0.1 % (v/v) polysorbate was added to the 50 mM NaCl buffer. However the reversal of enhanced adsorption under these conditions was not as pronounced as for the 10SP depth filter. Without knowing the precise composition of the depth filters it is difficult to speculate the cause of these changes in the observed adsorption of DNA, and this information was not available from the manufacturers. The extent to which hydrophobic interactions were responsible for adsorption of DNA in the salt free conditions at pH 7.5 were quantified by the use of polysorbate in the buffer and the operational capacity of the 90SP depth filter was largely unaffected by its presence indicating that adsorbtion in the absence of salt was largely by ionic interactions.

When Hou *et al.* published data regarding the adsorption of particles from solution, it was shown that the thermosetting resin employed for manufacture of the depth filters became uncharged at elevated pH (generally the efficiency of the depth filters began to decline as pH increased from 6.1, but for viruses, which were the smallest particles employed in the study the removal efficiency did not start to fall until pH 8.0). Therefore, two experiments were conducted at pH 8.8 to determine the role of the resin in adsorption of DNA to the depth filter surface. (Tris-HCl buffers will not buffer effectively above pH 8.8 (Fasman, 1989) so this value was employed to conduct the experiments. Other buffers could have been used but this may have made comparisons with other test conditions invalid.)

When challenged with a salt free TE buffer at pH 8.8 the operational capacity of the 90SP depth filters was drastically reduced from 1.055 μg DNA mm^{-2} at pH 7.5 to 0.214 μg DNA mm^{-2} at pH 8.8 indicating that the charge on the thermosetting resin played a key role in adsorption by electrostatic interactions in salt free conditions. Addition of 0.1 % (v/v) polysorbate 80 to the TE buffer at pH 8.8 had little impact on the operational capacity of the 90SP depth filter as compared with the same conditions in the absence of polysorbate, and this would appear to indicate that either a residual charge exists at this pH or hydrophobic interactions had not been entirely overcome by the presence of polysorbate at 0.1% (v/v). The former is more likely because Hou *et al.* did not observe complete reduction of adsorption for the charged depth filters at pH 9.0.

Therefore, for the 90SP depth filters adsorption of DNA was shown to be chiefly by ionic interactions in salt free conditions, but hydrophobic interactions were promoted by the presence of NaCl. The dramatic reduction in adsorption brought about by elevated pH was likely to be attributable to the thermosetting resin.

5.3.2. Microporous membranes

The adsorption of calf thymus DNA by positively charged 0.2 μm (sterilising grade) membranes under various conditions of ionic strengths and hydrophobicities was also examined (Figures 5-3 and 5-4).

For the Cuno Zetapor membrane the operational capacity of the membrane in salt free TE was 0.051 μg DNA mm^{-2}, representing a smaller capacity for DNA than either of the depth filters studied. When 50 mM NaCl was added to the TE buffer at pH 7.5, the operational capacity of the membrane was 0.083 μg DNA mm^{-2}, and 0.068 μg DNA mm^{-2} for the same TE buffer incorporating 100 mM NaCl. These two data indicate that hydrophobic interactions between the DNA and the membrane surface were promoted by the presence of NaCl at either concentration when compared with the salt free conditions. The hypothesis was tested by the addition of the uncharged detergent to the 50 mM and 100 mM NaCl conditions. In both cases the breakthrough curves shifted to the left indicating that 0.1% (w/v) polysorbate 80 had impeded hydrophobic interactions, resulting in operational capacities of 0.036 and 0.035 μg DNA mm^{-2}, respectively. In contrast to the results generated with the 10SP depth filter, the data generated when 100 mM NaCl was present in the challenge buffer did not differ greatly from that observed when 50 mM saline was present, irrespective of whether or not polysorbate 80 was in the buffer.

The manufacturers of the Zetapor membrane claim that it is largely uncharged at pH 8.8, and the role of charge in the adsorption of DNA in salt free conditions was tested accordingly. The data generated

in this study confirm their claim and corroborate the role of electrostatic effects in adsorption of DNA: the operational capacity of the membrane fell from 0.051 μg DNA mm^{-2} at pH 7.5 to 0.024 μg DNA mm^{-2} at pH 8.8 indicating that the charge on the membrane was playing a role in the adsorption of DNA at pH 7.5. Addition of polysorbate 80 at pH 8.8 reduced the operational capacity of the membrane further still to 0.017 μg DNA mm^{-2} although the profile of the two breakthrough curves performed at this pH were very similar indicating that hydrophobic interactions and electrostatic interactions between the surface of the membrane were not entirely overcome by the buffer components. Nevertheless, for the Zetapor membrane, as for both the depth filters, adsorbtion of DNA was by a combination of hydrophobic and electrostatic effects. A similar test was not performed on the Pall Posidyne membrane because the manufacturers claim it is positively charged up to pH 10 and TE does not buffer effectively at this point. A change in the buffer system may invalidate a comparison between the data sets.

The Pall Posidyne membrane had an operational capacity of 0.318 μg DNA mm^{-2} in salt free TE at pH 7.5 (Figure 5-4). This was over six times the operational capacity of the Cuno Zeta Plus membrane. In fact, under all conditions that the Pall Posidyne membrane was tested for adsorption of calf thymus DNA, it adsorbed more DNA than the Cuno Zeta Plus membrane under the same conditions. This finding led to a recommendation that the industrial sponsors should use the Posidyne membrane where sterilising grade membranes were required in the manufacture of monoclonal antibodies (such membranes are generally located to confer microbiological protection to downstream operations, prior to column chromatography for example).

As for the physio-chemical parameters governing the adsorption of DNA to the surface of the Posidyne membrane, enhanced removal of DNA was again observed (0.409 μg DNA mm^{-2} and >0.515 μg DNA mm^{-2} in TE at pH 7.5 including 50 and 100 mM NaCl, respectively) when compared with an operational capacity of 0.318 μg DNA mm^{-2} under salt free conditions at the same pH. When 0.1 % (w/v) polysorbate 80 was added to the saline buffers, the operational capacity of the membrane was reduced to 0.314 and 0.303 μg DNA mm^{-2} in the presence of 50 mM and 100 mM NaCl respectively.

The breakthrough curves for all the depth filters and sterilising grade membranes tested had extended tails whereby the dimensionless effluent concentration did not rapidly approach 1.0 after the operational capacity of the membrane had been exceeded. This phenomenon has been associated with dual rather than single interactions governing adsorption to adsorbate surfaces, and serves to further confirm the proposal that both electrostatic and hydrophobic interactions were responsible for the adsorption of DNA to the depth filter and membrane surfaces.

An increase in pressure drop across both the Pall Posidyne and Cuno Zetapor membranes was noted as DNA was adsorbed (typically increasing from 0.3 bar at the start of a run and increasing to 2.0 bar at the end of a challenge experiment). Such a response was not observed for any other units in this series of tests. This may be explained by the fact that the charge modifying agent for the Posidyne membrane is typically a high molecular weight polymer such as polethyleneimine, a well documented DNA precipitant (Atkinson and Jack, 1973), which is added to the $nylon_{66}$ dope prior to casting of the membrane (Gsell et al., 1983). The increase in pressure may have been caused by the progressive aggregation of DNA within the pores. If so, this may also explain why the Pall Posidyne membrane had a significantly greater capacity for DNA than the Zetapor membrane, which is charged following a two step chemical derivitisation after casting of the $nylon_{66}$ membrane (Ostreicher *et al.*, 1984). Although the patent published by Ostreicher *et al.* does not explicitly state the reagent which is used to confer charge to the surface of the membrane, the charge modifying agent is "preferably" a small organic group.

5.3.3. Adsorbent membrane

The Sartobind Q membrane was designed specifically as an anion exchange matrix to effect more rapid, adsorption of biomolecules than the equivalent column based ion-exchange matrices in pharmaceutical purification strategies. As such it would be expected to display minimal non-ionic (i.e. hydrophobic) interactions. Its operational capacities were determined in the same way as that for the depth filters and membranes, except the superficial velocity of the challenge material was increased thereby ensuring dispersal of the challenge material across the surface of the membrane as detailed in section 5.2. Breakthrough curves under the various conditions are shown in Table 5-1 and Figure 5-5 respectively. This data suggest that DNA is adsorbed on the basis of electrostatic interactions only, and the membrane achieves its design remit: there was no enhanced adsorption of DNA from solutions containing 100 mM and molar saline which would be expected to promote hydrophobic interactions. For this reason, tests were not performed using polysorbate 80 which had previously been used to confirm the presence of hydrophobic interactions. Because DNA was adsorbed on the basis of electrostatic interaction only, of the units tested here the Sartobind Q membrane was the most suitable for use in purification of DNA.

The profile of the breakthrough curves for the Sartobind Q membrane was unfavourable when challenged with DNA. Breakthrough of a proportion of the challenge material was immediate. For all the conditions used in this test there was no point at which the DNA was completely removed from the challenge solution which is in contrast to the data generated using the depth filters and microporous membranes. Because the effluent concentration of DNA rapidly rose above 10% of the challenge concentration, this indicated that the capacity of the membrane for DNA was not being

used as efficiently as possible. Ligands are used more efficiently if there is a point at which challenge adsorbates are removed completely from solution, and breakthrough thereafter is characterised by a rapid increase in concentration of the adsorbate in the effluent (Arnold et al., 1985). The problem of inefficient use of available ligands could be addressed in one of two ways. First, by expanding the diameter of the membrane surface, with the result that the slope of the breakthrough curve would become more shallow. In fact such an effect was observed when a 47 mm diameter membrane was employed and when the data from this breakthrough curve was compared to that produced for the 25 mm membranes on a per unit area basis, the breakthrough curves were identical indicating the scalability of these units. It also serves to confirm that that the 47 mm housing was distributing the challenge solution across the surface of the membrane efficiently (the 47mm diameter membrane had not been tested with bromophenol blue). Another method by which to make optimal use of the adsorptive potential of the membrane is to stack layers of adsorbent. This has the effect of shifting the breakthrough curves to the right whilst the gradient remains constant. This has the effect of allowing the membranes at the top of the stack to adsorb more DNA before breakthrough is realised at the base (although the membranes at the base of the stack will always behave sub-optimally). The potential for optimising adsorption by membranes has been demonstrated in modelling studies by Suen and Etzel (1992).

In all cases, breakthrough of DNA occurred after less than 0.050 μg DNA mm^{-2} had been challenged to the membrane surface indicating a capacity for DNA similar to that of the Cuno Zetapor membrane. Nevertheless, the Sartobind Q membranes differ from the sterilising grade membranes because they are designed to be regenerated after use rather than to be disposed of and they may be of use in contributing to DNA removal at some point in the mAb purification process. However, they should not be applied in the initial stages of antibody purification for the same reason that a column would not be placed here – the first chromatographic step would ideally capture substantial quantities of product with subsequent steps being designed to remove residual contaminants. Irrespective of challenge DNA concentration, superficial velocity, or available membrane area, the operational capacity and the profile of the breakthrough curves remained constant and whilst this membrane has been applied to the differential adsorption and elution of proteins from blood products with a degree of success, these properties mean that it may also find applications in the manufacture of biopharmaceuticals where DNA rather than protein is the product.

5.4. Challenge of process materials

The optimum configuration of the filtration train for removal of DNA from process supernatant can now be considered using the data generated from the calf thymus DNA challenge experiments. Assuming the depth filters and sterilising grade membrane are exhausted when C/Co = 0.1 and can

adsorb DNA as effectively as determined by this work in the best case scenario (i.e. the conditions under which most DNA was adsorbed from solution), at the 8000 litre process scale the Cuno ZetaPlus 10SP and 90SP depth filters and the Pall Posidyne membrane may adsorb 5.6, 19.9 and 2.3 grams of DNA respectively, a total of 27.8 grams. Assuming the concentration of DNA in 8000 litres of process material is 10 $\mu g\ ml^{-1}$, the total DNA challenge to the filters would be 80 grams of which 34.75% could be removed from useful product. A $\log_{10}$ clearance (generally the minimum clearance required to justify a process validation exercise) across the filtration train would most economically achieved by increasing the area of the 90SP filter from 10.8 m^2 to 36 m^2 at an increased cost of £1756.30 per batch (based on an additional 14 x 1.8m^2 filter cartridges @ £125.45 per cartridge, Cuno, Inc. 1998 Prices). This estimate is based on the removal of calf thymus DNA without any competing species and there must be an assessment of the performance of the depth filters when challenged with process material to verify this model.

The performance of the depth filters and membranes when challenged with process material was assessed in two ways. In the first set of experiments laboratory scale depth filters and a Pall Posidyne 0.2 μm sterilising grade membrane were challenged with a scaled down volume of cell culture supernatant because sampling of process materials in between the depth filters at the manufacturing scale was not feasible (it risked contaminating the preparation of clinical trial material). Flux was scaled on the basis of constant superficial velocity and volume was scaled on the basis of constant challenge volume per unit area. In a second series of experiments DNA was assayed in two sample types at the manufacturing scale: in the total quantity of DNA in the process material (i.e. all the high molecular weight DNA associated with whole cells and debris) or the concentration of DNA in the supernatant of process material was determined in samples prior to entry into the harvest step and at appropriate points in the harvesting step thereafter.

5.4.1. Scaled down model

Breakthrough curves for NS0 DNA from Cuno Zeta Plus 10SP and 90SP depth filters, and a Pall Posidyne membrane, sequentially challenged with clarified harvest material from a 8000 litre cell culture production vessel (Figure 5-6) indicated that these filters were rapidly saturated with DNA. So much so, that pre-manipulation of the challenge material or the configuration of depth filters in the harvest step could not economically result in a $\log_{10}$ reduction of the quantity of DNA in the process material. The permeate aliquots that were assayed always had C/Co >>0.1. One of the reasons that the depth filters were so rapidly overcome with DNA was because the concentration of DNA was much greater in the process material than that in the experimental work using calf thymus DNA. Thus, each unit was exposed to a significantly greater quantity of DNA per unit area than in the tests involving calf thymus DNA. Furthermore, the presence of RNA in cultured materials as

determined in Chapter 4, indicated that DNA had to compete for sites with other species that were capable of ionic or hydrophobic interactions with the surface of the depth filter. It was not surprising therefore to find that the depth filters and membrane in the harvest step could not economically reduce the concentration of DNA in the process material to less than $^{1}/_{10}$ of the challenge concentration. One of the predictions from this data is that the concentration of DNA should not be significantly reduced after passing through the harvest step, and accordingly the in-process samples were assayed for DNA using the fluorescence based method detailed in Chapter 4.

5.4.2. In-process sampling

Sampling and assay of DNA in process material at various points in the production scheme showed unequivocally that the concentration of DNA in this stage of the process was largely unaffected by its movement through the filters and membrane (Figure 5-7). This was true for process streams containing both mAbs A and B tested. Furthermore, DNA was concentrated with monoclonal antibodies in the ultrafiltration step that follows clarification. These observations demonstrate that a $\log_{10}$ clearance of DNA across this part of the purification scheme will not occur. This data resolves one of the research issues detailed in Chapter 1. The quantity of DNA that these depth filters remove at the process scale was unknown. The answer has been found to be effectively none, and accordingly the depth filters must be sized for debris removal. Furthermore, this data indicates that the successful partitioning of DNA and product must be demonstrated at other points in the process. Previously, the removal of DNA from therapeutic proteins has been demonstrated by immuno-affinity chromatography (Jiskoot *et al.*, 1991) and optimised by Tauer *et al.* (1995) and ion-exchange chromatography, and size exclusion chromatography (Ng and Mitra, 1994) and it is these unit operations that should be targeted for DNA clearance across the process.

In previous work it has been shown that removal of high molecular weight DNA from therapeutic protein is achieved through clarification of the culture broth (Chapter 3) and by quantifying the total amount of DNA in process material before and after centrifugation it is clear that for the harvest step, most DNA is removed by partitioning insoluble elements such as cells and debris from the broth in the centrifugation step (Figure 5-8).

The concentration of DNA in fermented material containing mAb A was 6.0 $\mu g\ ml^{-1}$ whereas for that containing mAb B it was in the range 15 to 20 $\mu g\ ml^{-1}$. The major difference in the production of these two antibodies is that cells secreting mAb A are cultivated for 7 days whereas cells secreting mAb B are cultured for 9 days. It is likely that these extra two days in the culture vessel are the reason for the elevated DNA levels and from this it is predicted that the quantity of DNA entering

the downstream process will be a function of the quantity of cell death that has preceded the purification.

Data described in this chapter was accepted for publication in *Bioseparations* in May 1999 (Charlton *et al., in press*).

Filter or Membrane (Area mm^2)	Conditions	Challenge DNA concentration ($ng\ ml^{-1}$)	Superficial velocity ($cm\ s^{-1}$)	Estimated DNA adsorbed when C/Co = 0.1 (μg DNA)	Effective capacity per unit area ($\mu g\ mm^{-2}$)
Cuno Zeta Plus 10SP (1257)	NaCl free, pH 7.5	1007	0.0265	241.2	0.192
	NaCl free, 0.1% Poly 80, pH 7.5	875	0.0265	180.5	0.144
	50mM NaCl, pH 7.5	1004	0.0265	433.9	0.345
	50mM NaCl, 0.1% Poly 80, pH 7.5	1119	0.0265	189.9	0.151
	100mM NaCl, pH 7.5	1064	0.0265	158.5	0.126
	150mM NaCl, pH 7.5	1227	0.0265	122.5	0.097
Cuno Zeta Plus 90SP (1257)	NaCl free, pH 7.5	1754	0.0265	1326	1.055
	NaCl free, pH8.8,	1348	0.0265	269.5	0.214
	NaCl free, 0.1% Poly 80, pH 7.5	1135	0.0265	1365	1.086
	NaCl free pH8.8, 0.1% Poly80	1442	0.0265	397.2	0.316
	50mM NaCl, pH 7.5	1133	0.0265	2315	1.842
	50mM NaCl, 0.1% Poly 80, pH 7.5	1461	0.0265	1923	1.530
Cuno Zetapor (1257)	NaCl free, pH 7.5	1032	0.0265	63.9	0.051
	NaCl free, pH8.8	976	0.0265	30.6	0.024
	NaCl free, 0.1% Poly 80, pH 7.5	944	0.0265	21.0	0.017
	50mM NaCl, pH 7.5	956	0.0265	104.0	0.083
	50mM NaCl, 0.1% Poly 80, pH 7.5	868	0.0265	45.6	0.036
	100mM NaCl, pH 7.5	956	0.0265	85.4	0.068
	100mM NaCl, 0.1% Poly 80, pH 7.5	976	0.0265	44.1	0.035
Pall Posidyne (1257)	NaCl free, pH 7.5	1474	0.0265	399.3	0.318
	50mM NaCl, pH 7.5	1372	0.0265	513.7	0.409
	50mM NaCl, 0.1% Poly 80, pH 7.5	1320	0.0265	428.8	0.341
	100mM NaCl, pH 7.5	716	0.0265	>647	>0.515
	100mM NaCl, 0.1% Poly 80, pH 7.5	1423	0.0265	380.9	0.303
Sartorius Sartobind Q					
(254)	NaCl free, pH 7.5	1176	0.0656	<12.8	<0.050
(254)	NaCl free, pH 7.5	184	0.0656	9.0	0.035
(254)	NaCl free, pH 7.5	981	0.5249	<25.4	<0.100
(1257)	NaCl free, pH 7.5	1302	0.0662	61.0	0.049
(254)	100mM NaCl, pH 7.5	1048	0.0656	<11.4	<0.045
(254)	1M NaCl, pH 7.5	1280	0.0656	<<10.0	<<0.039

Table 5-1: Summary table listing operational capacity of depth filters and membranes for calf thymus DNA in various test streams. The estimated operational capacity is the quantity of DNA adsorbed when the effluent concentration of DNA is 10% (i.e. C/Co=0.1) of the challenge concentration, as outlined in the text, section 5.3.1. Depth filters and membranes were challenged with calf thymus DNA at concentrations as stated in the table with solutions of various ionic strength and hydrphobicities. C is the effluent concentration of DNA and Co is the challenge concentration of DNA. All solutions were buffered with TE at the stated pH.

6. FILTER BLINDING AFTER INDUCTION OF CELL DEATH.

6.1. Overview

In the previous chapter it was clearly demonstrated that the depth filters and membranes employed in the monoclonal antibody harvest step did not adsorb significant quantities of DNA from process material. Since breakthrough of DNA was immediate and at a concentration close to that of the challenge material, an increase in filtration area would not elicit adequate separation of DNA from product. Therefore, the filters should be sized for debris removal. A straightforward filter sizing exercise employing typical process materials is not within the remit of this thesis. The remaining work attempts to address the issue of unpredictable filter blinding. The experimental work in this chapter focuses on the first filter in the filtration train: the Cuno Zeta Plus 10SP depth filter.

With historical pilot plant data (such as antibody concentration and viable or non-viable cell number) giving no insight into the durability of filtration processes, there was no obvious reason to pursue their role in filter life. However, the numbers of apoptotic or necrotic cells had not been determined throughout pilot-scale or large scale fermentations, and their numbers had subsequently been shown to vary considerably in a large-scale, 9 day, fed-batch fermentation (Figure 3-2). For these two reasons, cells that had suffered one of two types of cell death (apoptotic or necrotic), and their live counterparts, were assessed for their ability to affect filter life.

6.2. Filter blinding by healthy viable, non-viable apoptotic or non-viable necrotic cells

The relationship between the physical parameters governing filtration processes is described in Appendix 6. In the first experiment, only the pressure drop generated across a 10SP Cuno Zeta Plus depth filter was measured as a function of filtration time (since the filters were operated under constant flow rate mode, filtration time equates to filtration volume) when challenged with one of predominantly healthy viable cells, non-viable apoptotic cells or non-viable necrotic cells. This initial experiment acted to screen for any population of cells that may have an effect on the durability of the depth filter. The particle size distribution was also determined to see if this had any correlation with filter life. To ensure that the volume (and therefore mass) of particles deposited on the filter per unit volume of fluid was the same for each cell type, experiments were designed as follows.

A total of 1200 ml of suspended cells were grown for 5 days in 12 separate shake flasks. At the end of this time all the suspended cultures were pooled and cell numbers were determined by light and

fluorescent microscopy (Table 6-1). The impact of viable cells on the filtration process was determined by using 400 ml of the pooled cell suspension. Particle size analysis was determined prior to and following a filtration experiment using the 47 mm 10SP depth filter. This generated data to represent the ability of viable cell cultures to foul the depth filter. The remaining cells were split into two cultures and treated with 70 μM etoposide phosphate or 1 % (w/v) sodium azide to induce apoptosis and necrosis respectively. After 48 hours these samples were filtered in the same way that control cells had been. In this way, filters were treated with the same mass of cellular material (assuming cell division ceased after addition of the etoposide phosphate and sodium azide) consisting of either predominantly live and healthy cells or those that suffered chiefly apoptosis, or necrosis. Again, data from light and fluorescent microscopy which was used to establish cell numbers, and the cause of cell death for each experiment are shown in Table 6-1, below.

Culture type	Cell counts by light microscopy (10^6 cells ml^{-1})		Cell counts by fluorescence microscopy (10^6 cells ml^{-1})			
			Live		Dead	
	Live	Dead	Healthy	Apoptotic	Apoptotic	Necrotic
Viable	1.49	0.08	1.18	0.49	0.07	0.01
Apoptotic	0.02	1.09	0.04	0.39	1.08	0.0
Necrotic	0.0	1.02	0.0	0.0	0.0	1.05

Table 6-1: Cell counts by light and fluorescent microscopy of viable, apoptotic or necrotic cultures. 1200 ml of cell suspension were grown in 12 shake flasks for 5 days. At the end of this time all the cell cultures were combined and material was subsequently split into three distinct pools: viable; apoptotic and necrotic cultures. After cell counts had been performed the viable cultures were assessed for their filterability whilst the apoptotic and necrotic cultures were treated with 70 μM etoposide phosphate and 1% (w/v) sodium azide respectively. Cell counts, particles counts and filterability of these cultures was assessed 48 hours later. The time delay was to allow the respective reagents to induce cell death in the vast majority of cells, which generally took this long (see Figure 6-7). For the viable and necrotic cultures, the cells counted by the two separate procedures largely matched one another. For the apoptotic cultures the number of live cells detected by fluorescent microscopy was greater than that observed by erythrosin B exclusion procedures. This discrepancy may be explained by the fact that debris appears dark after staining with erythrosin B, and were excluded from cell counts. However, under fluorescent microscopy appear green and spherical and are scored as viable cells.

The data in Table 6-1 confirm the ability of etoposide phosphate and sodium azide to induce apoptotic and necrotic cell death, as previously reported by Pelliciari *et al.* (1996) and Franěk *et al.* (1992), respectively.

Figure 6-1, shows the particle size analysis of viable, non-viable apoptotic and non-viable necrotic cells grown in shake flasks (the same data is shown in Figures 6-2, 6-3 and 6-4 but in this instance it has been collated with the axis re-formatted to facilitate a comparison of the particle size distribution for each of the cultures). For the purposes of presention, all plots have been generated to show particles of up to 20 μm only (there were negligible numbers of particles greater than this size). The Coulter Channelyzer 256 was incapable of detecting particles below 2 μm. For analysis of the depth filter, the number of particles detected above or below 4 μm are considered, which is the nominal maximum pore size of the 10SP depth filter. The interpretation of this data is that viable cell cultures consist of whole cells and debris, but whole cells are chiefly in the range size 10 to 15 μm. The mean number of particles detected in the size range 2 to 4 μm was $7.68 \pm 0.33 \times 10^6$ ml^{-1} and the mean number of particles detected above 4 μm was $2.99 \pm 0.10 \times 10^6$ ml^{-1}.

For cells that had been killed with 1% (w/v) sodium azide a distinct population of cells was also visible albeit with somewhat reduced size range of 7.5 to 13 μm compared with a typical size range of 10 to 15 μm for the viable cells. Either cell shrinkage had occurred or the cells had fragmented into smaller particles, although the qualitative data from the particle size analysis of this culture would indicate the latter was more likely to be the case. The mean number of particles in the 2 to 4 μm size range was $11.39 \pm 0.31 \times 10^6$ ml^{-1} : significantly greater than the number observed in the viable cultures. This data would indicate that physical degradation of cells occurs following cell death resulting in an increased number of sub-cellular particles in the culture suspension. The mean number of particles above 4 μm was $2.62 \pm 0.04 \times 10^6$ ml^{-1} indicating a marginal decrease in the number of particles in this sub-population as compared with the viable cell culture.

For cells that had suffered apoptosis in the presence of 70 μM etoposide phosphate there was no clearly defined population of cells and the profile of the debris size distribution was strikingly different from that of the non-viable necrotic and viable cell cultures in that there was an increased number of particles in the range 3 to 9.5 μm. Indeed, inspection by microscopy of these materials confirmed the observation that many of the cells that had died by apoptosis were not intact i.e. their membranes had become fragmented and disrupted cells were visible. The mean number of particles in the range 2 to 4 μm was $21.96 \pm 1.85 \times 10^6$ ml^{-1} which was 1.9 times that observed in the necrotic cultures and 2.9 times that observed in the viable culture. Clearly the size and quantity of particulate matter in suspended cell cultures following cell death is related to both their viability and the method by which cells die. The mean number of particles observed above 4 μm was $8.43 \pm 0.11 \times 10^6$ ml^{-1},

again significantly greater than the numbers observed for the other two cell cultures serving to further confirm the population of debris after cell death is related to the manner in which cells die.

Sample	Pre-filter particle counts (2 to 4 μm) (10^6 ml^{-1})	Post-filter particle counts (2 to 4 μm) (10^6 ml^{-1})	Percentage of particles removed
Viable cells	**7.68** ± 0.33	**1.59** ± 0.09	**79.3**
Non-viable apoptotic cells	**21.96** ± 1.85	**2.11** ± 0.27	**90.3**
Non-viable necrotic cells	**11.39** ± 0.31	**0.89** ± 0.05	**92.2**

Table 6-2: Number of particles (10^6 ml^{-1}) with size 2 to 4 μm in each cell culture prior to and following passage through the 10 SP depth filter. The non-viable necrotic cells blinded the depth filter more rapidly than the other samples effectively only 66.7 % of this sample was filtered as compared to the volumes of other cultures that were filtered.

Sample	Pre-filter particle counts (4 to 20 μm) (10^6 ml^{-1})	Post-filter particle counts (4 to 20 μm) (10^6 ml^{-1})	Percentage of particles removed
Viable cells	**2.99** ± 0.10	**0.24** ± 0.03	**92.4**
Non-viable apoptotic cells	**8.43** ± 0.11	**0.17** ± 0.01	**97.9**
Non-viable necrotic cells	**2.62** ± 0.04	**0.19** ± 0.01	**92.9**

Table 6-3: Number of particles (10^6 ml^{-1}) with size 4 to 20 μm in each cell culture prior to and following passage through the 10 SP depth filter. The non-viable necrotic cells blinded the depth filter more rapidly than the other samples effectively only 66.7 % of this sample was filtered as compared to the volumes of other cultures that were filtered.

The particle clearance by the depth filter is shown also in Figures 6-2, 6-3 and 6-4 and summarised below in Tables 6-2 and 6-3. Inspection of the particle count plots indicated that cells and debris from all three of the culture types were effectively removed by the depth filter with little or no apparent breakthrough of particles above 4 μm in the filter effluent. Qualitative analysis largely confirmed this observation: for particles in the 2 to 4 μm range, over 90% were removed from

apoptotic and necrotic cultures and 79.3% from the viable cultures. For larger particles in the range 4 to 20 μm, over 90% of particulate matter was removed in each case considered. This data indicated the ability of the 10SP depth filter to remove a substantial proportion of particulate matter from various types of cell culture and in this respect it was a robust operation. However, this did not take into account the increase in pressure across the depth filter which must be taken into account in order to evaluate the performance of the depth filter when challenged with different process materials.

For the filter blinding experiments, each culture type differed significantly from one another in their ability to foul depth filters (Figure 6-5). The viable cells had the least impact on the depth filter. Cells in this culture were 94.6% viable, according to the erythrosin B dye exclusion test. The mean pressure drop across the depth filter recorded after three experimental runs increased from 1.5 ± 0.09 psi to 2.0 ± 0.15 psi, and this represented a small but significant increase in the pressure drop across the depth filter. For the apoptotic cultures, with viability of only 1.8% there was also a significant increase in the mean pressure drop across the depth filter from 1.5 ± 0.13 psi to 4.2 ± 0.35 psi. Evidently, the ability of the non-viable apoptotic cells for blinding the filter was over twice that of the live cells. The ability of the necrotic culture (with no viable cells at the time of filtration) to blind the depth filter was even greater still, such that the experiments had to be terminated after 3 minutes of filtration (other experiments involving the control and apoptotic cultures had lasted for 4.5 minutes) because the system was operating above its designated safety limit of 20 psi. The average pressure recorded over three blinding experiments after 3 minutes of filtration, using the necrotic culture, increased from 1.5 ± 0.1 psi to 24.7 ± 3.3 psi. This represents an ability of the dead necrotic cells to blind filters at least 15 times more effectively than viable cells and 9 times more effectively than cells that had suffered apoptosis. Such enhanced ability of the necrotic cells to reduce filter life may explain why filter blinding had previously been unpredictable: small changes in the number of necrotic cells from one batch to the next may have had a much greater impact on the filterability of the broth than variations in the number of non-viable apoptotic or viable cells.

Interestingly, the size distribution of the non-viable necrotic cells was very similar to that of the viable cultures, indicating that it was not the size distribution of debris and cells that was critical for predicting filter life in the system studied here. This conjecture was further supported by the fact that the apoptotic cultures had a significantly different particle size distribution from the viable and non-viable necrotic cultures, yet the apoptotic cultures were relatively benign in their ability to impact on the life of the filters as compared with the necrotic cultures.

One of the differences between non-viable necrotic and apoptotic cells that has been established by other workers is the condition of DNA following cell death. Franěk *et al.* (1992) showed that DNA

from cells that had been treated with 1% (w/v) sodium azide contained significantly more high molecular weight than cells which had died via the process of apoptosis. They did not consider the condition of DNA in the supernatant of the cell culture, i.e. DNA which had been released from the dying cells. It is proposed that the difference in the DNA released by the dead cells has an impact on the life of the subsequent filter used to remove cells from the culture broth. Therefore, an experiment was performed to determine the molecular weight of DNA in the supernatant of the culture broth from the three different cell types used in the initial filter blinding experiment. This experiment was embellished further by establishing the quantity of DNA released from each culture type and its ability to persist in the broth after its release. In this way the condition of DNA in the cell culture supernatant could be assessed for its ability to predict the durability of the depth filter.

6.3. Quantitative and qualitative analysis of DNA from dead cells

DNA released into the supernatant of the three types of cell culture (viable, non-viable apoptotic, and non-viable necrotic) was separated electrophoretically to establish its molecular weight distribution, and also analysed quantitatively using the PicoGreen assay.

6.3.1. Molecular weight of DNA

Figure 6-6 shows that DNA in the supernatants of both the viable and non-viable apoptotic cultures was very similar. The DNA content of both these samples was dominated by the oligonucleosomal fragments that have been reported previously by other workers who extracted intracellular DNA from the cells grown in bioreactors (Franěk *et al.*, 1992; Murray *et al.*, 1996). It was also similar to that observed in material taken from the large scale process, as detailed in Chapter 3. However, the DNA from the supernatant of the non-viable apoptotic cultures appeared to have a small quantity of material with molecular weight of around 506 to 1636 base pairs that was not present in the supernatant of viable cultures.

The principal difference between the DNA in the supernatant of the necrotic cultures and that of DNA in the supernatant of the non-viable apoptotic and viable cultures was the trace of high molecular weight material from 500 base pairs to >> 12,000 base pairs. Thus, DNA released into the supernatant from the cells that were exposed to 1 % (w/v) sodium azide had not suffered internucleosomal cleavage to the same extent as that from apoptotic cells. This data is compatible with that of Franěk *et al.* (1992) who reported that the intracellular DNA from cells cultured under such conditions was predominantly of high molecular weight. The DNA from the supernatant of the cells that had suffered necrosis also contained oligonulceosomal fragments but these stained less intensely than those observed in the non-viable apoptotic and viable cultures indicating that

apoptosis may not have been so prevalent in these cultures. Indeed, apoptotic cells had been observed in the fluorescent microscopy counts prior to the induction of necrotic cell death (Figure 6-7), and background levels of apoptosis were constantly present in all the NS0 cell cultures. This has also been reported by Murray *et al.,* (1996) who recognised that there was a constant turnover of apoptotic cells in NS0 cultures.

The similarity of DNA in the supernatant of viable cells and non-viable apoptotic cultures and the similarity of their filtration process in conjunction with the striking difference in the condition of the DNA from the supernatant of the non-viable necrotic cultures and its filtration profile, indicated that the condition of DNA in the process supernatant may be of importance in determining the longevity of the subsequent filter which used for clarification of the process stream. The difference in the molecular weight of DNA in the supernatant of the non-viable necrotic cultures as compared with the non-viable apoptotic or viable cultures may have been sufficiently large to aid in the formation of a mesh or grid of molecules over the pores of the filter, which could convert the depth filter from one operating by depth filtration to a surface straining mechanism.

There was no gross difference in the appearance of DNA on the gel between days 7 and 14 of culture for any of the experimental conditions, although there appeared to be a slight decrease in the quantity of DNA with between 1,636 and 506 base pairs in the supernatant of the non-viable apoptotic cells over the time period considered. In Chapter 4 it was shown that the concentration of DNA in sterile supernatants of mammalian cell cultures did not decrease when incubated at 37 $^{\circ}$C for prolonged periods. These two pieces of data taken together indicated that DNA released into the cell culture supernatant was not degraded extensively by nucleases in the cell culture media, and that its release leaves a permanent, possibly quantifiable record or footprint in the cell culture broth. This data confirmed the potential for using the condition or quantity of DNA in the culture broth as a marker for filter durability, and to evaluate this possibility, the quantity of DNA released from untreated, and etoposide phosphate or sodium azide treated cell cultures was determined.

6.3.2. Quantity of DNA released from dying cells

6.3.2.1. Experimental approach

The experimental procedures for this research were designed to establish the quantity of DNA released into the cell culture supernatant from necrotic and apoptotic cells. Variation in the quantity of DNA released from each cell type was also considered because in order for a predictive marker to be of benefit there must be a distinct, reproducible difference in the quantity of DNA released from the non-viable apoptotic, non-viable necrotic cells and viable cells. The release of DNA from the

viable cultures was also monitored to establish the quantity of DNA released as a natural consequence of cell death in healthy cultures.

Sample and Run Nº	C_{max} (10^6 cells ml^{-1})	Concentration of DNA at C_{max} (μg ml^{-1})	Max. concentration of DNA (μg ml^{-1})	DNA per dead cell (pg $cell^{-1}$)
Apoptosis 1	**0.60**	**0.56**	**7.00**	**10.73**
Apoptosis 2	**0.38**	**0.80**	**5.03**	**11.14**
Apoptosis 3	**0.34**	**1.07**	**5.35**	**12.60**
AVERAGE				**11.5±0.6**
Necrosis 1	**0.66**	**0.55**	**5.43**	**7.39**
Necrosis 2	**0.30**	**0.81**	**5.83**	**16.72**
Necrosis 3	**0.30**	**0.78**	**2.94**	**7.20**
AVERAGE				**10.4±3.1**

Table 6-4: Quantity of DNA released into cell culture supernatant from cell cultures. C_{max} is the maximum number of viable cells observed during the cell culture using the erythrosin B dye exclusion viability test. The quantity of DNA observed in the cell culture supernatant at C_{max} was subtracted from the maximum quantity of DNA observed in the cell culture. This figure was employed to determine the quantity of DNA released from the viable cell population. Raw data from which these figures were drawn is shown in Figures 6-7 to 6-10.

To provide material for use in evaluation of DNA and filtration blinding experiments following cell death, NS0 cells secreting monoclonal antibody A were grown in 250 ml shake flasks containing 100 ml culture volume. All cell cultures were grown in serum-free media and treated in one of three ways. Viable cultures consisted of cells that were grown without exogenous manipulations. Apoptotic cell cultures were produced by growing cells under the same experimental conditions as the viable cultures but with the addition of etoposide phosphate to a final concentration of 70 μM 44 hours after sub-culture of the cells. In this way the culture was dominated by healthy cells at the time of cell death and avoided complications from DNA released by cells that had died by necrosis. In the same manner, necrotic cell cultures were produced by inducing cell death with 1% (w/v) sodium azide (Franěk, 1992) after 44 hours of culture and DNA released by apoptotic cells was minimised. In the latter two cases cell death was induced after cells had been withdrawn for cell counting purposes. To gain an insight into the variability of the quantity of DNA released by the

dying cells three shake flasks containing each type of culture were prepared, and each of these was termed Run 1, 2, and 3 respectively. Cell suspensions were removed from each culture on days 0, 1, 2, 3, 4, 7, 10 and 14 for cell counting by light and U/V microscopy. This data is displayed in Figures 6-7 to 6-10, but various pertinent values have been drawn from this body of data. Quantitative analysis of DNA in the cell culture supernatant was performed on each of the samples that were withdrawn on the days stated above. Table 6-4 shows summary data from the experimental work using shake flasks to culture NS0 cells and quantities of DNA released from dying cells after control, apoptotic and necrotic cell death.

The control cells released an average of 5.9 ± 0.7 pg DNA per dead cell. Since these cells died without chemical manipulation it is assumed that cells dying in fermenters would release approximately the same quantity of DNA. A concentration of DNA of 20 $\mu g\ ml^{-1}$ would then correspond to the death of 3.4×10^6 cells ml^{-1}. Since a population of NS0 cells can exceed this number, and such concentrations of DNA in the fermenter have been observed, this estimate has some corroborating evidence. Data from the U/V microscopy cell counts indicated that the dominant mode of cell death in the control cultures was apoptosis, and consequently it is also assumed that the majority of DNA present in the cell culture supernatant was derived from apoptotic cell death.

The quantities of DNA released from cells that died by apoptosis and necrosis were higher than those observed in the viable, or control cultures. The quantity of DNA in the cell culture supernatant of the apoptotic and necrotic cultures was 11.5 ± 0.6 and 10.3 ± 3 pg DNA per dead cell, respectively. This data may indicate that the apoptotic cells die via a different apoptotic pathway from those cells which died in the control culture. The concentration of etoposide phosphate can elicit various apoptotic pathways, and it is possible that the quantity of DNA released by apoptotic cells is related to the biochemical pathway that is employed to instigate and pursue cell death.

From inspection of the plots in Figure 6-10, it can be seen that DNA from the apoptotic culture is released most rapidly, reaching its maximum concentration two days after induction of cell death. The concentration of DNA in cell culture supernatant from necrotic cells appeared to reach their maximum 5 days after the addition of azide. Once these values reached their maxima there was little or no reduction in the measured concentration of DNA which further confirms that DNA is not degraded in the culture broth supernatant. Whilst this is of interest, the fact that cells which suffered necrosis or apoptosis released quantities of DNA that were quantitatively indistinguishable indicates that quantitative DNA analysis of cell culture supernatants will not indicate the longevity of subsequent depth filters.

A final set of experiments were performed to establish whether DNA released from necrotic cells was the cause of premature filter blinding whereby necrotic cell cultures were treated with DNase I: if the DNA in the culture supernatant was affecting the filterability of cells, then the removal of DNA should extend the life of a filter when compared to one that was challenged with a similar, but DNase I free solution. Indeed, Mercille and Massie (1994) have shown extension of tangential flow membrane life in a harvest step of NS0 cells secreting monoclonal antibody by treating the suspended culture with DNase I. They envisage that DNA is an aid to the blinding mechanism, but targeted apoptotic cells as the culprits rather than necrotic cells. The feasibility of employing benzonase to perform this role was also evaluated. Benzonase is applied in industrial situations because it is cheaper and has fewer regulatory implications than DNase I. It also acts on RNA as well as DNA so, arguably, the role of RNA in filtration processes was also assessed by performing this work.

Also to complete the unknowns in the equation detailed in Appendix 6, the viscosity of relevant solutions was determined, since high concentrations of DNA in solution may significantly affect their rheology.

6.4. Filter blinding following enzymatic treatment of cell cultures

Sample	Viscosity (cP)	Concentration of DNA ($\mu g\ ml^{-1}$)	r v (m) x 10^6	Pressure drop across 10SP depth filter (psi)
Viable cells	**1.04**	**1.20**	**1.5**	**1.4** ± 0.2
Non-viable necrotic cells	**1.06**	**6.80**	**27.0**	**26.4** ± 7.4
Non-viable necrotic cells, treated with DNase I	**1.00**	**0.39**	**8.4**	**7.8** ± 3.8
Non-viable necrotic cells, treated with benzonase	**1.01**	**0.29**	**7.0**	**6.5** ± 1.0

Table 6-5: Viscosities, pressure drop and **r** *v (as detailed in Appendix 6) after 3.0 minutes of filtration, and corresponding DNA concentration of various suspended GS-NS0 cell cultures . The viable cell number was 1.155 x 10^6 cells ml^{-1}. Necrotic cells were produced by treating a portion of this culture with 1% (w/v) sodium azide. For the enzyme treated cultures, DNase I or benzonase was added to a concentration of 20 units ml^{-1} after adding 1M MgCl to a final concentration of 10 mM.*

Figure 6-11 shows the effect of the addition of two different nucleases to the culture media on the filterability of the cultured cells, and this data along with that presented in Table 6.5 was used to calculate a value for **r** v, as detailed in Appendix 6. The effect of material derived from non-viable

necrotic cells being able to induce a significantly greater pressure drop across the depth filter when compared to a similar mass of viable cells was shown to be reproducible.

Digestion of cell culture broths with DNase I or benzonase brought about a reduction in the viscosity of the necrotic cell culture from 1.06 cP to 1.00 and 1.01 cP, respectively. From inspection of the equation describing filtration processes it is implicit that there should be a proportional decrease in the pressure drop generated across the depth filtration by challenge of these materials when all other parameters remain unchanged. The pressure drop of the enzyme treated cultures, after 3 minutes, was significantly lower than that which would be indicated by the decrease in viscosity observed here, when compared to the untreated cultures. Using the experimental data to calculate a value for $\mathbf{r}_v$, the resistance due to filtration of the various solutions was decreased after incubation with the nucleases (Table 6-5). Since there are no other parameters in the equation that have not been accounted for, the increase in filterability of this material indicates that removal of DNA from the broth has a significant impact on the durability of the depth filter that is subsequnetly used to clarify the process material which is not ordinarily described by the equations governing the process. Therefore, the addition and incubation of either DNase I or benzonase to suspended NS0 cell cultures which had suffered necrosis significantly reduced the ability of these cultures to foul the depth filter, and this change was brought about by a change in the constitution of the culture broth.

Since DNase I cleaves phophodiester bonds on DNA only whereas benzonase will hydrolyse phophodiester bonds on both DNA and RNA, this experiment established that the use of benzonase and concomitant destruction of RNA in the cell culture led to no significant extension of depth filter life. Therefore, this work showed the importance of DNA in culture broth for the longevity of a depth filter employed to remove cells and debris from solution. Furthermore, it can be concluded that the high impact that high molecular weight DNA has on the durability of the depth filter be a greater effect than that produced by low molcular weight DNA.

7. DISCUSSION

The research scenario was defined by two issues. First the ability of two depth filters and a terminal sterilising grade membrane, all of which carried a positive charge under typical processing conditions, to adsorb DNA from process material was unknown. Second, the inability of the filter train to reproducibly clarify mammalian cell culture broth from batch to batch manifested itself in premature filter blinding. This resulted in either the loss of large quantities of fermented materials and hence useful product, or a time penalty which was incurred whilst a new set of filters were fitted.

These two issues meant that optimum process validation strategies could not be developed and there was a risk of losing a considerable portion of each fermented batch which is undesirable in itself, but also indicates a lack of batch to batch consistency which can prevent the granting of a licence to market pharmaceutical preparations.

The initial work in this thesis was executed to develop a valid assay for DNA in mammalian cell culture. Since DNA is a polymer, and various procedures for its assay generally respond differently to the size of the polymer, it was necessary to evaluate the size of DNA passing through the monoclonal antibody harvest step. This was achieved by electrophoretic separation of DNA in agarose which generates qualitative data. DNA in the process stream was shown to be predominately low molecular weight whilst high molecular weight DNA, probably intact genomic, was substantially cleared from the broth after passage through a disc stack centrifuge. The profile of the molecular weight distribution of DNA appeared to be unaffected by its passage through the depth filters and a sterilising grade membrane, possibly indicating that its was not removed from the process stream by depth filtration. A small amount of DNA with molecular weight of up to 6000 base pairs was detected after concentration of the culture broth by ultrafiltration. The DNA from cell culture supernatant showed the characteristic pattern of internucleosomal cleavage of chromatin when fractionated by electrophoresis but the presence of both necrotic and apoptotic cells throughout the fermentation meant that the mechanism of origin of the fragmented DNA could not be unequivocally determined.

The incidence of apoptotic and necrotic cells appeared to correlate loosely with the quantities of glucose and lactate which became respectively depleted and accumulated during the decline phase of the culture. Such phenomena have previously been reported by Mercille and Massie (1994).

On the basis of the data generated in this large-scale study, an assay for DNA was developed using a fluorochrome, namely PicoGreen, which was able to generate fluorescent signals from low

molecular weight materials without, reportedly, incurring interference from other biomolecules (Singer, 1997; Ahn *et al.* 1996).

The validity of the DNA assay was assured by extensive work which assessed the impact of numerous pertinent substances on PicoGreen induced fluorescence of DNA including, fresh culture media, monoclonal antibodies, host cell protein, culture broth and RNA. As a result of this work, samples derived from mammalian cell culture containing unquantified contaminants and high levels of monoclonal antibody could be assayed for DNA following digestion with RNase A and appropriate dilutions with TE at pH 8.8 including 100 mM NaCl. Singer *et al.* (1997) have shown that the specific fluorescent enhancement of PicoGreen in the presence of linear dsDNA is constant and independent of source organism whilst Ahn *et al.* (1996) demonstrated that PicoGreen can bind DNA of 150 base pairs with the same sensitivity and efficiency as larger strands of DNA. Experimental procedures in this thesis demonstrate that PicoGreen can be used to quantify DNA in the presence of protein concentrations that previously had been prohibitive for fluorochromes (Cesarone *et al.*, 1979). The combined data provide explicit evidence endorsing the use of PicoGreen for the unequivocal quantification of DNA in crude mammalian cell cultures.

Armed with such an assay for DNA in mammalian cell cultures, characterisation of the depth filters employed in the monoclonal antibody harvest step became a possibility. Considerable time was also spent in assessing the performance of the filters for DNA adsorption in various test streams. This data showed that the positively charged depth filters and membranes were indeed capable of DNA adsorption. Buffers which reduced or neutralised the depth filter or membrane charge, and those that impeded hydrophobic interactions were shown to affect their capacity, demonstrating that DNA was adsorbed by a combination of electrostatic and hydrophobic interactions. The adsorption profile of DNA by an anion exchange membrane showed immediate breakthrough, irrespective of challenge DNA concentration or flow rate, and in this case adsorption was by electrostatic interactions only.

Removal of DNA from harvest broths at the production scale containing therapeutic protein by partitioning of cells and debris from by centrifugation reduced the total quantity of DNA in the process material from 79.8 $\mu g\ ml^{-1}$ to 9.3 $\mu g\ ml^{-1}$ which confirmed the qualitative findings that substantial removal of high molecular weight DNA occurred in the centrifugation step. The concentration of DNA in the supernatant of subsequent of pre- and post-filtration samples had only marginally reduced DNA content: from 6.3 to 6.0 $\mu g\ ml^{-1}$ respectively. DNA was concentrated to 27.3 $\mu g\ ml^{-1}$ along with monoclonal antibody in the subsequent ultrafiltration step. This data applied to monoclonal antibody A and similar effects were observed for four other batches of monoclonal antibody B.

In this way, one of the research goals were achieved, the filters should be sized for debris removal only, because of their inability to partition DNA and product at the process scale.

Historical data, such as viable and non-viable cell numbers or product titre, from pilot plant and production scale fermentations gave no insight into the durability of depth filters. However, fluorescence based microscopy which had been applied for detection and quantification of viable, viable apoptotic, non-viable apoptotic and non-viable necrotic cells had not been applied to fermentations when unpredictable filter blinding had been an issue. Therefore, experiments were conducted to evaluate the impact of such NS0 cell types on the first depth filter in the depth filtration train. Culture broths containing necrotic cells were shown to dramatically reduce the ability of this depth filter to capture cells because the pressure drop across the depth filter was significantly greater than that produced by challenging with apoptotic or viable cultures. Particle size distribution of these cultures gave little or no insight into the durability of the depth filter even though a significant difference in the profile of debris and cells from each culture was observed. Previous workers had shown that the condition of DNA in necrotic cells to be predominantly high molecular weight (Franěk *et al.,* 1992), which constitutes a significant difference in the condition of DNA from viable or non-viable apoptotic cultures. The DNA released in the supernatant of the cultures studied here was also assessed and found to be compatible with data produced by Franěk *et al.* Hence, the importance of DNA in blinding of depth filters was confirmed by treatment of culture broth with DNase I. Such treatment was able to elicit greater than a ten fold reduction in the measured quantity of DNA in the culture broth. Whilst this had a small impact in reducing the viscosity of the culture broth (by 6.0%), the pressure drop brought about by the enzyme treated cells was reduced by 70.4% as compared with the untreated necrotic cultures. Benzonase, which is much cheaper than DNase I, can be applied to bio-therapeutics to elicit substantial removal of both DNA and RNA without invoking major regulatory hurdles, was also assessed to perform the same role and was found to largely reproduce the effects of DNase I application. However, assaying for DNA in culture broth to predict filter life was shown to be unfeasible because the quantity of DNA released from apoptotic and necrotic cell cultures was similar in quantity which is in contrast to their impact on the durability of the depth filter studied. Therefore, DNA is implicated in the blinding of depth filters but its molecular weight appears to have a more important role to play than the quantity of DNA released into the cell culture supernatant.

7.1. Recommendations for future work

Research is an ongoing process and this thesis would be incomplete without making recommendations for the direction of future work resulting from the findings or omissions of the experiments described herein. Suggestions for future work can be conveniently divided into those

that directly relate to the scientific discoveries of the work described herein or that have general implications for bioprocessing; and those specifically relating to the process employed by the industrial sponsors of this project.

7.1.1. Future evaluations (general aspects)

One issue that has repeatedly occurred throughout this work is the lack of knowledge regarding the structure and mode of action of PicoGreen. Since the manufacturers have elected not to share structural knowledge of this molecule with the scientific community at large it is difficult to make further insights resulting from the investigative procedures cited here. However, there are two areas where further work might be performed. First, a definition of the minimum number of base pairs that will elicit a linear fluorescent response would be extremely useful for future development work using this chemical. Second, it was proposed in chapter 4 that the effect of increasing pH in the presence of a high pI antibody resulted in loss of overall charge on the surface of the antibody which meant that it failed to bind DNA. An alternative explanation could be that conformational changes in the antibody result in its failure to bind DNA and hence the return of the fluorescent signal at elevated pH. Therefore, the role that surface charge plays in the DNA/antibody interaction could be investigated further by performing experiments a low pH, when the polyphosphate backbone of DNA becomes protonated. This should give valuable information regarding the necessity of DNA to maintain a negatively charged polyphosphate backbone to ensure the emission of a fluorescent signal from intercalators such as PicoGreen.

The low pH work described above could also be applied to the adsorption of DNA by the membranes and depth filters studied and, as such may result in a clearer understanding of the mode of DNA adsorption. Clearly, it has been argued here that a mixed mode type of interaction is taking place between DNA and the surface of the depth filters and membranes. By causing DNA to become uncharged at low pH, electrostatic interactions effects are effectively removed and purely hydrophobic interactions, if they are truly taking place, may be observed by introducing a second factor that might minimise hydrophobic effects. This work could be expanded further by observing the presence of a chaotrophic agent such as ethanol, ethylene glycol or polysorbate, all of which will absolve hydrophobic interactions. Alternatively, high concentrations of a chaotrophic salt such as thio-cyanate that can simultaneously eliminate electrostatic and hydrophobic interactions could be used to provide further insights into the mode of adsorption by the filters and membranes studied here (Roper and Lightfoot, 1995).

There is much more scope for further developmental work regarding the depth filters and membranes. One question that should be asked is: how valid is it to produce scale down models on

the basis of chromatographic parameters rather than on the basis of filtration theory? For example, the scale down model described in section 2.2.8 was based on maintaining constant superficial velocity and constant challenge volume per unit area. If filtration theory were applied to generate the model when operating under constant flow rate, the same parameters would be applied to generate a scaled down model. However, if the system operated under constant pressure the model would be less valid because there would be variations in the superficial velocity through the filter and the challenge volume could not be controlled. Since the system studied here was largely operated under constant flow, the application of chromatographic techniques is co-incidentally appropriate, but future work could appraise the impact on adsorption of operating under various operating parameters of pressure and flow rate.

Another aspect of the work that demands greater scrutiny is the extent to which the depth filters and membranes truly act as anion exchangers. There may be some benefit in examining the ability of each of the units tested to adsorb purely negatively charged species (chloride ions, for example). Such an experiment would provide a foundation for the theory that each of the units tested is truly capable of anion exchange. Similar experiments might also be performed where the adsorption of a hydrophobic species is examined.

The work involving the application of bromophenol blue to determine the distribution of fluid over the surface of the adsorbent membranes was valuable for identifying the performance of membrane housings. This work could be expanded further by monitoring the breakthrough of a low molecular weight solvent such as acetone. Acetone is commonly applied for determination of height equivalent theoretical plates (or HETPs as they are more commonly referred to) because it is readily miscible with water; is of low molecular weight and therefore high diffusivity; and it has a strong UV adsorbance. Therefore, passing a bolus of acetone through a chromatographic system can give useful information regarding the axial diffusion, mixing and displacement of fluid within that system.

Finally, the data generated for many of the membranes could be applied to determine coefficients such as their dynamic capacity (Q_{max}), and ratio of adsorption to desorption (K_m or k_1/k_2). Such data is useful because it can open new avenues of exploration in terms of scaling up; prediction of the impact of competing species and their selective elution; and the cost and scheduling of a processing option. Indeed, it is recognised that the discovery of such coefficients enables more accurate prediction of the performance of chromatographic materials, including membranes, at the large scale (Suen and Etzel, 1992; Thommes and Kula, 1995).

7.1.2. Future work related to the bioprocessing of mAbs

With regard to the bioprocess itself, there is clear evidence here that the condition of material in the upstream fermentation can have a major impact on the operation of the downstream process, although this was shown using shake flasks and a scaled down filtration model. Future work could be approached by using a scaled down model of the fermentation using an alternative necroticide to sodium azide, ammonia or lactate for example, which would indicate whether or not the impact that necrotic cells have on depth filters is reproducible under more realistic simulations of the process. If this is found to be the case, then the incidence of necrotic cells must be minimised to ensure filterability of process broths. Identification of necrotic agents that naturally accumulate in the broth and their on-line measurement, would also aid in predicting filter life in downstream operations.

As for DNA removal from the therapeutic protein, other parts of the process must be identified that are able to partition DNA and product. The most likely candidates for this are the Protein A affinity chromatography step and ion exchange chromatography on SP-Sepharose, as these steps have already been identified by other researchers as being able to elicit such separations (Jiskoot, *et al.*, 1989; Ng and Mitra, 1994). Should these two steps elicit insufficient partitioning of DNA and product, then additional steps may need to be introduced to the process.

One type of chromatographic separation that could be usefully applied is a membrane ion-exchanger that can bind DNA. This would enable more rapid separations than conventional column chromatographic separations, with the benefit that the system could readily cope with a wide range of DNA molecular weights because diffusion of the adsorbate to the ligands is not a limiting step and is not the cause of restrictions in the flow rate at which these units work. The problem of unfavourable breakthrough curves reported herein would have to be addressed: this might be achieved by stacking the membranes.

With specific reference to monoclonal antibody B, the high pI of this antibody may make it harder to elicit adequate DNA clearance across the process because it may remain bound to DNA unless a high pH chromatographic step is introduced which should separate the protein and nucleic acid.

This work has not precisely identified the charged ligands, or other substances that bind DNA. As demand for the purification of DNA for pharmaceutical applications increases, there will be a demand for knowledge of substances that will effectively bind to DNA. Future work might readily involve successful methods for capture and elution of DNA from membrane surfaces by

identification of useful ligands. One such ligand might be based on the properties of PicoGreen which was shown by this work to be extremely effective for DNA binding whilst apparently having minimal interactions with other biological substances.

The redundancy of the filtration train for DNA removal, and the duplication of roles by the disc stack centrifuge and first depth filter in the filtration train has been clearly identified. This means that alternative methods for configuration and capture of product can be considered. Two methods are immediately apparent. First the use of expanded beds which allow the adsorption of proteins in feed-stocks containing particulate matter. This technique has been identified as having the potential to eliminate centrifugation, filtration and concentration steps from the purification strategy (Chase, 1994), and successful incorporation of this into a process could also confer significant time saving advantages to the manufacturers. Second, the filtration train and ultrafiltration units could be replaced by a single ultrafiltration unit that is capable of partitioning the solid and liquid phases of the feed-stream. However, ultrafiltration has already been shown to be sensitive to DNA in process materials (Mercille and Massie, 1994). A membrane should be selected that does not interact with DNA: Mercille and Massie used a polycarbonate based membrane and advances in membrane technology may now mean that regenerated cellulose or polyether sulphone could be more usefully applied to avoid interactions that cause fouling of ultrafiltration processes. Successful development of ultrafiltration in this part of the process this could confer significant time and cost saving advantages to the manufacturers. A small feasibility study for application of either of these alternative purification routes could be usefully performed. The data gathered here would indicate that the best system to operate would be one that is immune to the condition of DNA in the process material and this issue should be addressed by laboratory work. In fact, there may be a justification for determining the effect of adding high molecular weight DNA to a small scale harvest system to find if it can elicit the problems highlighted by this work. This information could be applied to the feasibility study and would inform on the benefit of minimising necrotic cell death other than those benefits accrued purely by reducing the rate of cell death in bioreactors.

Whilst the research issues outlined in the introduction of this text have been resolved, an alternative harvest step has inadvertently been developed. By treating the culture broth with benzonase prior to filtration, the concentration of DNA was reduced from 6.8 to 0.29 $\mu g\ ml^{-1}$ which is greater than a log_{10} reduction, the minimum reduction often demanded in industrial settings to justify a process validation exercise. This treatment also extended the life of the first depth filter in the filter train. Therefore this step, with some optimisation and further evaluation, may be applicable to the large scale manufacture of monoclonal antibodies because it could offer substantial removal of DNA whilst significantly reducing the risk of unpredictable filter blinding. It also has the added advantage of not incurring major changes to the architecture of the industrial process which has already been

built and commissioned. This is in contrast to the alternative suggestions of evaluating the use of ultrafiltration or expanded beds for a harvest step. The most favourable of each could be established by a feasibility study which would have to consider the change in costs incurred in the downstream process. This might involve the extra cost incurred to guarantee the removal of benzonase from monoclonal antibody.

As a final note, the effectiveness of depth filters which do not carry a charge could also be assessed for their ability to clarify various process streams. This is suggested because the charged depth filters may posses curtailed durability as a result of being positively charged. Removal of this charge may make the depth filters less susceptible to the impact of high molecular weight DNA, hence extending their durability in the presence of debris. Such depth filters are commercially available and typically contain cellulose only, hence diatomaceous earth is not employed in their manufacture, and binding of DNA should be minimal. Furthermore, as bio-pharmaceutical manufacturing begins to embrace the purification of plasmid DNA for application in gene therapies, the value of filters which do not adsorb DNA, and hence maximise product recovery, will gather importance.

8. APPENDICES

8.1. Appendix 1: Monoclonal antibodies employed in this study

The initial stages of mAb purification were studied using three different humanised antibodies. All were type IgG1, secreted by GS-NS0 cells with molecular weight of 155 KDa. The technique for generation of such cells was pioneered by Bebbington *et al.* (1992). For the purposes of this work, these three glycoproteins have been termed monoclonal antibody A, B and C. Information relating to these antibodies was personally communicated by Dr. Julian Relton.

Monoclonal antibody A

Monoclonal antibody A binds to antigen which is present at high levels on the surface of a large number of carcinomas. Evidently, there are numerous potential applications for such an antibody. However, given the difficulty with which mAbs permeate tumours, such antibodies are not intended for use in direct confrontation of carcinoma. They are for use in post-operative settings to prevent the growth of metastases from single disrupted carcinoma cells.

Monoclonal antibody B

Monoclonal antibody B recognises an antigenic determinant on the macrophage cell surface. The rational for treatment with this antibody is to block the release of inflammatory reagents from macrophages, reducing the progression of rheumatiod arthritis, and its concomitant inflammation and pain.

Monoclonal antibody C

Monoclonal antibody C (recognises an antigenic determinant on the T-cell surface). The antigenic determinant plays a role in the interaction between antigen-presenting cells and T-cells. By blocking this interaction between T-cells and antigen presenting cells, auto-immune diseases may be regulated. One of the most common auto-immune diseases is RA whereby cartilage and bone is progressively destroyed. Accordingly, mAb C has been devised as a therapeutic agent in this disease.

Material containing monoclonal antibody C was used during the early developmental work for this thesis but its development as a product stopped following the generation of data from Phase II Clinical Trials. Consequently, data relating to this mAb appears briefly in Chapter 4 only.

8.2. Appendix 2: The structure of DNA

The structure of DNA has been extensively characterised over the past 45 years. This intriguing biological polymer consists of two complementary polymeric chains twisted about each other to form a right handed double helix* . Each chain is a polynucleotide whereby each nucleotide is bound to subsequent nucleotides via a phosphate group bound to the deoxyribose component of each nucleotide. The phosphate groups are negatively charged at physiological pH, and do not protonate until pH is decreased to pH 2 or 3. The five carbon sugar is always bound to the phosphate group by the same carbon atoms (3' and 5' by a phosphodiester linkage) and consequently the sugar phosphate backbone of DNA is very regular, and easily defined. This is in extreme contrast to the series of purines (double ringed groups, adenine – A, and guanine – G) and pyrimidines (single ringed groups, cytosine – C, and thymine –T) which extend perpendicular to the axis of the helix from carbon 1' of the deoxyribose by a glycosidic bond. The order of the bases is often unique to each polymer and *in vivo* this sequence defines the structure of proteins, gene control mechanisms or may, enigmatically, have no apparent role whatsoever to play in an organisms life.

At the centre of the helix the relatively water insoluble bases always hydrogen bond with the same complementary base (A with T, and C with G) thereby binding the two polynulceotides together and simultaneously ensuring that one chain is complementary to the other. The two glycosidic bonds attached to each base pair do not lie precisely opposite one another, resulting in the helix having a major and minor groove. The chemical groups forming the floor of these grooves are predominantly oxygen and nitrogen, but the floor of the major groove is defined by base pair sequence moreso than that of the minor groove making it a target for sequence specific hydrogen bonding proteins. Thus, the polyphosphate backbone of DNA and the nature of bases in the grooves of the helix enable numerous types of interactions with other molecules, and this is discussed further in terms of fluorescent enhancement of DNA intercalaters in section 1.7.4, and DNA adsorption in section 5.3.

The mode of fluorochrome intercalation is extensively discussed in chapter 4. The sketch below is included to embellish these descriptions. Precise data regarding the structure and mechanism of PicoGreen / DNA interaction has not been published, therefore the sketch is based on models of bisintercalators (i.e. having two chromophores linked by a single arm) such as TOTO and YOYO which generally have greater affinity for DNA than monointercalators such as ethidium bromide (Galzer, and Rye, 1992).

---

* This discussion is confined to the B form of DNA which is most commonly encountered in physiological circumstances. A-DNA, whilst maintaining a right handed helix is a shorter, more squat molecule when compared with B-DNA of the same number of base pairs, and is formed when relatively little water is available to interact with the helix. Z-DNA has a left handed helix and is formed by methylation of cytosine residues often within regions of high d(CG) repeats. For greater detail on the structure of DNA see Watson *et al.* (1987) or Lewin (1997).

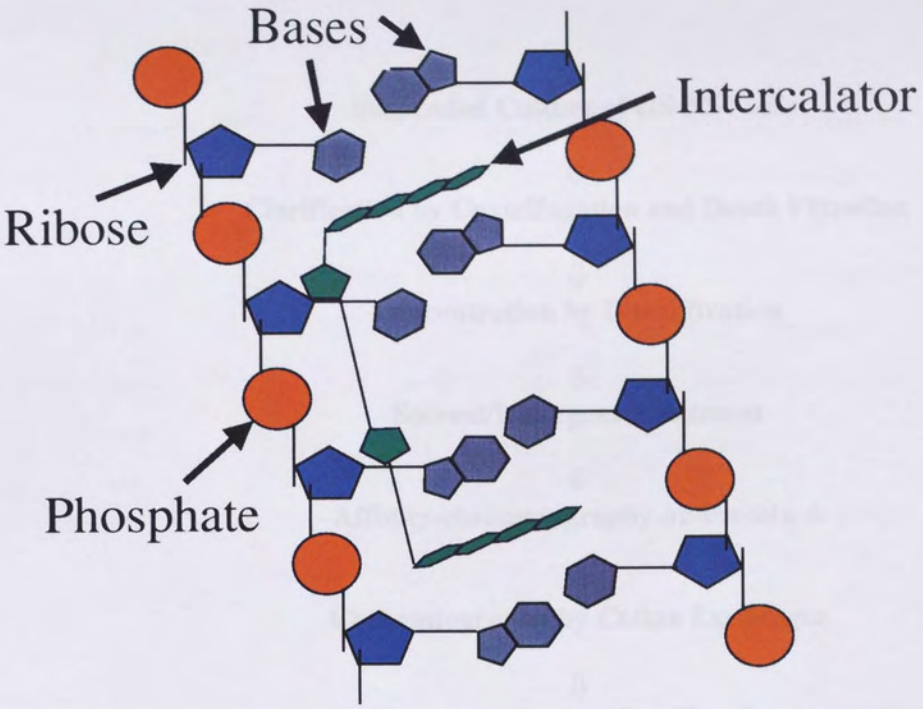

Figure A2-1: Sketch to represent the intercalation of a bisintercalator within double stranded DNA.

8.3. Appendix 3: Schematic of monoclonal antibody purification.

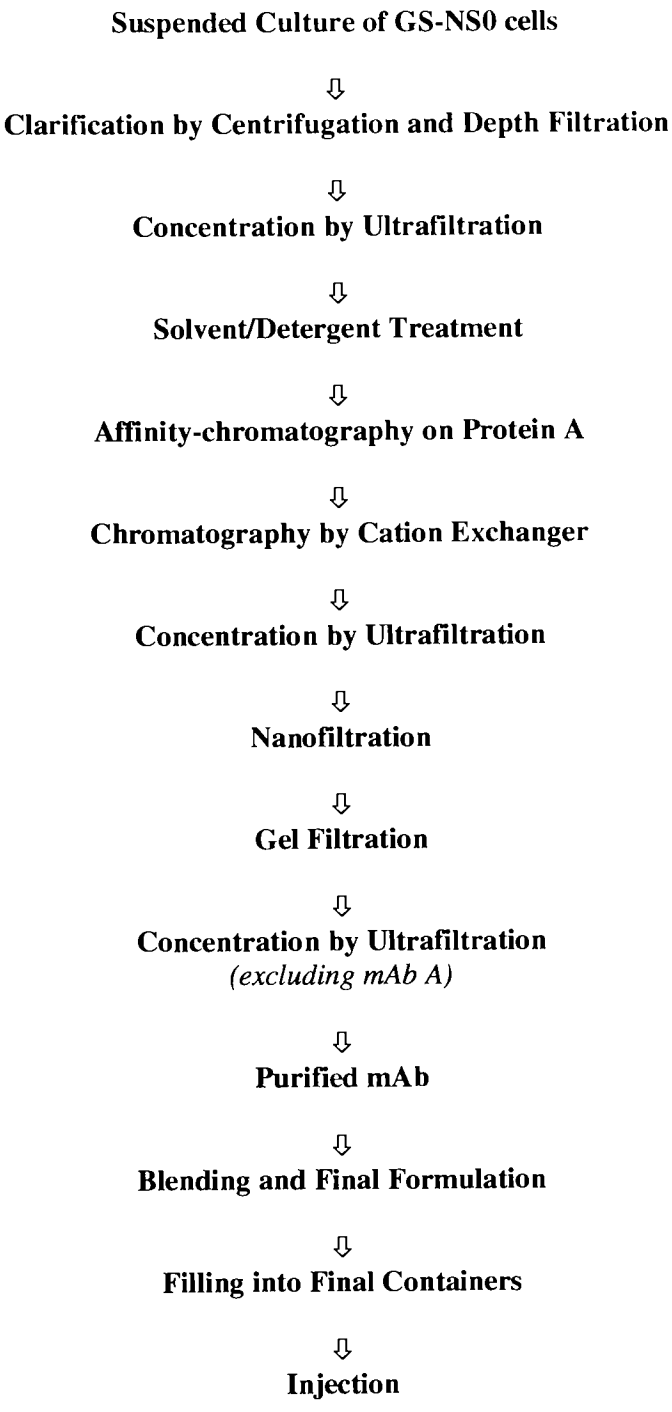

Figure A3-1: Schematic of the generic mAb process employed by industrial sponsors. This figure was reproduced with the permission of Julian Relton.

8.4. Appendix 4: Validation of Millex GV sterilising grade membranes for use in preparation of DNA assay samples.

To ensure that the Millex GV 0.2 μm membrane did not adsorb DNA which would invalidate its application for preparation of samples prior to DNA assay, two solutions of calf thymus DNA were prepared at concentrations of approximately 5 μg ml^{-1} and 500 ng ml^{-1}. Samples were assayed for their DNA content using PicoGreen prior to and following passage of 5 ml of each sample through a 4 cm^2 Millex GV 0.2 μm membrane, the same membrane that was intended for use in the determination of DNA in samples derived from mammalian cell cultures. The results are shown in the table below.

Concentration of DNA (μg ml^{-1})		
Pre-filtration	**Post-filtration**	**% Recovery**
5.73 ± 0.02	5.82 ±0.026	101.7
0.692 ± 0.026	0.698 ± 0.030	99.5

Table A-1: Quantity and recovery of DNA in solutions employed to challenge a Millex GV 0.2 μm membrane.

This data indicates that DNA is recovered quantitatively in each case. This data indicate that the Millex GV membrane can be employed for preparation of samples prior to assay for DNA.

8.5. Appendix 5: Distribution of fluid across membranes in various membrane housings

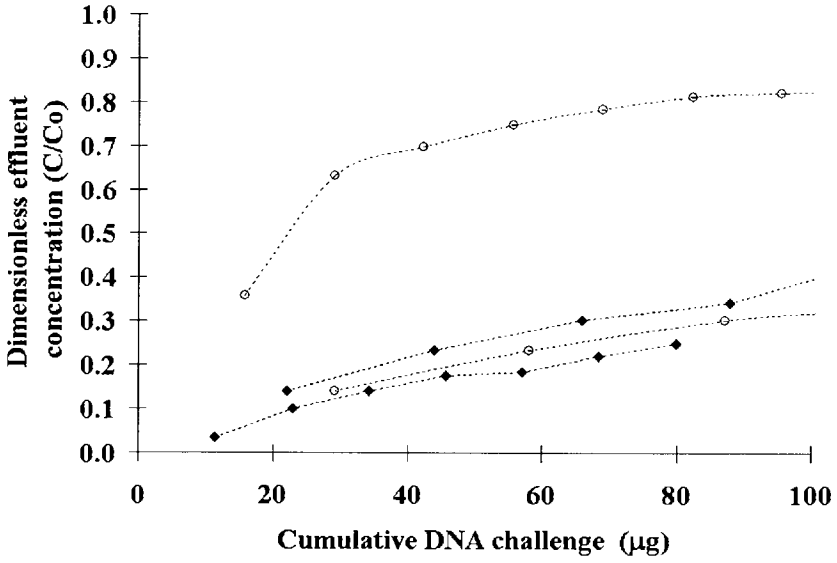

Figure A5-1: Breakthrough curves for Sartorius Sartobind Q membrane held in the capsule provided by the manufacturer. Fractions were collected and assayed for DNA using PicoGreen. Black diamonds, calf thymus DNA in 100 mM NaCl, TE at pH 7.5; open circles, calf thymus DNA in salt free TE at pH 7.5. In all cases the concentration of challenge DNA was approximately 1.0 μg ml^{-1}.

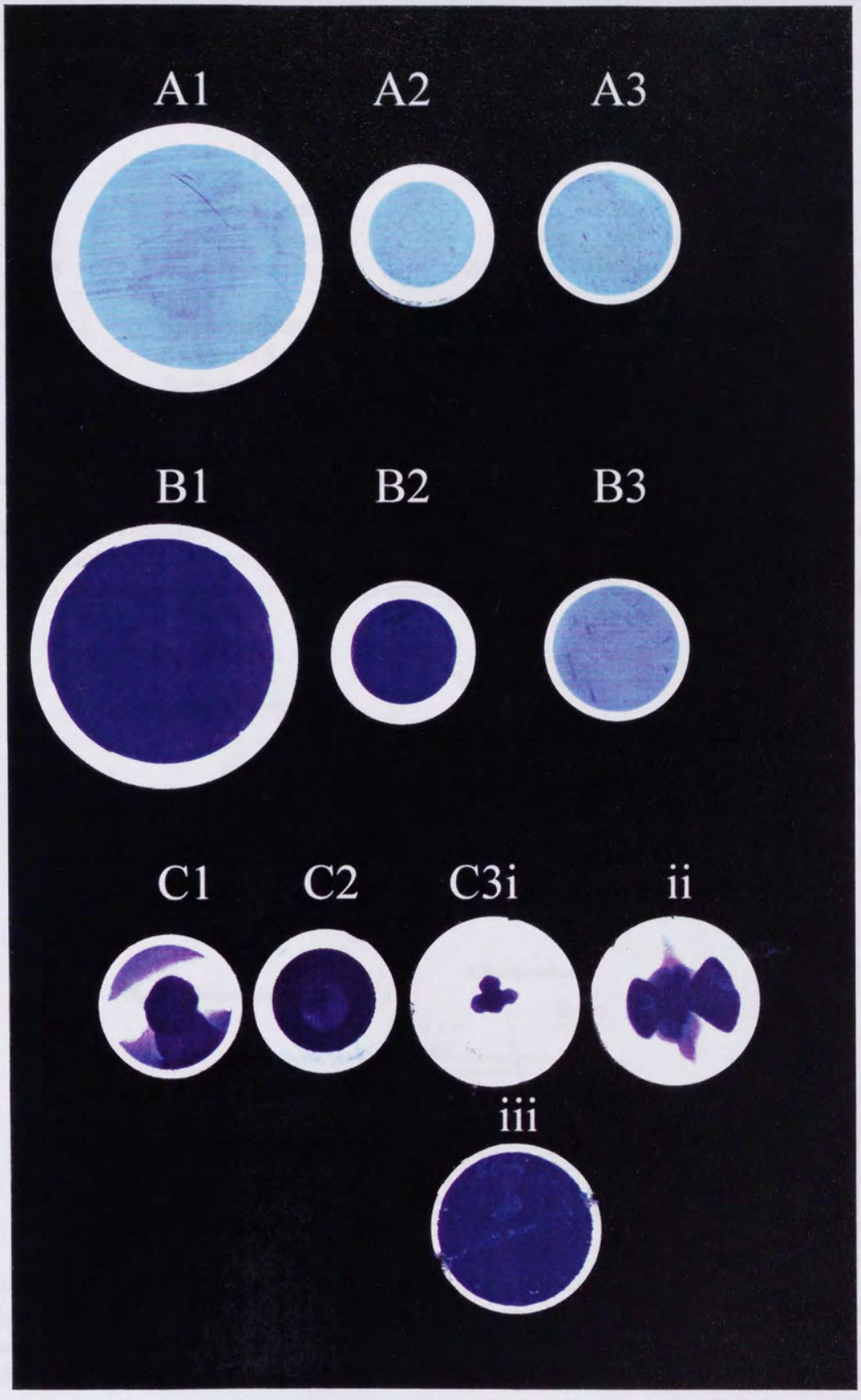

Figure A5-2: Pall Posidyne (A), Cuno Zetapor (B) and Sartorius Sartobind Q (C) membranes were held in various housings and challenged with bromophenol blue at a concentration of 10 μg ml^{-1} as detailed in Table A2-1, below.

Photographic reference	Membrane	Housing manufacturer, material, and diameter (mm)	Flow rate (ml min^{-1})
A1	Pall Posidyne	Pall, SS316, (47mm)	21.0
A2	Pall Posidyne	Millipore, SS316, (25mm)	5.8
A3	Pall Posidyne	Millipore, Polyethylene, (30mm)	6.5
B1	Cuno Zetapor	Pall, SS316, (47mm)	21.0
B2	Cuno Zetapor	Millipore, SS316, (25mm)	5.8
B3	Cuno Zetapor	Millipore, Polyethylene, (30mm)	6.0
C1	Sartorius Sartobind Q	Millipore, Polyethylene,(30mm)	6.5
C2	Sartorius Sartobind Q	Millipore, SS316, (25mm)	6.0
C3I	Sartorius Sartobind Q	Sartorius pre-formed capsule, (30mm)	6.0
C3ii	Sartorius Sartobind Q	Sartorius pre-formed capsule, (30mm)	50.0
C3iii	Sartorius Sartobind Q	Sartorius pre-formed capsule, (30mm)	430.0

Table A2-1: Details of membranes, membranes housings and flow rates for challenge with bromophemol blue to reveal flow distribution patterns across the membrane surfaces at various flow rates. No increase in pressure drop was observed for any of the parameters employed.

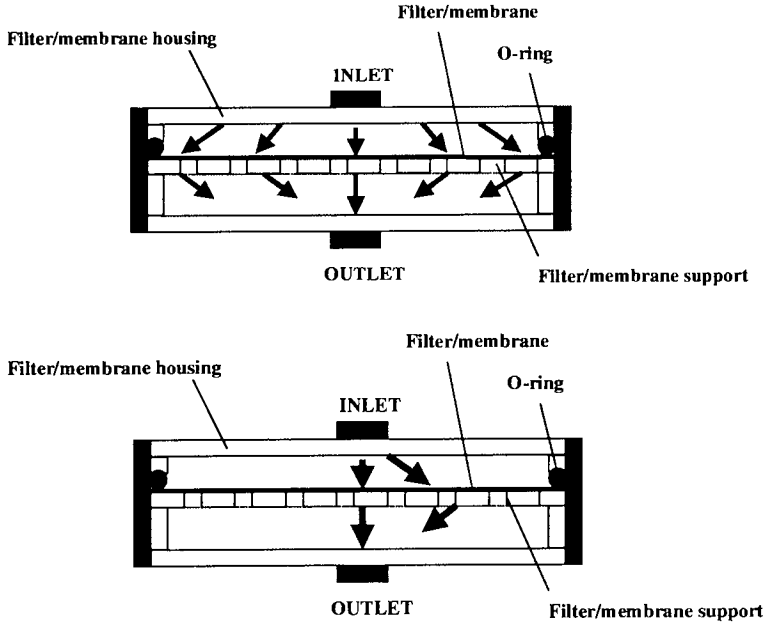

Figure A5-3: Sketches to represent ideal fluid distribution across the membrane or depth filter surface (upper sketch) whereby fluid is distributed evenly across their surface, and representation of an unwanted instance where fluid is distributed unevenly across the surface of the membrane or depth filter (lower sketch). Arrows represent the hypothetical path of the challenge fluid.

8.6. Appendix 6. Filtration theory and its application to calculation of resistance of filtered cells in depth filtration.

The basic relationship between time, filtration volume, and pressure drop across a filter is described by the following equation:

$$\frac{dV}{dt} = \frac{A^2 (-\Delta P)}{\mathbf{r} \mu \nu V} \qquad (6.1)$$

where

V = volume of liquid flowing in time t (m^3)

t = time (s)

A = filtration area (m^2)

ΔP = drop in pressure across filter (Pa, or N m^2)

r = specific resistance due to accumulation of particles (m^{-2})

μ = viscosity of fluid (Pa s)

ν = volume of particles deposited on filter per unit volume of fluid (m^{-3})

In section 1.6.2 the operation of the depth filters at the process scale was described, and the work in this chapter attempts to mimic the constant rate of filtration by the which the depth filters operate.

For filtration at constant rate:

$$\frac{dV}{dt} = \frac{V}{t} = \text{constant, or } Q_v \qquad (6.2)$$

where

Q_v = volumetric flow rate

therefore,

$$Q_v = \frac{A^2 (-\Delta P)}{\mathbf{r} \mu \nu V} \qquad (6.3)$$

The filtration area was constant for each experiment at 1256 x 10^{-6} m^2. The variation in pressure across the scaled down 10SP depth filter was recorded throughout the experiment. The viscosity of the challenge fluid was determined for appropriate solutions, although it was confined to the range 1.00 to 1.06 cP. The cumulative volume of liquid flowing in time was established during the

filtration experiments using a measuring cylinder. The volume of particles deposited on the filter could not be accurately determined. Therefore, it was assumed that the density of the particles being filtered were similar to one another and the mass of cellular material was constant within each comparative experiment. This meant that the volume of particles deposited on the filter was also assumed to be constant, but could not be quantified. In this way a comparison of the resistance attributable to the cellular material from various cell types was facilitated by calculating a value for **r** v.

The rig adopted for use in the pressure drop measurements is shown below.

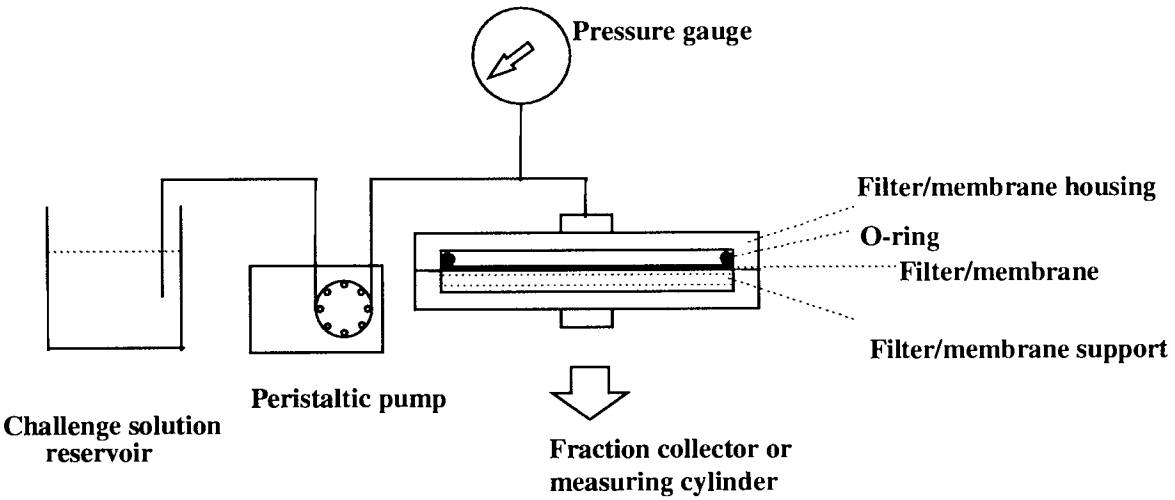

Figure A6-1: Sketch of test equipment employed for determination of pressure drop across the 10SP depth when challenged with control, apoptotic or necrotic cells. The same rig was also employed for generation of DNA breakthrough curves by the various depth filters and membranes.

9. References

Ahn, S.J., Costa, J., and Emanuel, J.R. Pico Green quantitation of DNA: effective evaluation of samples pre- or post-PCR. *Nucleic Acids Research* **24**(13):2623-2625, 1996.

Al-Rubeai, M., Mills, D., and Emery, A.N. Electron microscopy of hybridoma cells with special regard to monoclonal antoibody production. *Cytotechnology* **4**:13-28, 1994.

Al-Rubeai, M., Singh, R.P., Goldman, M.H., and Emery, A.N. Death mechanisms of animal cells in conditions of intensive agitation. *Biotechnology and Bioengineering* **45**:463-472, 1994.

Arnold, F.H., Blanch, H.W., and Wilke, C.R. Analysis of affinity separations. I: Predicting the performance of affinity adsorbers. *Chemical Engineering Journal* **30**:B9-B23, 1985.

Atkinson, A. and Jack, G.W. Precipitation of nucleic acids with polethyleneimine and the chromotography of nucleic acids and proteins on immobilised polyethyleneimine. *Biochimica and Biophysica Acta* **308**:41-52, 1973.

Bebbington, C.R., Renner, G., Thomson, S., King, D., Abrams, D., and Yarranton, G.T. High-level expression of a recombinant antibody from myeloma cells using a glutamine synthetase gene as an amplifiable selectable marker. *Bio/technology* **10**:169-175, 1992.

Bhattacharya, S. and Mandal, S.S. Interaction of surfactants with DNA. Role of hydrophobicity on intercalation and melting. *Biochimica et Biophysica Acta* **1323**:29-44, 1997.

Bibila, T.A. and Robinson, D.K. In pursuit of the optimal fed batch process for monoclonal antibody production. *Biotechnology process* **11**:1-13, 1995.

Blankstein, L.A. and Dohrman, L. an advanced affinity membrane for immunodiagnostic tests. a*m. Clin. Prod. Rev.* **11**:33-41, 1985.

Boer, G.J. a simplified microassay of DNA and RNA using ethidium bromide. *Analytical Biochemistry* **65**:225-231, 1975.

Borrebaeck, C.A.K. (Ed). Antibody Engineering, 2nd Edition. Oxford University Press, New York. 1995.

Brandt, S., Goffe, R.A., Kessler, S.B., O'Connor, J.L., and Zale, S.E. Membrane-based affinity technology for commercial scale purifications. *Bio/technology* **6**:779-782, 1988.

Breifs, K.-G. and Kula, M.-R. Fast protein chromatography on *Analytical* and preparative scale using modified microporous membranes. *Chemical Engineering Science* **47**:141-149, 1992.

Briggs, J. and Panfili, P.R. Quantitation of DNA and protien impurities in biopharmaceuticals. *Analytical Chemistry* **63**:850-859, 1991.

Brown, S. and Fuller, A.C. Depyrogenation of pharmaceutical solutions using submicron and ultrafilters. *Journal of Parenteral Science and Technology* **47**:285-288, 1993.

Carter, P., Kelley, R.F., Rodrigues, Snedecor, B., Covarrubias, M., Velligan, M.D., Wong, W.L.T., Rowland, A.M., Kotts, C.E., Carver, M.E., Yang, M., Bourell, J.H., Shepard, H.M., Henner, D. High level *Eschericia coli* expression and production of a bivalent humanized antibody fragment. *Bio/Technology* **10**: 163-167, 1992.

Cesarone, C.F., Bolognesi, C., and Santi, L. Improved microfluorimetric DNA determination in biological material using 33258 Hoescht. *Analytical Biochemistry* **100**:188-197, 1979.

Champluvier, B. and Kula, M. Microfiltration membranes as pseudo-affinity adsorbents: modification and comparison with gel beads. *Journal of Chromatography* **539**:315-325, 1991.

Charlton, H.R., Relton, J.M., and Slater, N.K.H. DNA from clarified, large scale, fed-batch, mammalian cell culture is of predominantely low molecular weight. *Biotechnology Letters* **20**:789-794, 1998.

Charlton, H.R., Relton, J.M., and Slater, N.K.H. Characterisation of a generic monoclonal antibody harvesting system for adsorption of DNA by depth filters and various membranes. *Bioseparations, in press.* 1999.

Charlton, H.R., Relton, J.M., and Slater, N.K.H. Fluorometric determination of DNA in mammalian cell cultures by PicoGreen. *Biotechnology Techniques, in press.* 1999.

Collins, R.J., Harmon, B.V., Gobe, G.C., and Kerr, J.F.R. Internucleosomal DNA cleavage should not be the sole criterion for identifying apoptosis. *International Journal of Radiation Biology* **61**:451-453, 1992.

Coulson, J.M. and Richardson, J.F. (with Backhurst, J.R. and Harker, J.H.). Chemical Engineering, Volume 2, 4th Edition. Butterworth Heinemann, Oxford, U.K. 1996.

Daniels, D.L., Schroeder, J.L., Szybalski, W., Sanger, F., Coulson, A.R., Hong, G.F., Hill, D.F., Petersen, G.B., and Blattner, F.R. Appendix 2: Complete Annotated Lambda Sequence. In *Lambda II.* Edited by Hendrix, R.W., Roberts, J.W., Stahl, F.W., and Weisberg, R.A. Cold Spring Harbour Laboratory, Cold Spring Harbour, N.Y. 1983.

Devitt, A., Moffat, O.D., Raykundalia, C., Capra, J.D., Simmons, D.L., and Gregory, C.D. Human CD14 mediates recognition and phagocytosis of apoptotic cells. *Nature* **392**:505-509, 1998.

Dick, H.M. Monoclonal antibodies in clinical medicine. *British Medical Journal* **291**:762-764, 1985.

Dickson, A.J. apoptosis regulation and its applications to biotechnology. *Tibtech* **16**:339-342, 1998.

Doran, P.M. Bioprocess Engineering Principles. Academic Press, London, U.K. 1995.

Dortant, P.M., Claasen, I.J.T.M., van Kreyl, C.F., van Steenis, G., and Wester, P.W. Risk assessment on the carcinogenic potential of hybridoma cell DNA: implications for residual contaminating cellular DNA in biological products. *Biologicals* **25**:381-390, 1997.

Dutton, M.D., Varhol, R.J., and Dixon, D.G. Technical considerations for the use of ethidium bromide in the quantitative analysis of nucleic acids. *Analytical Biochemistry* **230**:353-355, 1995.

Duxbury, M., Jezuit, M., Letwin, B., and Wright, J. DNA in plasma of blood for transfusion. *Biologicals* **23**:229-231, 1995.

Emery, S.C. and Adair, J.R. Humanised monoclonal antibodies for therapeutic applications. *Exp.Opin.Invest.Drugs* **3**:241-251, 1994.

Enger, O. Use of fluorescent dye Pico Green for quantification of PCR products after agarose gel electrophoresis. *BioTechniques* **21**:372-374, 1996.

Franěk, F. and Dolnikova, J. Nucleosomes occuring in protein-free hybridoma cell culture. *FEBS* **284**:285-287, 1991.

Franěk, F., Vomastek, T., and Dolnikova, J. Fragmented DNA and apoptotic bodies document the programmed way of cell death in hybridoma cultures. *Cytotechnology* **9**:117-123, 1992.

Freshney, R.I. *Culture of animal cells. A Manual of Basic Technique.* Alan R. Liss, New York, 1983.

Frost and Sullivan. The market for monoclonal antibody in the U.S. – market overview, total market, veterinary, contract manufacturing and research reagents. April 1996. www.profound.com.

Galfre, G., Howe, S.C., Milstein, C., Butcher, G.W., and Howard, J.C. Antibodies to histocompatibility antigens produced by hybrid cell lines. *Nature* **266**:550-552, 1977.

Garem, A., Daufin, G., Maubois, J.L., and Leonil, J. Selective separation of amino acids with a charged inorganic nanofiltration membrane: effect of physicochemical parameters on selectivity. *Biotechnology and Bioengineering* **54**:291-302, 1997.

Gebauer, K.H., Thommes, J., and Kula, M. Plasma protein fractionation with advanced membrane adsorbents. *Biotechnology and Bioengineering* **54**:181-189, 1997.

Glazer, A.N. and Rye, H.S. Stable dye-DNA intercalation complexes for high sensitivity fluorescence detection. *Nature* **359**:859-861, 1992.

Goergen, J.L., Marc, A., and Engasser, J.M. Determination of cell lysis and death kinetics in continuous hybridoma cultures from the measurement of lactate dehydrogenase release. *Cytotechnology* **11**:189-195, 1993.

Griffiths, E. WHO expert committee on biological standardization highlights of the meeting of October 1996. *Biologicals* **25**:359-362, 1997.

Gsell, T.C., Joffee, I.B., and Degen, J.P. Polyamide membrane with controlled surface properties and process for its production. European Patent No:87228B2:1, 1983.

Horowitz, B., Wiebe, M.E., Lippin, A., and Stryker, M.H. Inactivation of viruses in labile blood derivatives. *Transfusion* **25**:516-522, 1985.

Hou, K., Gerba, C.P., Goyal, S.M., and Zerda, K.S. Capture of latex beads, bacteria, endotoxin, and viruses by charge-modified filters. *Applied and Environmental Microbiology* **40**:862-896, 1980.

Hou, K.C. and Mandaro, R.M. Bioseparation by by ion exchange cartridge chromatography. *BioTechniques* **4**:358-367, 1986.

Jacobson, M.D. and Raff, M.C. Programmed cell death and Bcl-2 protection in very low oxygen. *Nature* **374**:814-816, 1994.

Jiskoot, W., Van Hertrooij, J.J.C.C., Klein Gebbinck, J.W.T.M., Van der Velden-de Groot, T., Crommelin, D.J.A., and Beuvery, E.C. Two-step purification of a murine monoclonal antobody intended for therapeutic application in man. *Journal on immunological methods.* **124**:143-156, 1989.

Junowicz, E., and Spencer, J. Studies on bovine pancreatic deoxyribonuclease A. 1. General properties and activation with different bivalent metals. *Biochimica et Biophysica Acta* **312**:72-84, 1973.

Kai, K., Foegeding, P.M., and Swaisgood, H.E. Isolation of RNA and DNA fragments using diatomaceous earth. *Biotechnology Techniques* **12**:549-552, 1998.

Karsten, U. and Wollenberger, A. Determination of DNA and RNA in homogenised cells and tissues by surface fluorometry. *Analytical Biochemistry* **46**:135-148, 1972.

Kohler, G. and Milstein, C. Continuous cultures of fused cells secreting antibody of predefined specificity. *Nature* **256**:495-497, 1975.

Kung, V.T., Panfili, P.R., Sheldon, E.L., King, R.S., Nagainis, P.A., Gomez Jr, B., Ross, D.A., Briggs, J., and Zuk, R.F. Picogram quantitation of total DNA using DNA-binding proteins in a silicon sensor-based system. *Analytical Biochemistry* **187**:220-227, 1990.

Kuo, M.T. and Hsu, T.C. Bleomycin causes release of nucleosomes from chromatin and chromosomes. *Nature* **271**:83-84, 1978.

Labarca, C. and Paigen, K. A simple, rapid, and sensitive DNA assay procedure. *Analytical Biochemistry* **102**:344-352, 1980.

Lee, S-M. Affinity purification of monoclonal antibody from tissue culture supernatantusing protein A-sepharose CL-4B. In: Commercial production of monoclonal antibodies: A guide for scale up, (Ed Seaver, S.S.). Marcel Dekker Inc. New York, U.S.A. 1987.

Le Pecq, J. and Paoletti, C. a new fluorimetric method for RNA and DNA determination. *Analytical Biochemistry* **17**:100-107, 1966.

Liddel, J.E. and Cryer, A. A practical guide to monocloanl antibodies. Courier International. Tiptree, Colchester, 1991.

Markovits, J., Roques, B.P., and Le Pecq, J. Ethidium dimer: a new reagent for the fluorimetric determination of nucleic acids. *Analytical Biochemistry* **94**:259-264, 1979.

McKnabb, S., Randall, R., and Tedesco, J.L. Measuring contaminating DNA in bioreactor derived immunoglobins. *Bio/technology* **7**:343-347, 1989.

Mercille, S. and Massie, B. Induction of apoptosis in nutrient-deprived cultures of hybridoma and myeloma cells. *Biotechnology and Bioengineering* **44**:1140-1154, 1994.

Mercille, S. and Bernard, M. Induction of apoptosis in oxygen deprived cultures of hybridoma cells. *Cytotechnology* **15**:117-128, 1994.

Meltzer, T.H. (Ed). Filtration in the pharmaceutical industry. Marcel Decker Inc., New York, N.Y., U.S.A. 1987.

Miller, R.A., Oseroff, A.R., Stratte, P.T., and Levy, R. Monoclonal antibody therapeutic trials in seven patients with T-cell lymphoma. *Blood* **62**:988-995, 1983.

Mirsky, A.E. and Silverman, B. Blocking by histones of accessibility to DNA in Chromatin. *Proceedings of the National Academy of Science* **69**:2115-2119, 1972.

Moe, D., Garbarsch, C., and Kirkeby, S. The protein effect on determination of DNA with Hoechst 33258. *Journal of Biochemical and Biophysical Methods* **28**:263-276, 1994.

Muller, J.G., Ng, M.M.P., and Burrows, C.J. Hydrophobic vs coulombic interactions in the binding of steroidal polyamines to DNA. *Journal of Molecular Recognition* **9**:143-148, 1996.

Murray, K., Ang, C.-E., Gull, K., Hickman, J.A., and Dickson, A.J. NS0 Myeloma cell death: Influence of bcl-2 Overexpression. *Biotechnology and Bioengineering* **51**:298-304, 1996.

Ng, P. and Mitra, G. Removal of DNA contaminants fron therapeutic protein preparations. *Journal of Chromatography A* **658**:459-463, 1994.

Oshima, K.H., Evans-Strickfaden, T.T., Highsmith, A.K., and Ades, E.W. The use of a microporous polyvinylidene fluoride (PVDF) membrane filter to separate contaminating viral particles from biologically important proteins. *Biologicals* **24**:137-145, 1996.

Persidis, A. Biotechnologies to watch. *Biotechnology Nature* **15**:1409-1411, 1997.

Petricciani, J.C. and Hennesse, W. Developments in Biological Standardization. *Dev. Biol Stand* **68**, 1986.

Petricciani, J.C. and Horaud, F.N. DNA, dragons and sanity. *Biologicals* **23**:233-238, 1995.

Petricciani, J.C. and Regan, P.J. Risk of neoplastic transformation from cellular DNA: claculations using the oncogene model. *Journal of Biological Standardization* **68**: 43-49, 1986.

Phillips, M.W. and DiLeo, A.J. A validatable porosimetric technique for verifying the integrity of virus-retentive membranes. *Biologicals* **24**:243-253, 1996.

Pimpinelli, S., Gatti, M., and De Marco, A. Evidence for heterogeneity in Heterochromatin of Drosophila melongaster. *Nature* **256**:335-337, 1975.

Prunnel, A., Kornberg, R.D., Klug, L.L.A., Levitt, M., and Crick, F.H.C. Periodicity of deoxyribonuclease I digestion of chromatin. *Science* **204**:855-858, 1979.

Ramage, P.I.N. and Allen, G. Purified CDW52-Specific Antibodies. International Patent No: PCT/GB91/01816 (WO 92/07084), 1992.

Ratafia, M. Mammalian Cell Culture: Worldwide Activities and Markets. *Bio/technology* **5**:692-694, 1987.

Reichmann, L., Clark, M., Waldmann, H., and Winter, G. Reshaping human antibodies for therapy. *Nature* **332**:323-327, 1988.

Rodrigues, M.T.A., Raw, I., and Moro, A.M. Residual DNA from hybridoma cultures: decorrence of apoptosis? In: *Animal Cell Technology*, edited by Carrondo, M.J.T., Griffiths, B., and Moreira, J.L.P. Kluwer Academic Publishers, Dordrecht, Boston, and London: 1997. pp 467-472.

Roper, D.K. and Lightfoot, E.N. Separation of biomolecules using adsorptive membranes. *Journal of Chromatograhy A* **702**:3-26, 1995.

Sambrook, J., Fritsch, E.F., Maniatis, T. Molecular cloning: A laboratory manual. Cold Spring Harbour Laboratory Press, Cold Spring Harbour, N.Y., 1989.

Seewoster, T. and Lehmann, J. Cell size distribution as a parameter for the predetermination of exponential growth during repeated batch cultivation of CHO cells. *Biotechnology and Bioengineering* **55**:793-797, 1997.

Seville, M., West, A.B., Cull, M.G., and McHenry, C.S. Fluorometric assay for DNA polymerases and reverse transciptase. *BioTechniques* **21**:664-672, 1996.

Sharp, P.A., Sugden, B., and Sambrook, J. Detection of two restriction endonuclease activities in *Haemophilus parainfluenzae* using *Analytical* agarose-ethiduim bromide electrophoresis. *Biochemistry* **12**:3055-3063, 1973.

Shi, Y., Sahai, B.M., and Green, D.R. Cyclosporin A inhibits activation-induced cell death in T-cell hybridomas and thymocytes. *Nature* **339**: 625-626, 1989.

Shimizu, S., Eguchi, Y., Kosaka, H., Kamiike, W., Matsuda, H., and Tsujimoto, Y. Prevention of hypoxia induced cell death by Bcl-2 and Bcl-xl. *Nature* **374**:811-813, 1995.

Simpson, N.H., Singh, R.P., Perani, A., Goldenzon, M., and Al-Rubeai, M. In hybridoma cultures, deprivation of any single amino acid leads to apoptotic death, which is supressed by the expression of the *bcl-2* gene. *Biotechnology and Bioengineering* **59**:90-98, 1998.

Singer, V.L., Jones, L.J., Yue, S.T., and Haugland, R.P. Characterization of PicoGreen reagent and development of a fluorescence-based solution assay for double stranded DNA quantitation. *Analytical Biochemistry* **249**:228-238, 1997.

Singh, R.P., Al-Rubeai, M., Gregory, C.D., and Emery, A.N. Cell death in bioreactors: a role for apoptosis. *Biotechnology and Bioengineering* **44**:720-726, 1994.

Skeidsvoll, J. and Ueland, P.M. Analysis of double stranded DNA by capilliary electrophoresis with laser induced fluorescence detection using the monomeric dye SYBR Green 1. *Analytical Biochemistry* **231**:359-365, 1995.

Smith, C.A., Williams, G.T., Kingston, R., Jenkinson, E.J., and Owen, J.J. Antibodies to CD3/T-cell receptor complex induce death by apoptosis in immature T cells in thymic cultures. *Nature* **337**: 181-184, 1989.

Smith, P.K., Krohn, R.I., Hermanson, G.T., Mallia, A.K., Gartner, F.H., Provenzano, M.D., Fujimoto, E.K., Goeke, N.M., Olson, B.J., and Klenk, D.C. Measurement of Protein Using Bicinchoninic Acid. *Analytical Biochemistry* **150**:76-85, 1985.

Southern, E.M. Detection of specific sequences among DNA fragments separated by gel electrophoresis. *Journal of Molecular Biology* **98**:503-517, 1975.

Spier, R. Animal cells in culture: moving into exponential phase. *Tibtech* **6**:2-6, 1988.

Stein, K.E. Overcoming obstacles to monoclonal antibody product development and approval. *Tibtech* **15**:88-90, 1997.

Suen, S.-Y. and Etzel, M.R. A mathematical analysis of affinity membrane bioseparations. *Chemical Engineering Science* **47**:1355-1364, 1992.

Tauer, C., Buchacher, A., and Jungbauer, A. DNA clearance in chromotography of proteins, exemplified by affinity chromotography. *Journal of Biochemical and Biophysical Methods* **30**:75-78, 1995.

Tsukakoshi, S. and Yamazaki, K. Mechanisms of nucleic acid transfer - nucleic acid. *Membrane* **21**:379-385, 1996.

Van Doorne, H. Sorption of bacterial endotoxin and retention of bacteria by positively charged membrane filters. *Journal of Parenteral Science and Technology* **47**:192-198, 1993.

Weidle, U.H., Borgya, A., Mattes, R., Lenz, H. and Buckel, P. Reconstitution of functionally active antibody directed against creatine kinase from separately expressed heavy and light chains in non-lymphoid cells. *Gene* **51**:21-9, 1987.

Wierenga, D.E., Cogan, J., and Petricciani, J.C. Administration of tumor cell chromatin to immunosuppressed and non-immunosuppressed non-human primates. *Biologicals* **23**:221-224, 1995.

Wolfert, M.A. and Seymour, L.W. Atomic force microscopic analysis of the influence of the molecular weight of poly(L)Lysine on the size of polyelectrolytecomplexes formed with DNA. *Gene Therapy* **3**:269-273, 1996.

Wongsamuth, R. and Doran, P.M. Production of monoclonal antibodies by tobacco hairy roots. *Biotechnology and Bioengineering* **54**:401-415, 1997.

Wu, Y.-C. and Horvitz, H.R. C.elegans phagocytosis and cell-migration protein CED-5 is similar to human DOCK 180. *Nature* **392**:501-504, 1998.

Wyllie, A.H. Glucocorticoid-induced thymocyte apoptosis is associated with endogenous endonuclease activation. *Nature* **284**:555-556, 1980.

Wyllie, A.H. Apoptosis: an overview. *British Medical Bulletin* **53**:451-465, 1997.

Xie, L. and Wang, I.C. High cell density and high monoclonal antibody production through medium design and rational control in a bioreactor. *Biotechnology and Bioengineering* **51**:725-729, 1996.

Zierdt, C.H. Adherence of bacteria, yeast, blood cells, and latex spheres to large-porosity membrane filters. *Applied and Environmental Microbiology* **38**:1166-1172, 1979.

Zola, H. Monoclonal Antibodies, The Second Generation. Information Press Ltd. Oxford, U.K. 1995.

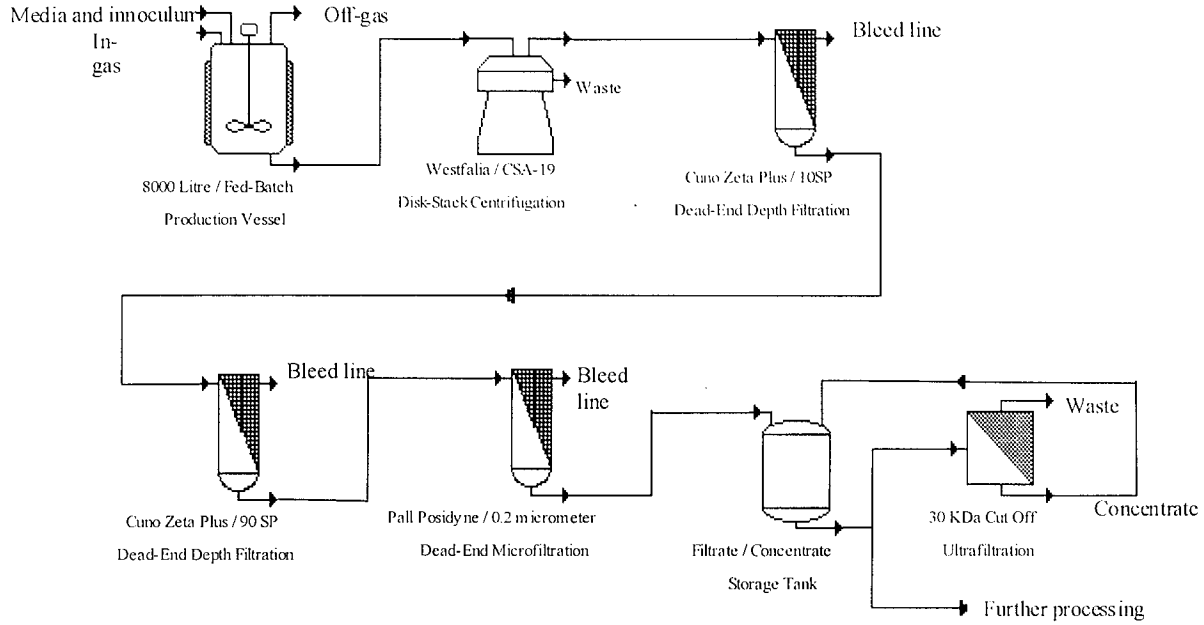

Figure1-1: Schematic of the initial stages of a generic monoclonal antibody purification scheme.

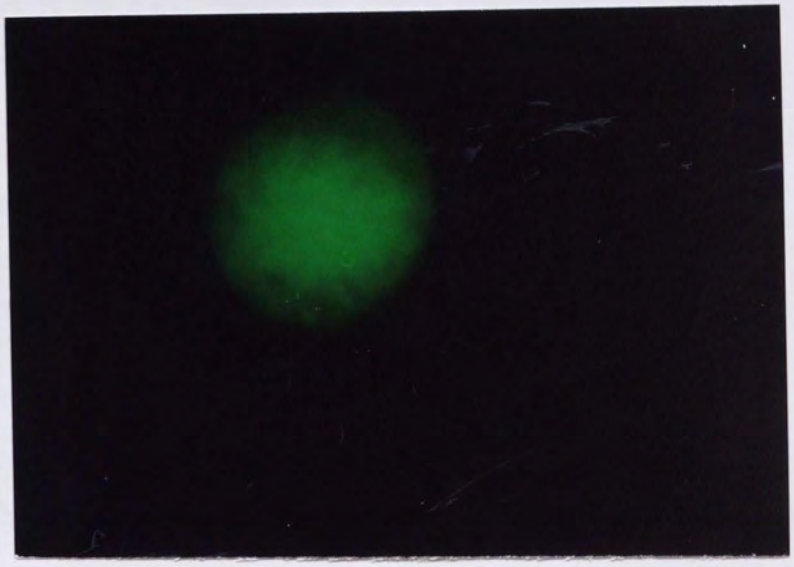

Figure 2-1: Fluorescent photomicrograph of a viable non-apoptotic NS0 cell stained with acridine orange and ethidium bromide. The cell viability is identified by relatively homogeneous green staining and uniform, near-circular morphology as detailed in the Methods chapter.

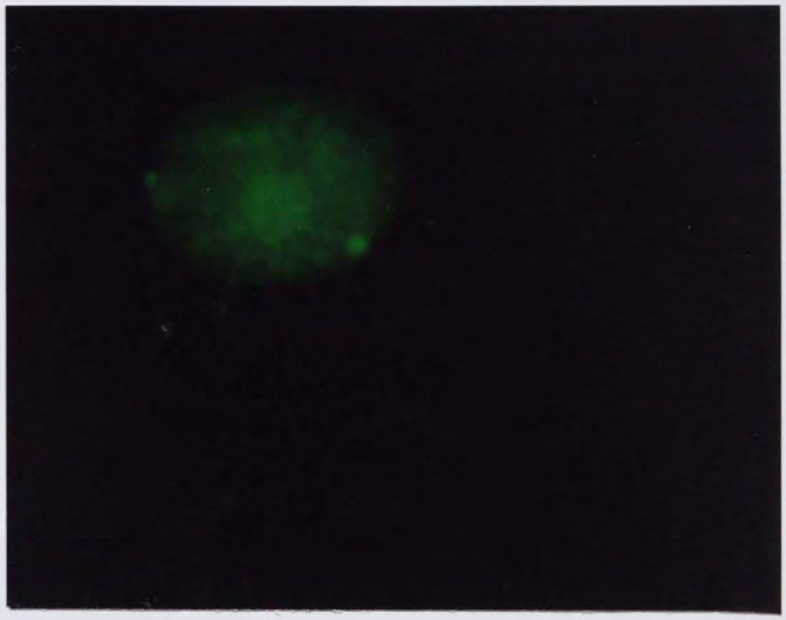

Figure 2-2: Fluorescent photomicrograph of a viable, early apoptotic NS0 cell stained with acridine orange and ethidium bromide. The cell viability is identified by heterogeneous green staining due to chromatin compaction whilst cell surface blebbing is still minimal and the gross morphology of the cell remain intact indicating that apoptosis is at an early stage in the cells demise.

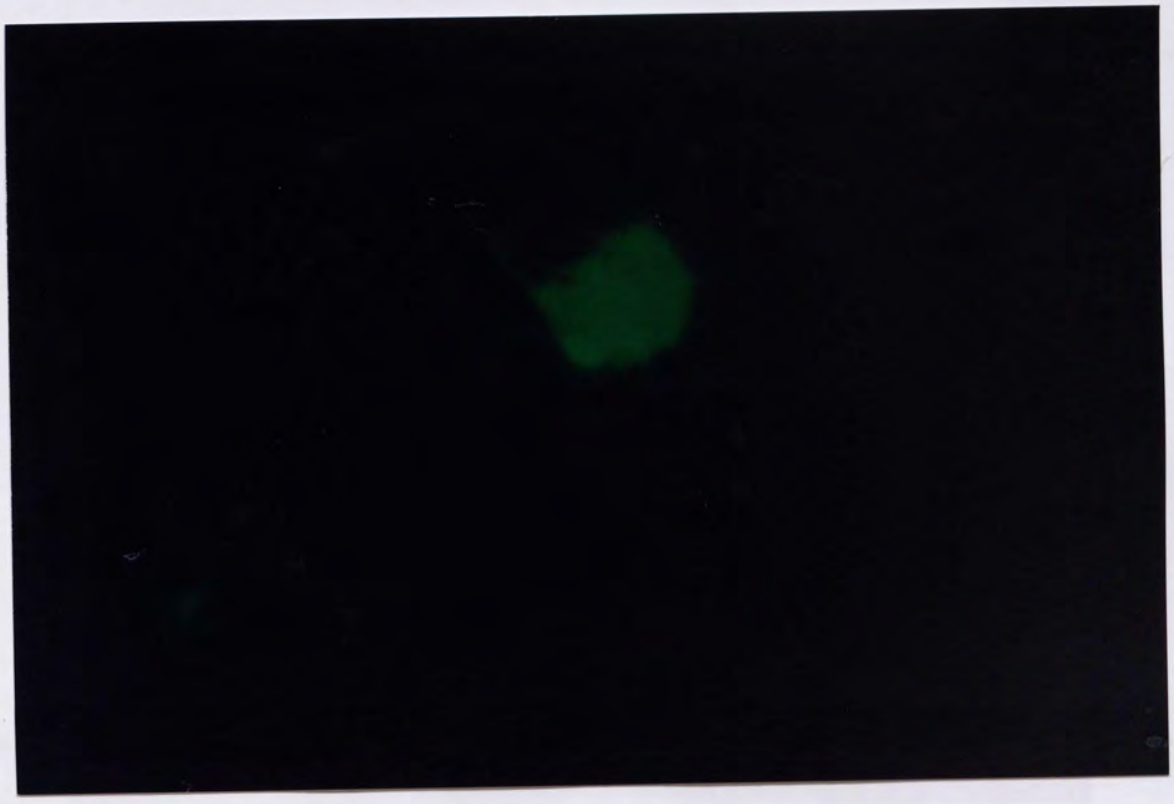

Figure 2-3: Fluorescent photomicrograph of a viable, late apoptotic NS0 cell stained with acridine orange and ethidium bromide. The cell viability is identified by heterogeneous green staining due to chromatin compaction whilst cell surface blebbing is advanced and the gross morphology of the cell has distorted, indicating that apoptosis is at a late stage in the cells demise.

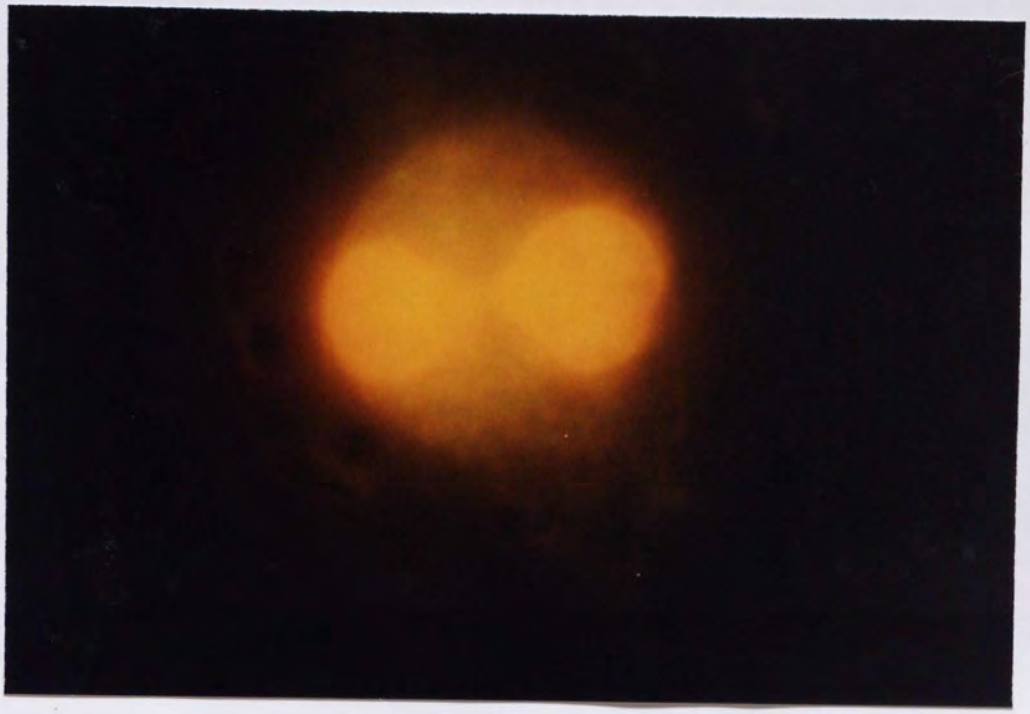

Figure 2-4: Fluorescent photomicrograph of a non-viable apoptotic NS0 cell stained with acridine orange and ethidium bromide. The cell viability is identified by orange staining due to the ingress of ethidium bromide following loss of membrane integrity. The mode of cell death is identified by the morphological changes associated with apoptosis including heterogeneous staining and cell surface disruptions.

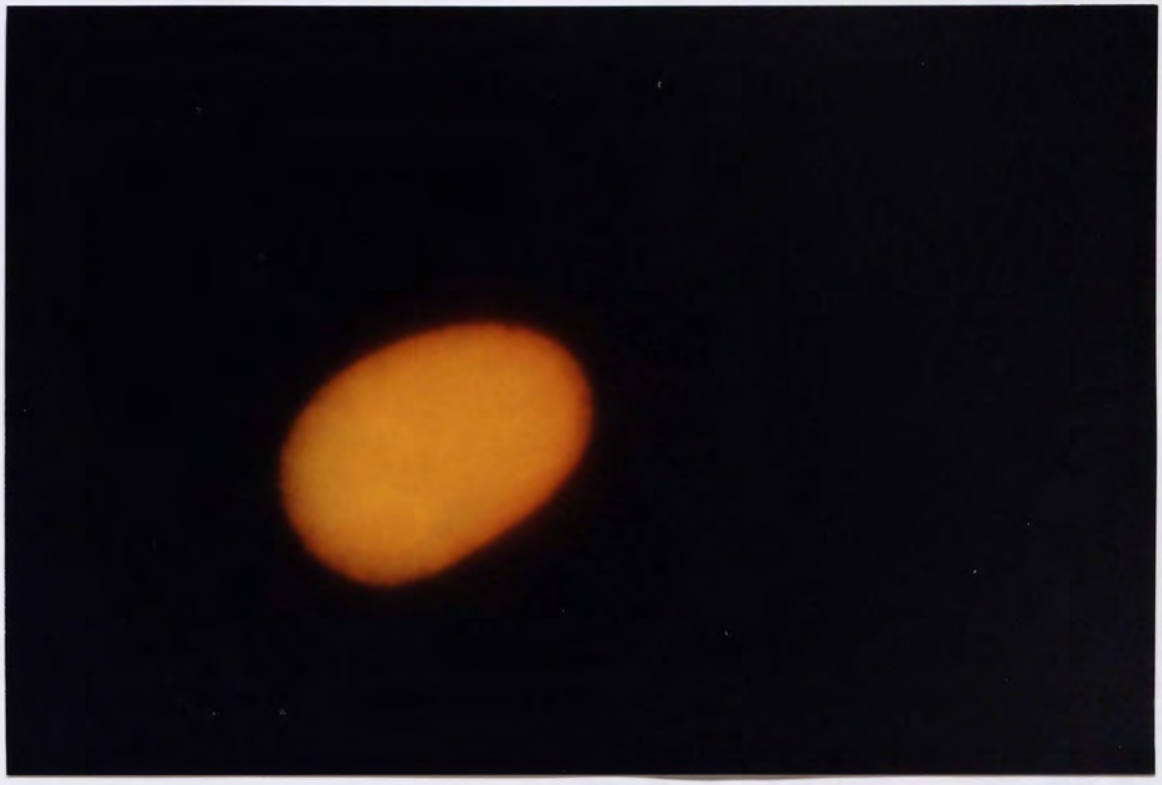

Figure 2-5: Fluorescent photomicrograph of a non-viable necrotic NS0 cell stained with acridine orange and ethidium bromide. The cell viability is identified by orange staining due to the ingress of ethidium bromide following loss of membrane integrity. The mode of cell death is identified by the morphological changes associated with necrosis including relatively homogeneous staining and minimal cell surface disruptions.

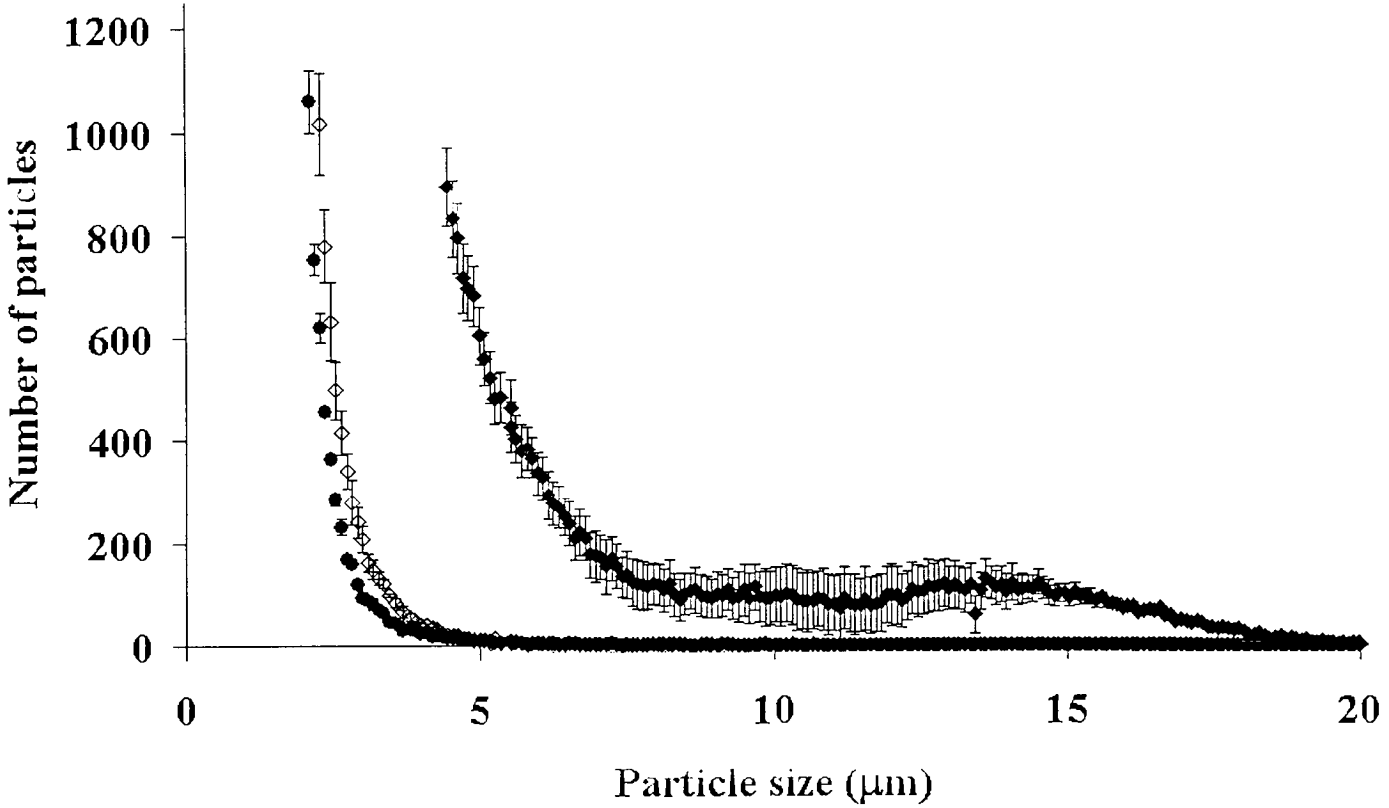

Figure 3-1: Particle size distribution of material from a 8000 litre culture vessel after a 9-day fed-batch fermentation of cells secreting monoclonal antibody B (◆), following centrifugation by a Westfalia CSA-19 disc stack centrifuge (◇), and after filtration by a 47 mm 10SP depth filter (●), scaled on the basis of constant superficial velocity. Particles counts were determined in triplicate for all samples by a Coulter Channelyzer 256 after samples had been diluted 1:200 with PBS. The sample volume was 500 μl. Error bars represent the standard deviation.

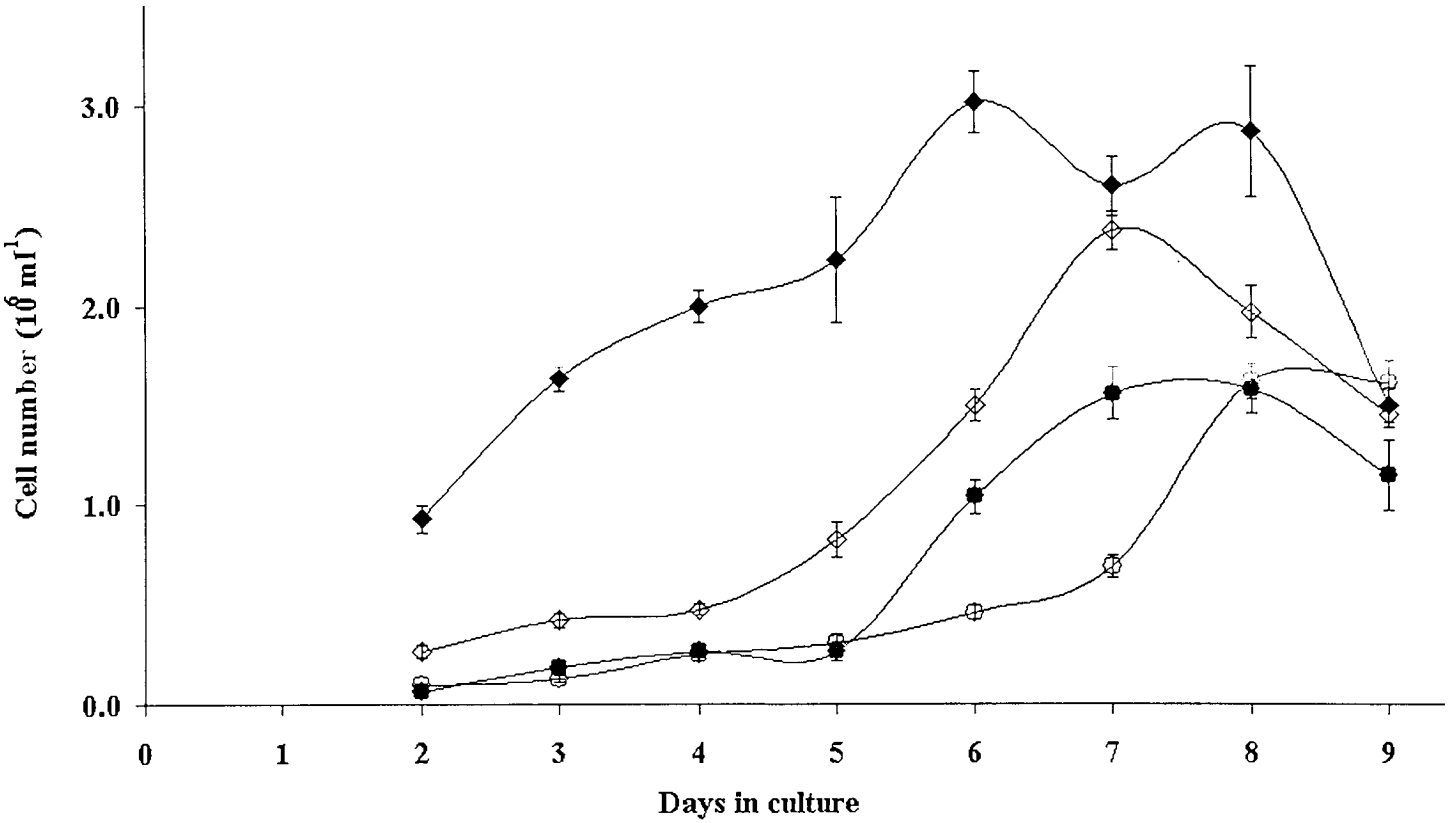

Figure 3-2: Cell counts from a 8000 litre culture vessel, 9-day, fed-batch fermentation of NS0 cells secreting monoclonal antibody B after staining with Acridine Orange and ethidium bromide as described in section 2.2.2.2: viable non-apoptotic (◆), non-viable necrotic (●), viable apoptotic (◇), non-viable apoptotic (○). Cells were scored in four squares of a haemacytometer and the average score plotted for each cell type. Error bars represent the standard error of the mean.

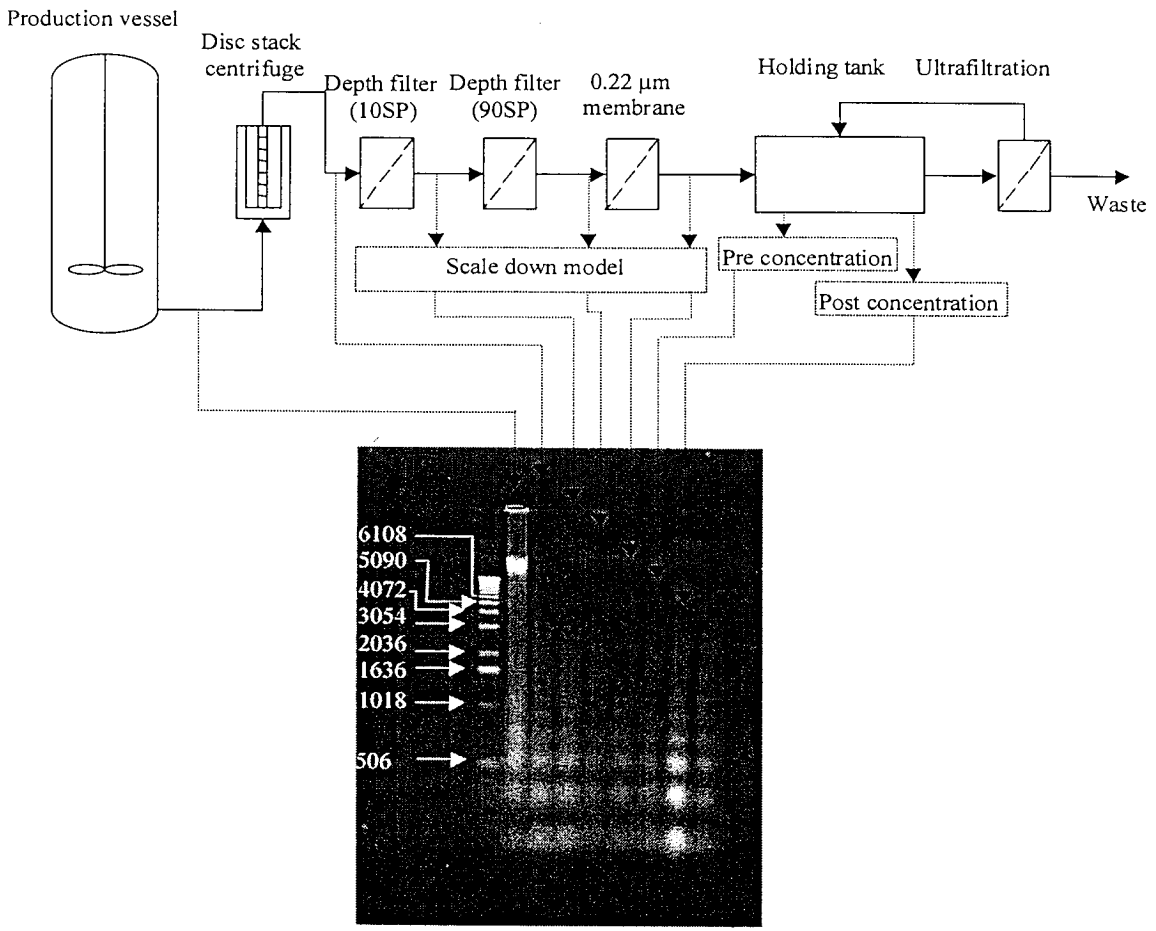

Figure 3-3: Samples were taken from either the large scale process or the scale down model at the points denoted by the dotted lines. Following treatment with Ribonuclease and Proteinase K, DNA was extracted, run on a 1.5% agarose gel and stained with ethidium bromide. The far left hand lane contains a 1 Kb ladder of DNA molecules, 12,216 bp being the largest strand. DNA molecules of strand length 6108 to 506 base pairs were clearly resolved and have been labelled accordingly. The far right hand lane contains DNA extracted from the supernatant of production vessel material after centrifugation for 5 mins at 7,200g.

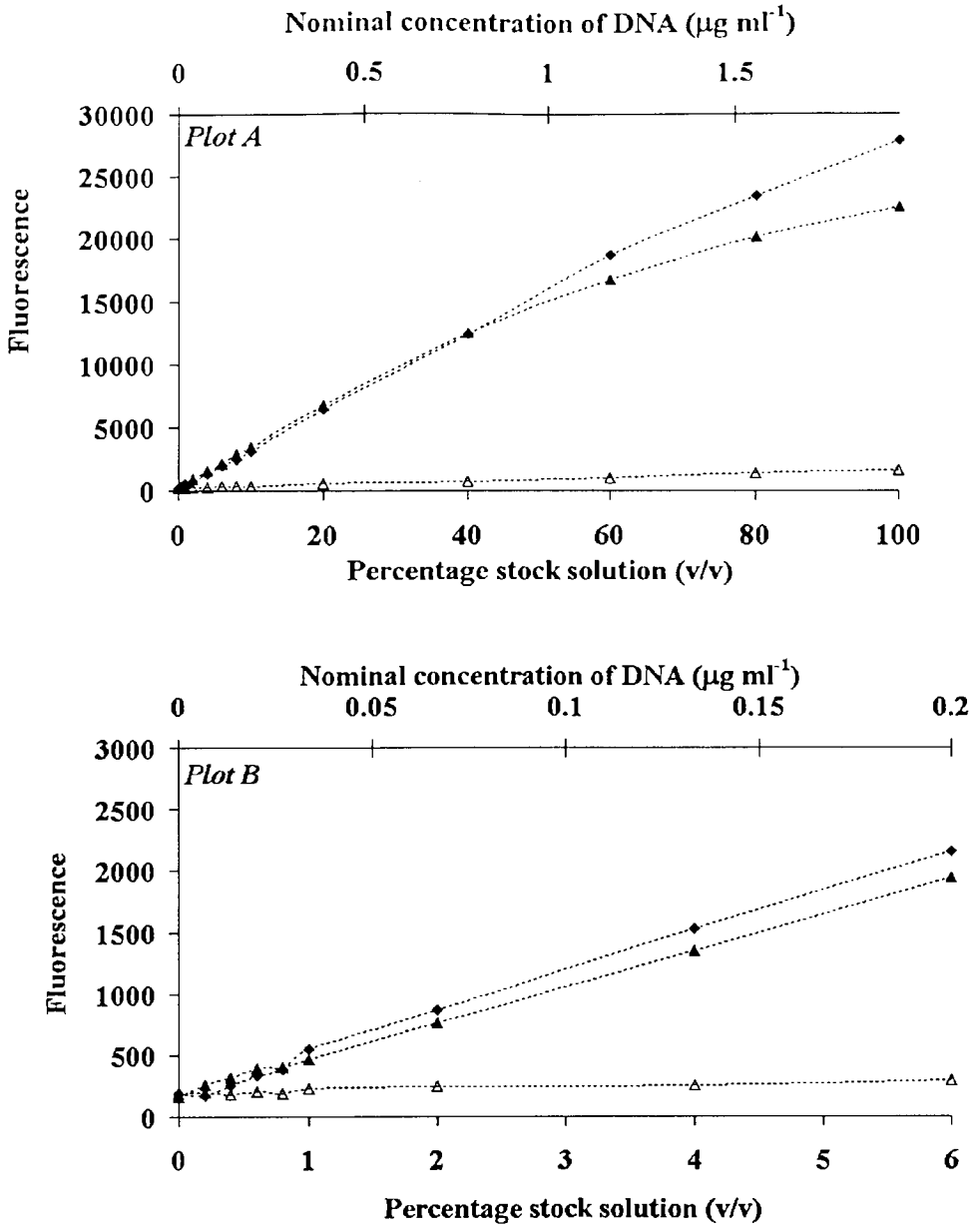

Figure 4-1: Effect of unused culture media on fluorescence. Three stock solutions were employed: 1) unused culture media (△) 2) calf thymus DNA made up in unused culture media (▲) and 3) as a control, calf thymus DNA in TE, pH 7.5 (♦). Solutions (1) and (3) were subsequently diluted with (TE), and solution (2) was subsequently diluted with unused culture media. Stock solutions (2) and (3) had nominal DNA concentrations of 1.95 μg ml^{-1}. Fluorescence of the resultant solutions in the presence of PicoGreen was determined and plotted as a function of percentage stock solution. Plots A and B differ only in the range of stock solution concentrations.

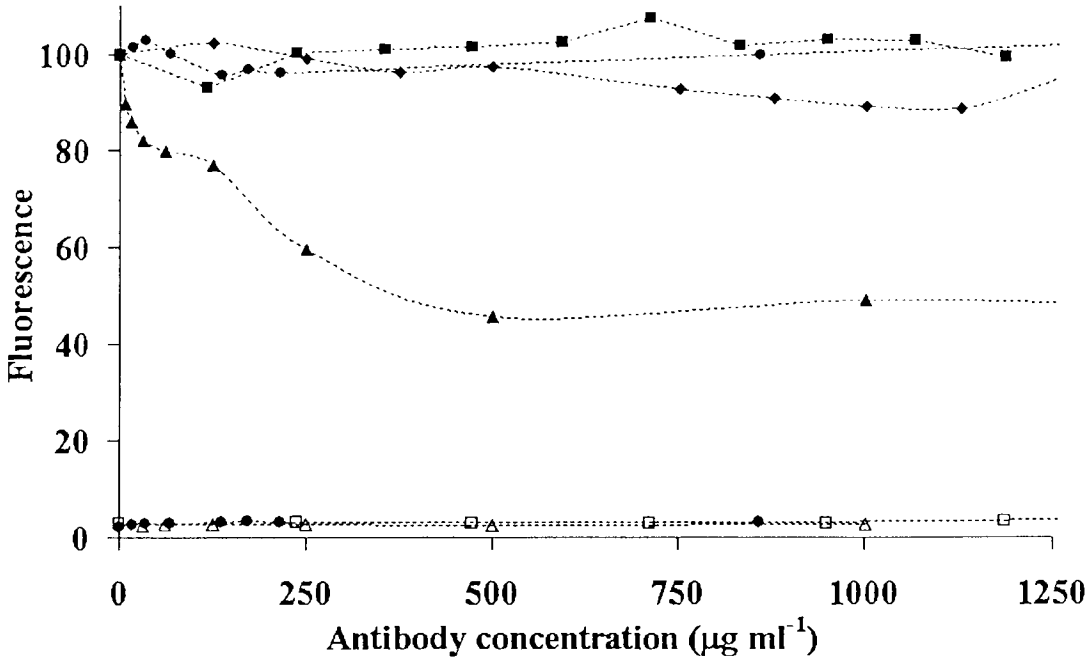

Figure 4-2: The effect of monoclonal antibodies A, B, and C on fluorescence of PicoGreen prior to and following spiking with calf thymus DNA. Antibodies were purified in accordance with standard operating procedures for generation of clinical trial material and were largely free of DNA. Formulated material was initially diluted 1:40 with TE, pH 7.5 or TE at pH 8.8 containing 100mM NaCl, and subsequent dilutions were made with the same buffers that the antibodies were initially diluted with. These preparations were spiked with calf thymus DNA resulting in a final concentration of 650 ng DNA ml^{-1} or left unspiked as a control. For presentation purposes the fluorescence of antibody free solutions spiked with DNA were normalised to 100 fluorescence units. The same factor was applied to the fluorescence of the DNA spiked antibody solutions and plotted as a function of antibody concentration. Symbols: antibody A in TE, spiked (■), unspiked (□), antibody B in TE pH 7.5, spiked (▲), unspiked (△) and in TE pH 8.8 100mM NaCl, spiked (◆), antibody C in TE pH 7.5 spiked (●) and unspiked (○).

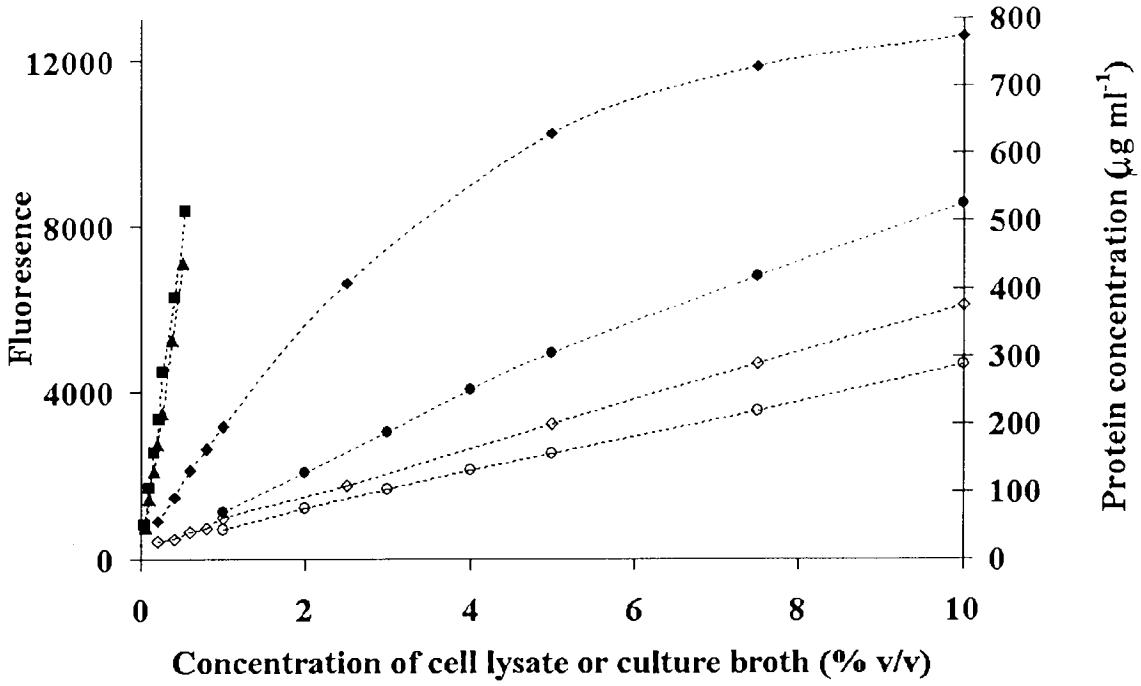

Figure 4-3: Protein concentration and fluorescence of cell culture broth. NS0 cells secreting antibody A were grown for 7 days with nutrient supplements on days 2,4 and 6 in a 1.5 litre cell culture vessel and fluorescence was determined in diluted clarified cell culture broth (●) or following lysis of cells with SDS (▲) as described in the Methods chapter. NS0 cells secreting antibody B were grown for 9 days with nutrient supplements on days 2,4 and 6 in an 8000 litre cell culture vessel and fluorescence was determined in diluted clarified cell culture broth (◆) or following lysis of cells with SDS (■). Protein concentration was determined in the clarified culture broth only; antibody A (○), antibody B (◇) using the bicinchoninic acid assay. Baseline fluorescence was subtracted from the fluorescence reading of each sample prior to plotting the graph and all dilutions were performed using TE, pH 8.8, 100 mM NaCl.

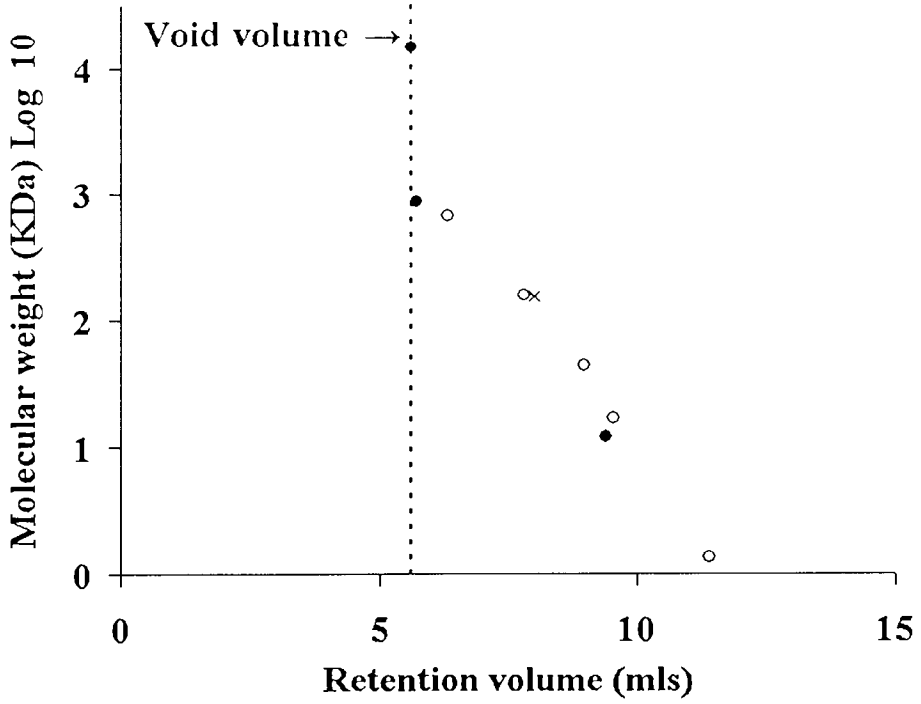

Figure 4-4: Size exclusion chromatography of various proteins (○) and nucleic acids (●) for calibration of the HPLC system employing a BIOSEP SEC S3000 column (7.8 mm ID x 300 mm; Phenomonex, CA, U.S.A.), flow rate 1 ml min^{-1}, isocratic elution with TE, pH 8.8, 100 mM NaCl. For injection of nucleic acids, sequential fractions were collected and assayed for fluorescence with PicoGreen. The apex of each fluorescent peak for each sample was interpreted to indicate the retention time of the largest fragment of DNA present in the sample used. Three nucleic acid samples were employed: calf thymus DNA (23,000 to 100 base pairs); ΦX174 HaeIII digest (Daniels *et al.*, 1983) (1,353 to 72 base pairs); and $dN_{5\text{-}19}$ synthetic oligonucleotides. The retention times of individual proteins were established after spectrophotometric analysis of eluted material following a single injection of a Bio-Rad Gel Filtration Standard (Hemel Hampstead, Herts, U.K.). Regression analysis of the components that were not excluded from the matrix gave the equality y=-0.538x+6.3087 which was used to predict the retention time of nucleic acids and monoclonal antibodies. The void volume is indicated and the retention volume of monoclonal antibodies A and B were found to be identical at 8.0 ml which is denoted by the symbol: X.

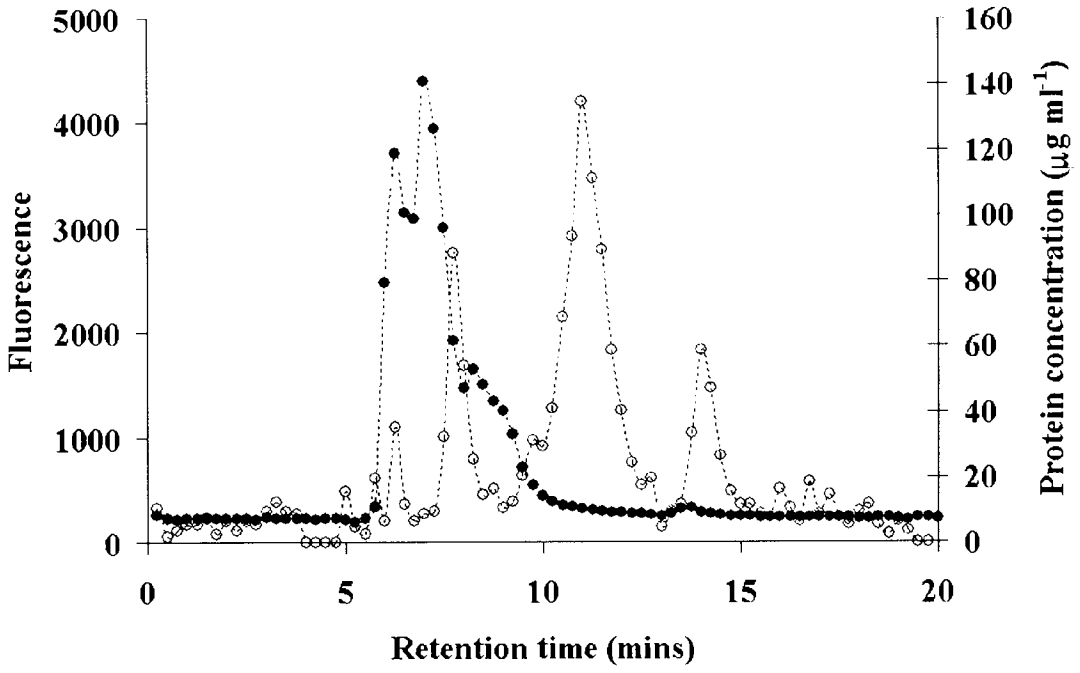

Figure 4-5: Size exclusion HPLC of clarified culture broth containing monoclonal antibody A. Sequential fractions were collected and 100 μl were assayed for fluorescence in the presence of PicoGreen (●) or protein using bicinchinoic acid (○). The HPLC system employed a BIOSEP SEC S3000 column (7.8 mm ID x 300 mm; Phenomonex, CA, U.S.A.), flow rate 1 ml min^{-1}, isocratic elution with TE, pH 8.8, 100 mM NaCl.

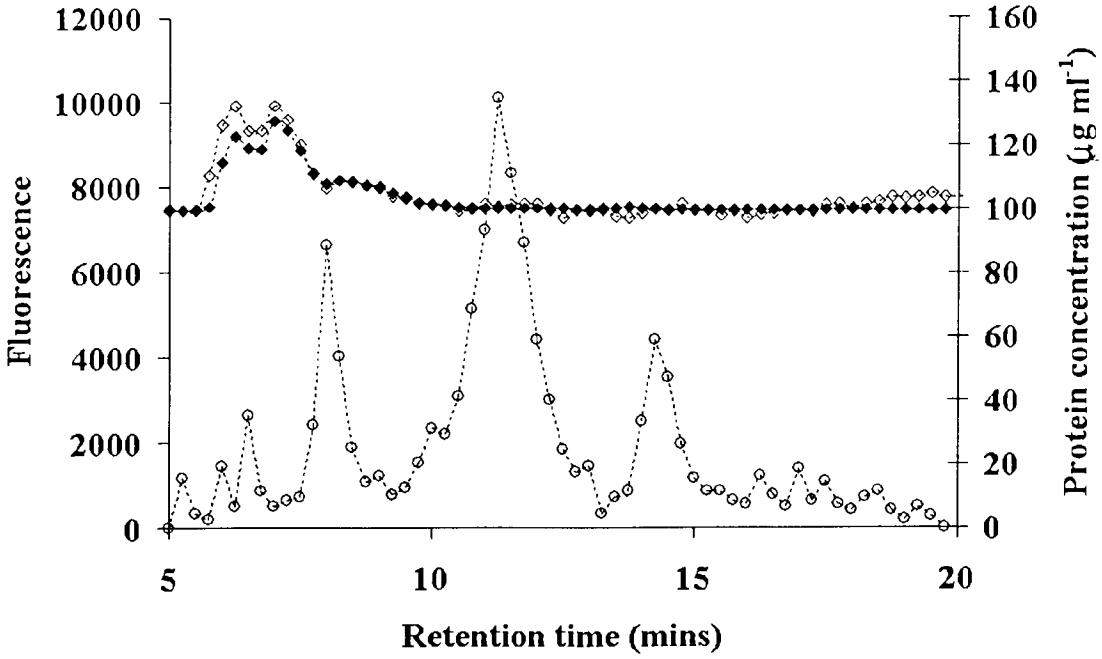

Figure 4-6: Size exclusion HPLC of clarified culture broth containing monoclonal antibody A. 50 µl of a 1.3 µg ml^{-1} calf thymus DNA stock solution in TE, pH 8.8, 100 mM NaCl was combined with 50 µl of the same fractions as those used to produce figure 4-6. Fluorescence predictions were calculated on the basis of adding 50 µl blank TE, pH 8.8, 100 mM NaCl to 50 µl of the calf thymus DNA stock solution and adding this figure to 50% of the above baseline fluorescence observed in the fractions collected: fluorescence after spiking (◆) and predicted fluorescence (◇). Protein determinations were made using bicinchinoic acid (○). The HPLC system employed a BIOSEP SEC S3000 column (7.8 mm ID x 300 mm; Phenomonex, CA, U.S.A.), flow rate 1 ml min^{-1}, isocratic elution with TE, pH 8.8, 100 mM NaCl.

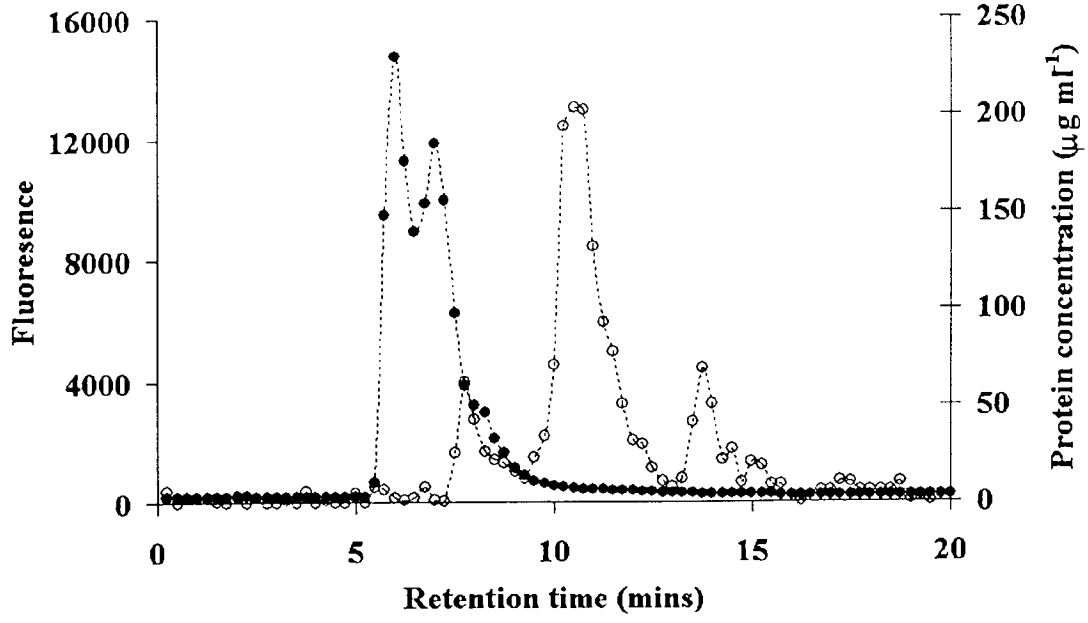

Figure 4-7: Size exclusion HPLC of clarified culture broth containing monoclonal antibody B. Sequential fractions were collected and 100 µl were assayed for fluorescence in the presence of PicoGreen (●) or protein using bicinchinoic acid (○). The HPLC system employed a BIOSEP SEC S3000 column (7.8 mm ID x 300 mm; Phenomonex, CA, U.S.A.), flow rate 1 ml min^{-1}, isocratic elution with TE, pH 8.8, 100 mM NaCl.

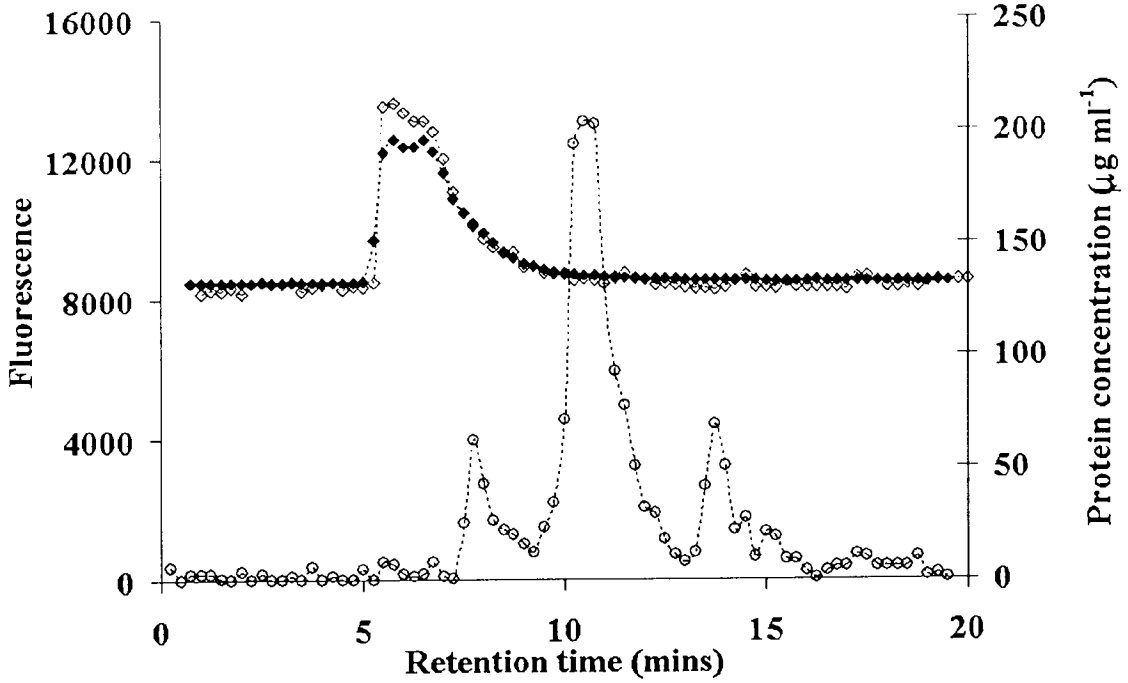

Figure 4-8: Size exclusion HPLC of clarified culture broth containing monoclonal antibody B. 50 µl of a 1.3 µg ml^{-1} calf thymus DNA stock solution in TE, pH 8.8, 100 mM NaCl was combined with 50 µl of the same fractions as those used to produce figure 4-6. Fluorescence predictions were calculated on the basis of adding 50 µl blank TE, pH 8.8, 100 mM NaCl to 50 µl of the calf thymus DNA stock solution and adding this figure to 50% of the above baseline fluorescence observed in the fractions collected: fluorescence after spiking (◆) and predicted fluorescence (◇). Protein determinations were made using bicinchinoic acid (○). The HPLC system employed a BIOSEP SEC S3000 column (7.8 mm ID x 300 mm; Phenomonex, CA, U.S.A.), flow rate 1 ml min^{-1}, isocratic elution with TE, pH 8.8, 100 mM NaCl.

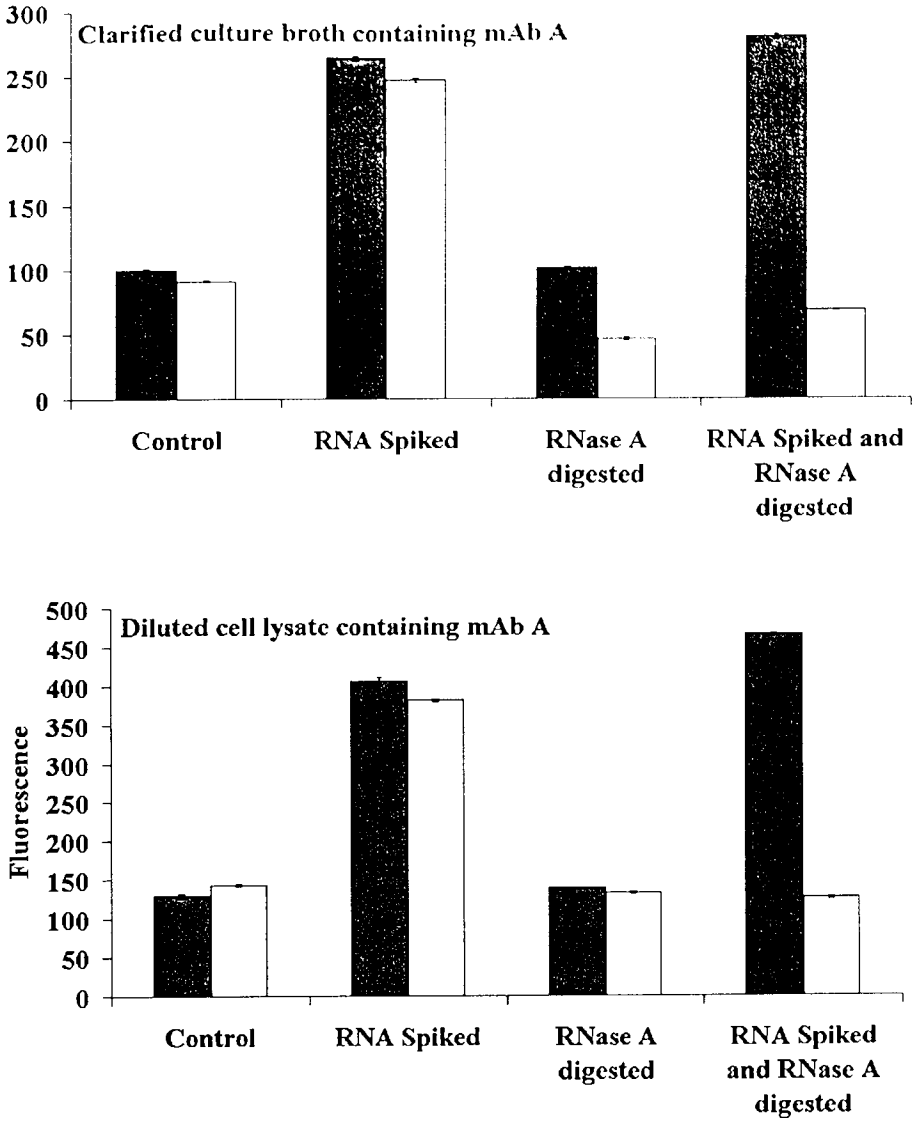

Figure 4-9: The effect on fluorescence of incubating clarified culture broth or diluted cell lysate containing mAb A without RNase A ("Control" and "RNA Spiked") and with approx. 50 μg ml^{-1} RNase ("RNase A digested" and "RNA Spiked and RNase A digested") for one hour at 37°C. Prior to (grey bars) and following incubations (white bars), clarified culture broth and diluted cell lysate was diluted to within the linear fluorescence range as determined in Figure 4-3, both with TE, pH 8.8, 100mM NaCl. All digestions were performed in triplicate. For presentation purposes, fluorescence of the control clarified culture broth samples were normalised to 100 and the same factor was applied to the fluorescence of other samples. Error bars represent the standard deviation.

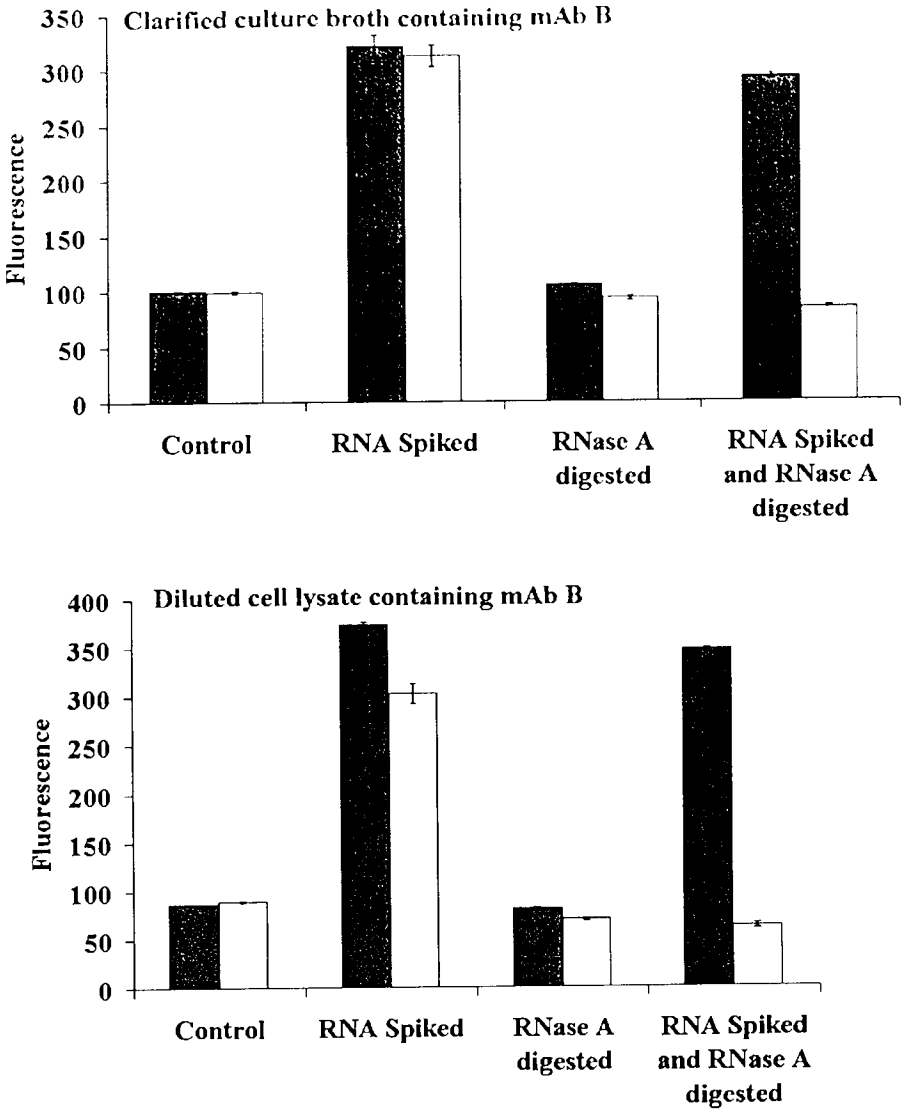

Figure 4-10: The effect on fluorescence of incubating clarified culture broth or diluted cell lysate containing mAb B without RNase A ("Control" and "RNA Spiked") and with approx. 50 μg ml^{-1}RNase ("RNase A digested" and "RNA Spiked and RNase A digested") for one hour at 37°C. Prior to (grey bars) and following incubations (white bars), clarified culture broth and diluted cell lysate was diluted to within the linear fluorescence range as determined in Figure 4-3, both with TE, pH 8.8, 100mM NaCl. All digestions were performed in triplicate. For presentation purposes, fluorescence of the control clarified culture broth samples were normalised to 100 and the same factor was applied to the fluorescence of other samples. Error bars represent the standard deviation.

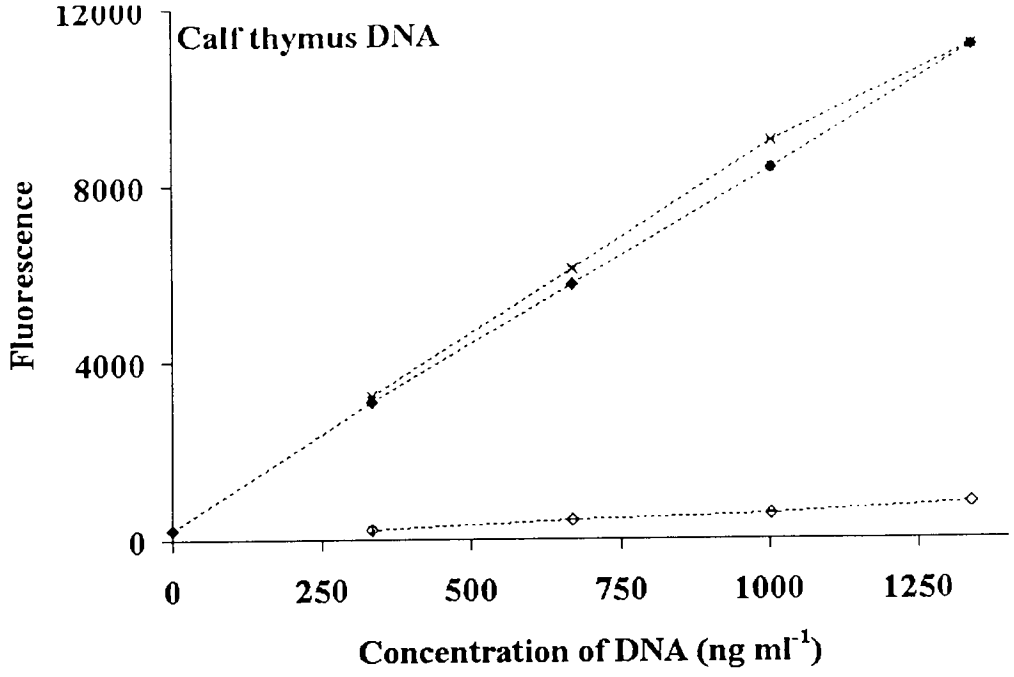

Figure 4-11: Fluorescence of calf thymus DNA prior to and following incubation with 5 units DNase I ml^{-1} for one hour at 37 ^{0}C, with appropriate controls. Calf thymus DNA was employed at a concentration of 13.4 $\mu g\ ml^{-1}$. Samples were treated in one of three ways: unincubated (♦); incubated with 10mM $MgCl_2$ only (x); or incubated with 10mM $MgCl_2$ and DNase I (◇). Following incubation samples were diluted with TE, pH 8.8, 100mM NaCl to those concentrations shown on the plot prior to determination of fluorescence in the presence of PicoGreen. Error bars represent the standard deviation.

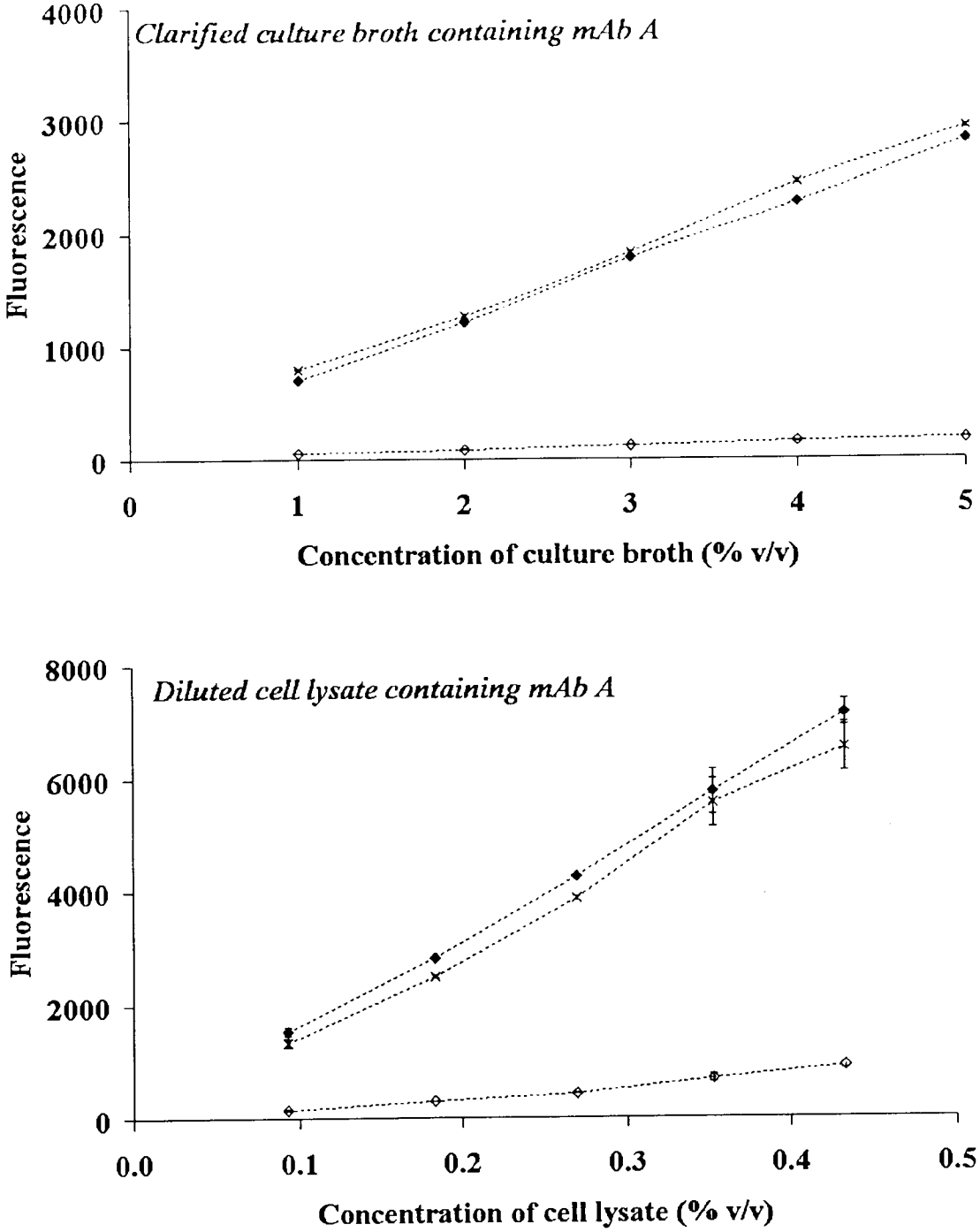

Figure 4-12: Fluorescence of cultured materials containing mAb A prior to and following incubation with 5 units DNase I ml^{-1} for one hour at 37 ^{o}C, with appropriate controls. Samples were treated in one of three ways: unincubated (♦); incubated with 10mM $MgCl_2$ only (x); or incubated with 10mM $MgCl_2$ and DNase I (◇). Following incubation samples were diluted with TE, pH 8.8, 100mM to those concentrations shown on the plot prior to determination of fluorescence in the presence of PicoGreen. Error bars represent the standard deviation.

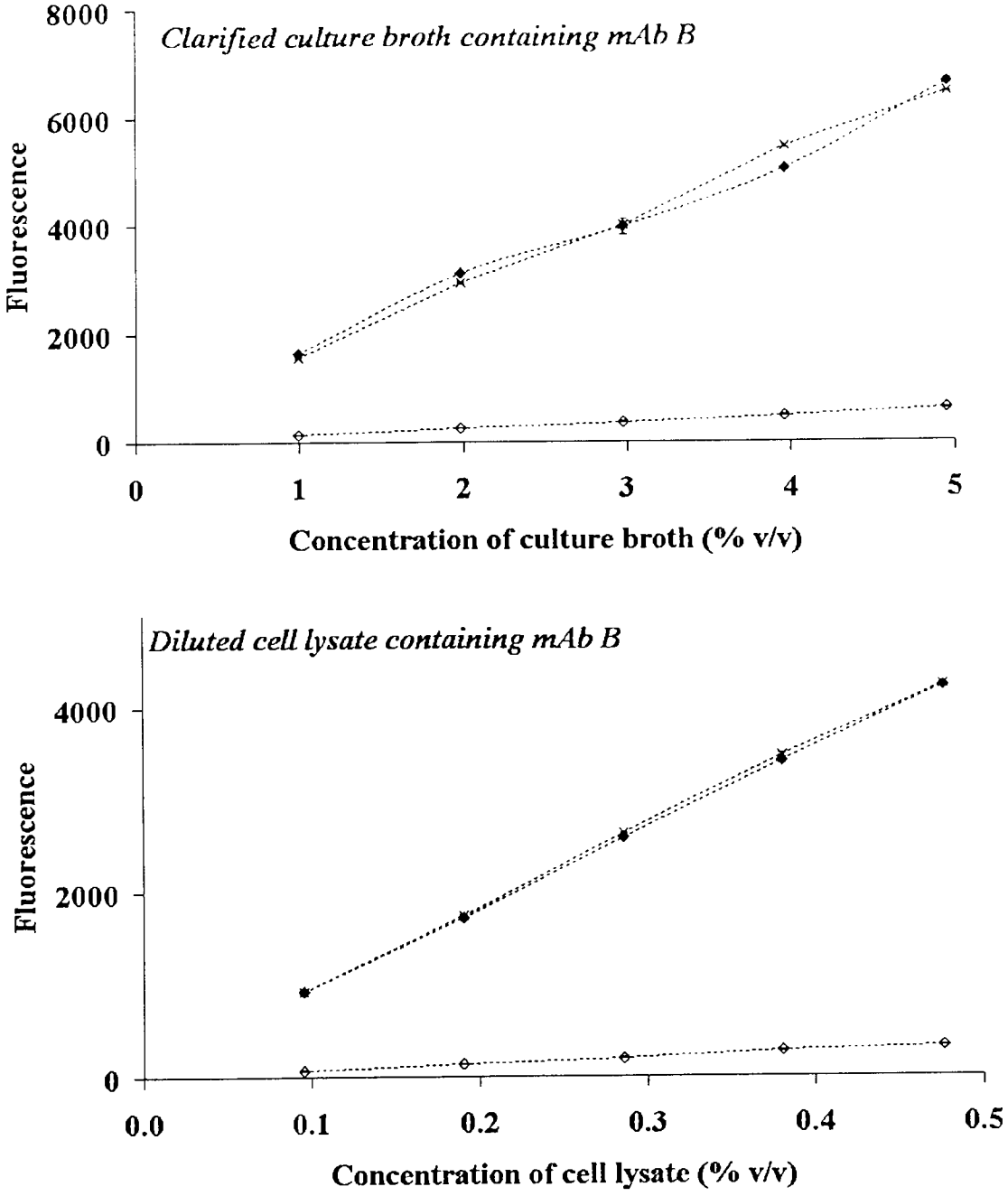

Figure 4-13: Fluorescence of cultured materials containing mAb A prior to and following incubation with 5 units DNase I ml^{-1} for one hour at 37 ^{o}C, with appropriate controls. Samples were treated in one of three ways: unincubated (♦); incubated with 10mM $MgCl_2$ only (x); or incubated with 10mM $MgCl_2$ and DNase I (◇). Following incubation samples were diluted with TE, pH 8.8, 100mM to those concentrations shown on the plot prior to determination of fluorescence in the presence of PicoGreen. Error bars represent the standard deviation.

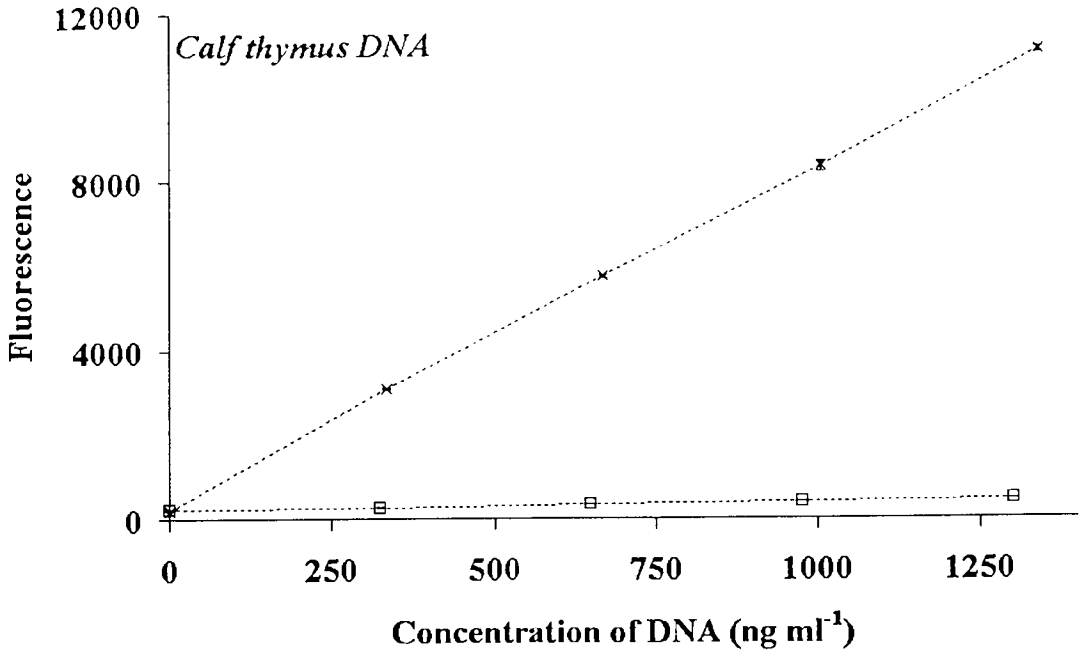

Figure 4-14: Addition of poly-L-lysine to calf thymus DNA. A stock solution of calf thymus DNA at a concentration of 13.4 μg ml^{-1} was diluted with TE, pH 8.8, 100 mM NaCl to the concentrations shown in the plot and fluorescence in the presence of PicoGreen was determined prior to (x) or following addition of a 590 μg ml^{-1} stock solution of poly-L-lysine to a final concentration of 16 μg ml^{-1} (□). Error bars represent the standard deviation.

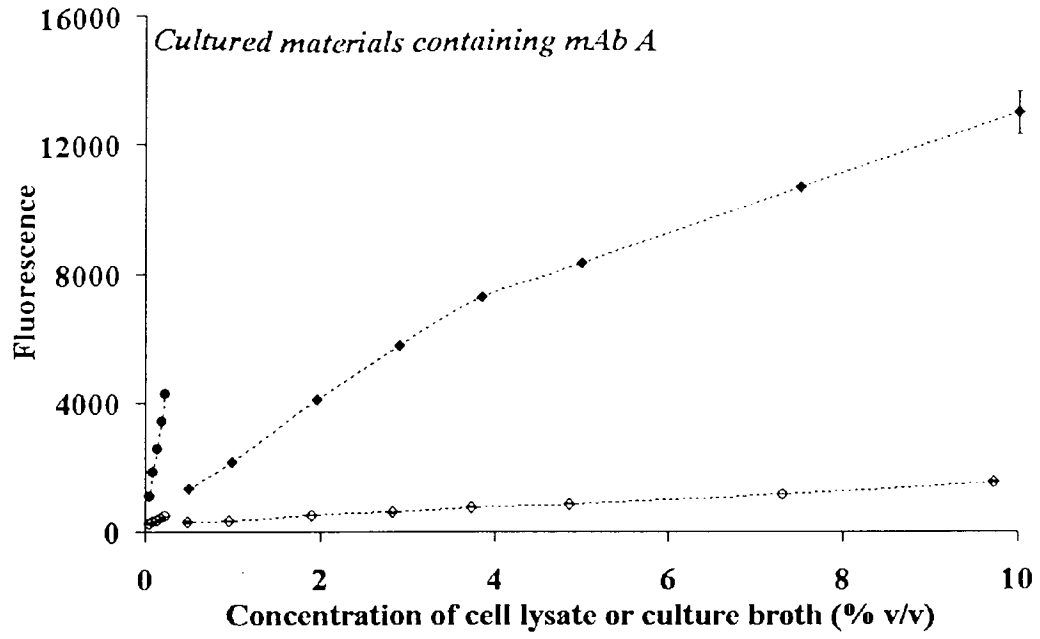

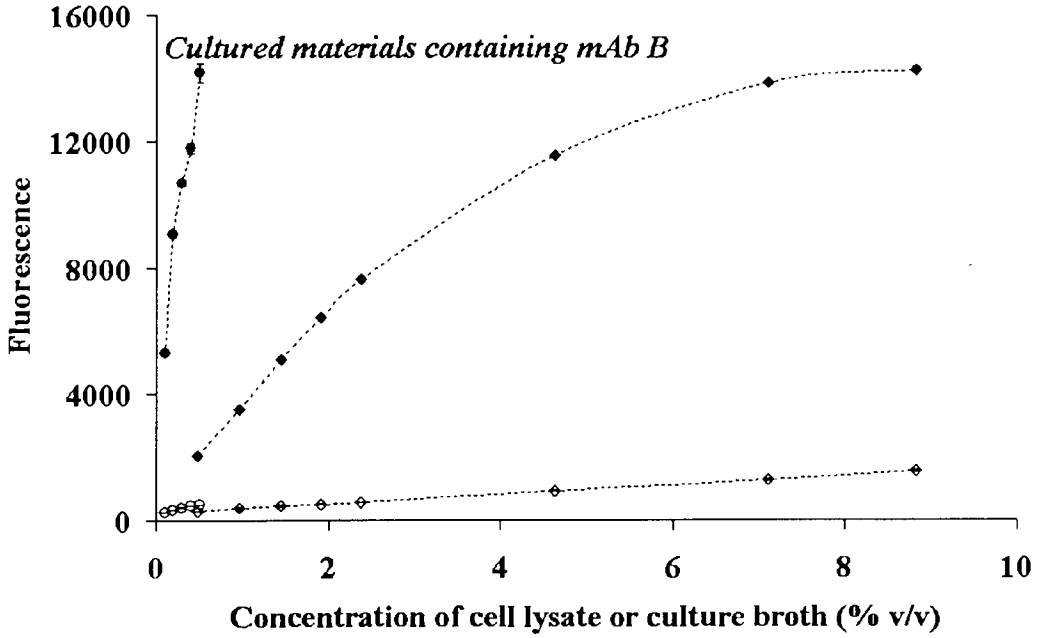

Figure 4-15: Addition of poly-L-lysine to diluted cell lysate, clarified cell culture containing mAbs A and B. Plots are labeled accordingly. Solutions were prepared by dilution with TE, pH 8.8, 100 mM NaCl and then assayed for fluorescence (diluted cell lysate; ●, clarified culture broth; ♦) or after addition of a 590 μg ml^{-1} stock solution of poly-L-lysine to a final concentration of 16 μg ml^{-1} (diluted cell lysate; ○, clarified cell culture broth; ◇). Error bars represent the standard deviation.

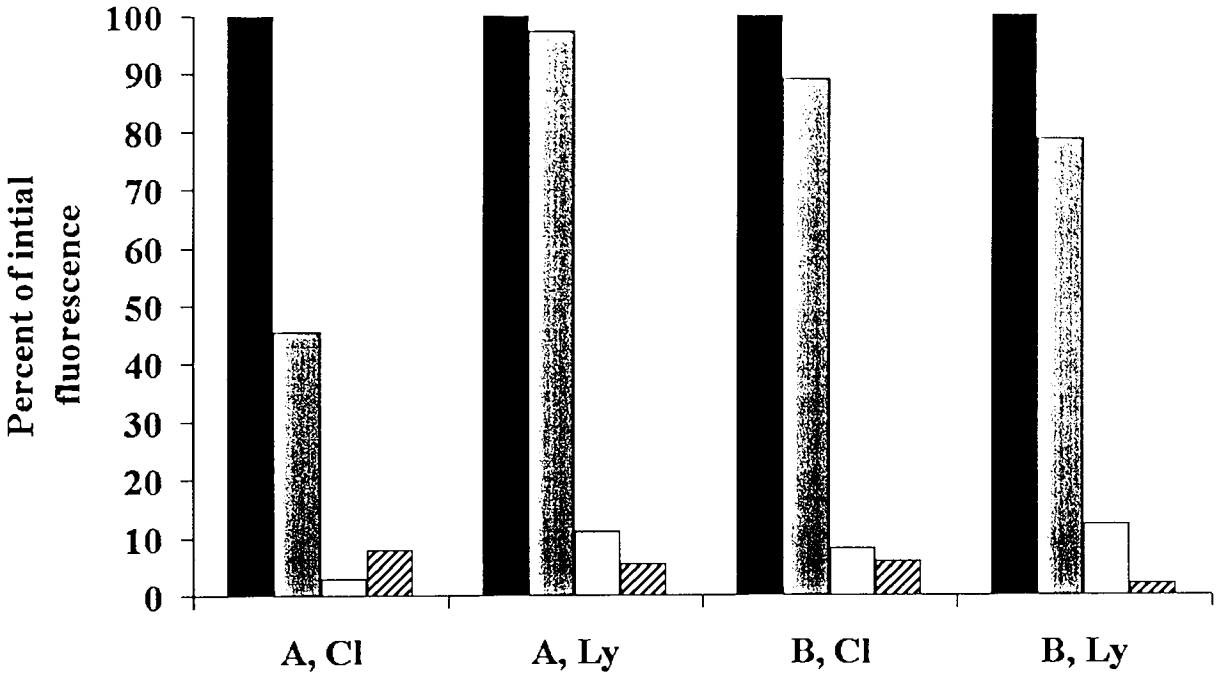

Figure 4-16: Composite graph of data presented in Figures 4-10, 4-11, 4-13, 4-14 and 4-16 to demonstrate the relative contributions of RNA and DNA to the total fluorescent signal in clarified culture broth (denoted **Cl** on the graph), diluted cell lysate (denoted **Ly** on the graph) containing antibodies A or B, labelled accordingly. Black bars represent percentage fluorescence prior to incubation, grey bars represent the percentage fluorescence after incubation with RNase and white bars represent the percentage fluorescence after incubation with RNase then DNase I. Hatched bars represent percentage remaining fluorescence after treatment with poly-L-lysine.

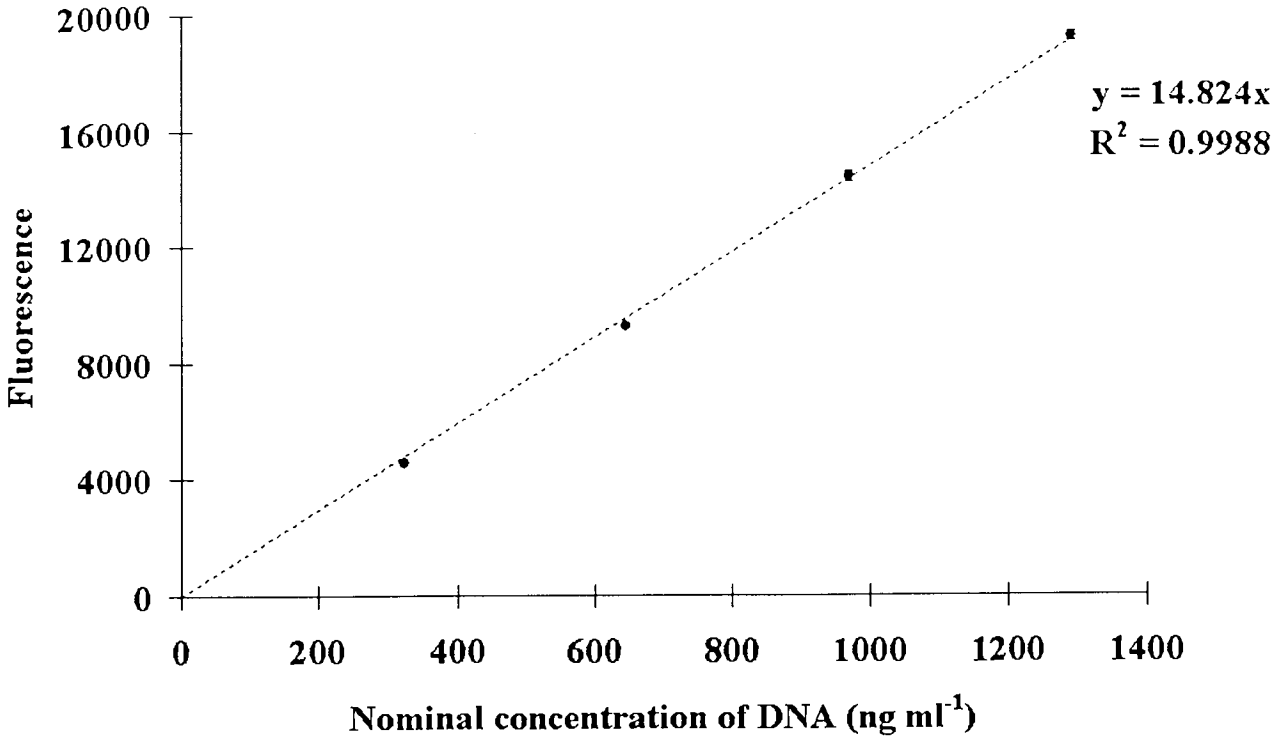

Figure 4-17: Typical calibration plot for determination of DNA in unknown samples. The concentration of DNA in a stock solution was established as 12.9 μg ml^{-1} by spectrophotometry. In this example subsequent dilutions of the stock solution were performed with TE, pH 7.5. In other expermients dilutions were performed with buffers that samples had been diluted or made up in. Fluorescence of each sample, including a blank, was determined in 3 wells of a 96 well plate. The average fluorescence in the three wells was plotted and error bars represent the standard deviation. Fresh calibration plots were performed for each 96 well plate. The concentration of DNA in unknown samples was determined by subtracting the average blank reading from the average fluorescence in three wells and dividing the resultant figure by the gradient, as determined by applying a regression analysis to the above plot.

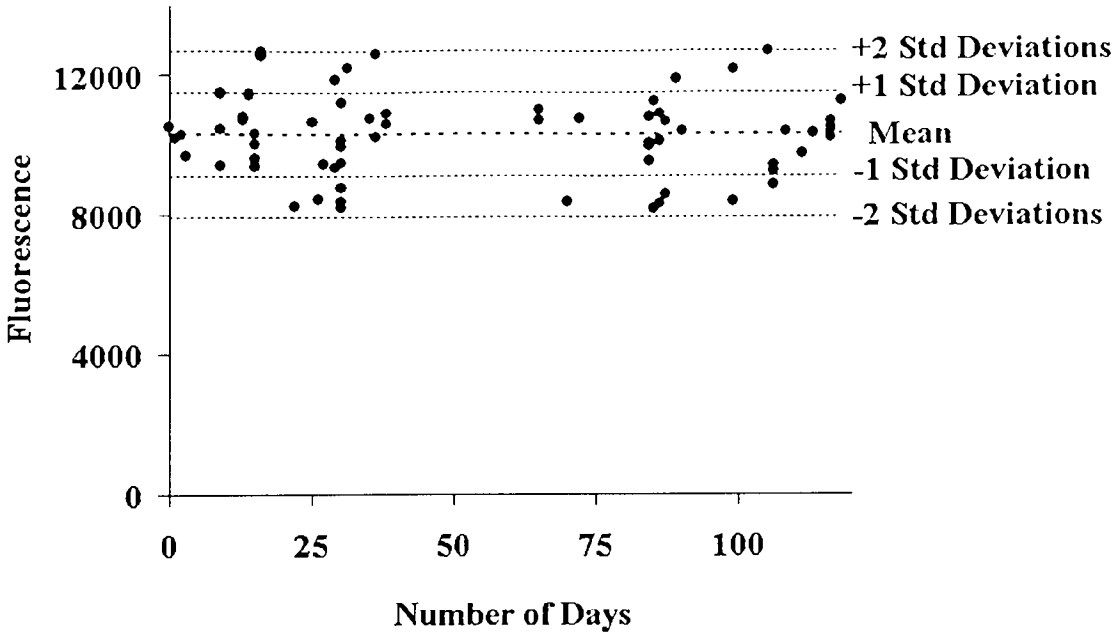

Figure 4-18: Fluorescence of a calf thymus DNA sample with nominal concentration of 1.003 μg ml^{-1} as determined for calibration plots used in 71 experiments over a period of 118 days. The stock solution employed was stored at –20 ^{0}C. The mean fluorescence of triplicate samples was determined and plotted as a function of the number of days since the stock solution was first prepared.

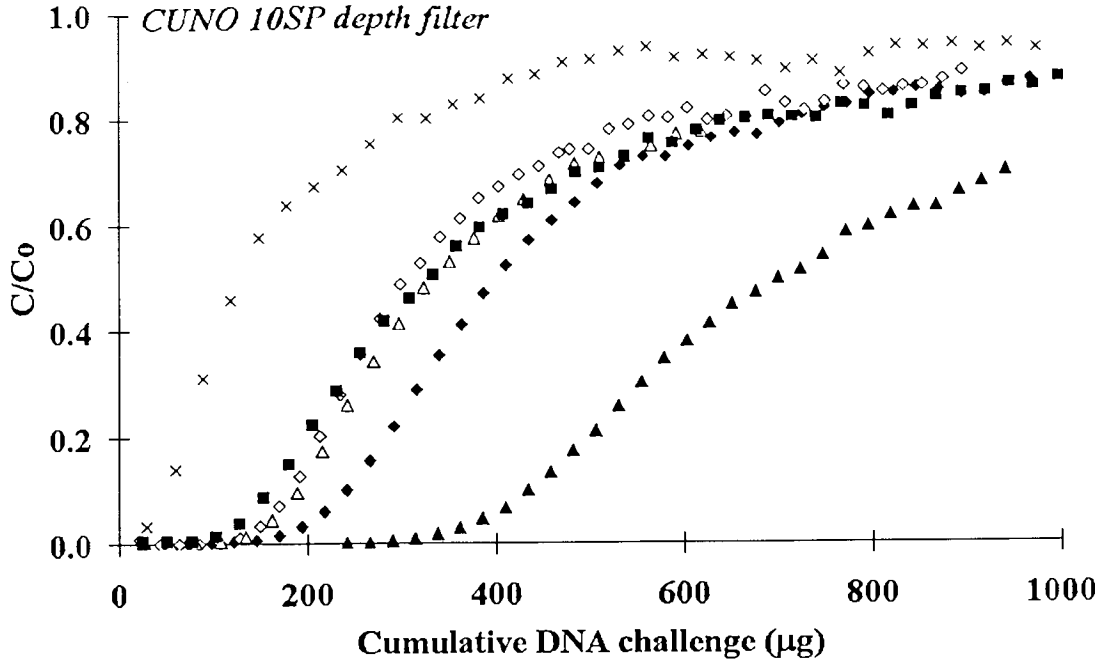

Figure 5-1: Breakthrough curves for Cuno Zeta Plus 10SP 47 mm diameter depth filter after challenge with calf thymus DNA. In all cases the initial flow rate was 20 ml min^{-1} and the concentration of challenge DNA was approximately 1000 ng ml^{-1}(see Table 5-1). Fractions were collected and assayed for DNA using the fluorescent dye PicoGreen. C=effluent concentration of DNA and Co=challenge concentration of DNA. Challenge solution compositions and symbols used (TE was employed as a buffer at pH 7.5): salt free TE (◆), salt free TE including 0.1% (v/v) polysorbate 80 (◇), 50 mM NaCl (▲), 50 mM NaCl including 0.1% (v/v) polysorbate 80 (△), 100 mM NaCl (■), 150 mM NaCl (×).

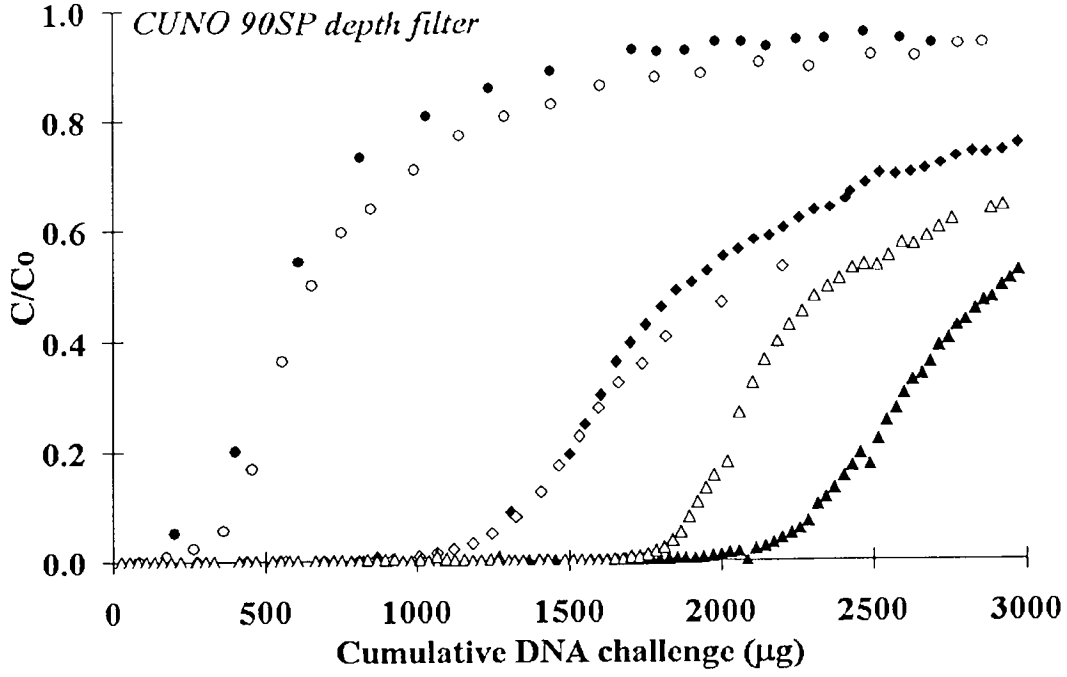

Figure 5-2: Breakthrough curves for Cuno Zeta Plus 90SP 47 mm diameter depth filter after challenge with calf thymus DNA. In all cases the initial flow rate was 20 ml min^{-1} and the concentration of challenge DNA was between 1133 and 1754 ng ml^{-1}(see Table 5-1). Fractions were collected and assayed for DNA using the fluorescent dye PicoGreen. C=effluent concentration of DNA and Co=challenge concentration of DNA. Challenge solution compositions and symbols used (TE was employed as a buffer at pH 7.5 unless otherwise stated): salt free TE (◆), salt free TE including 0.1% (v/v) polysorbate 80 (◇), 50 mM NaCl (▲), 50 mM NaCl including 0.1% (v/v) polysorbate 80 (△), salt free TE at pH 8.8(●), and salt free TE at pH 8.8 including 0.1% (v/v) polysorbate 80 (○).

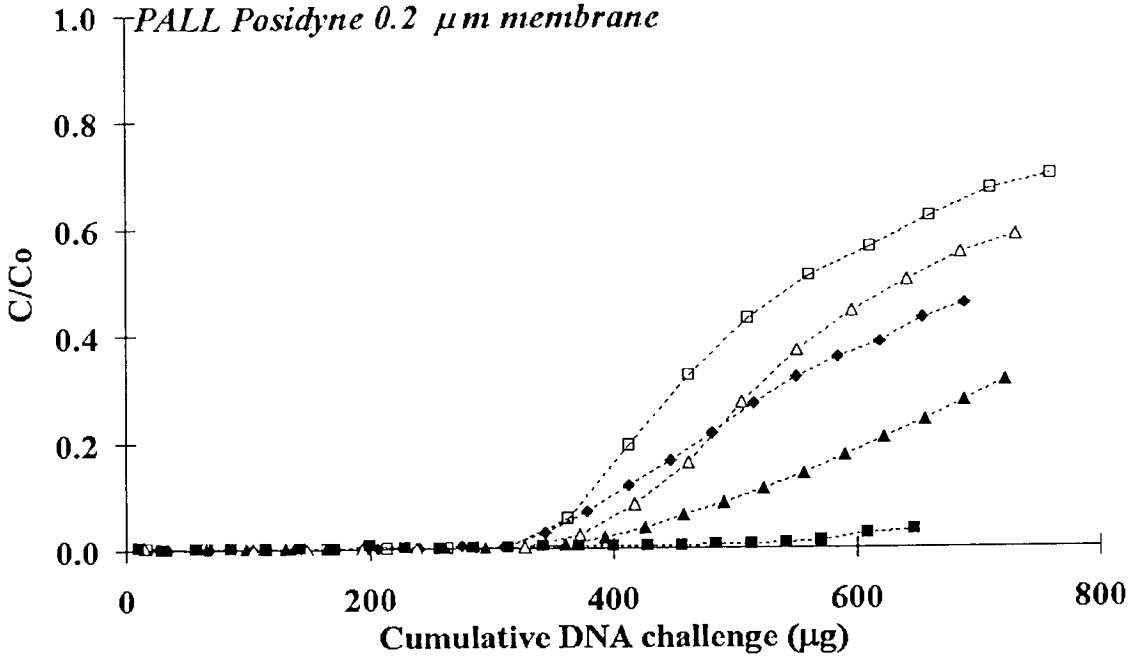

Figure 5-3: Breakthrough curves for Pall Posidyne 47 mm diameter sterilising grade microporous membrane after challenge with calf thymus DNA. In all cases the initial flow rate was 20 ml min^{-1} and the concentration of challenge DNA was between 716 and 1474 ng ml^{-1}(see Table 5-1). Fractions were collected and assayed for DNA using the fluorescent dye PicoGreen. C=effluent concentration of DNA and Co=challenge concentration of DNA. Challenge solution compositions and symbols used (TE was employed as a buffer at pH 7.5): salt free TE (◆), 50 mM NaCl (▲), 50 mM NaCl including 0.1% (v/v) polysorbate 80 (△), 100 mM NaCl (■), 100mM NaCl including 0.1% (v/v) polysorbate 80 (□).

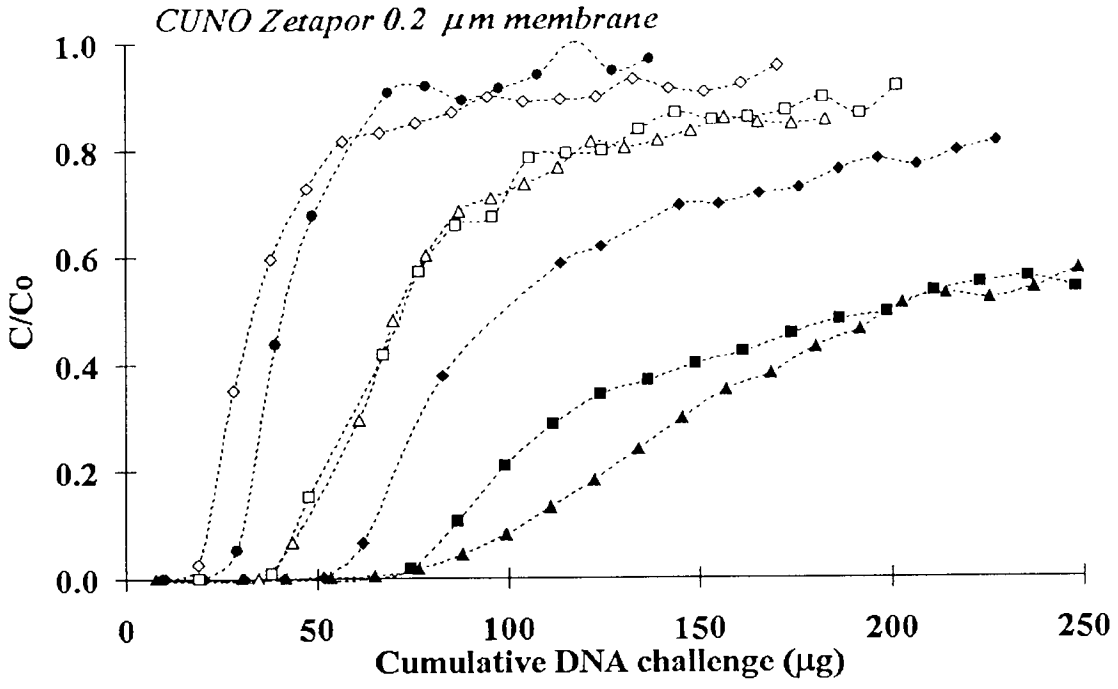

Figure 5-4: Breakthrough curves for Cuno Zetapor 47 mm diameter sterilising grade microporous membranes after challenge with calf thymus DNA. In all cases the initial flow rate was 20 ml min^{-1} and the concentration of challenge DNA was between 868 and 1032 ng ml^{-1}(see Table 5-1). Fractions were collected and assayed for DNA using the fluorescent dye PicoGreen. C=effluent concentration of DNA and Co=challenge concentration of DNA. Challenge solution compositions and symbols used (TE was employed as a buffer at pH 7.5 unless otherwise stated): salt free TE (◆), salt free TE including 0.1% (v/v) polysorbate 80 (◇), 50 mM NaCl (▲), 50 mM NaCl including 0.1% (v/v) polysorbate 80 (△), 100 mM NaCl (■), 100mM NaCl including 0.1% (v/v) polysorbate 80 (□), and salt free TE at pH 8.8(●).

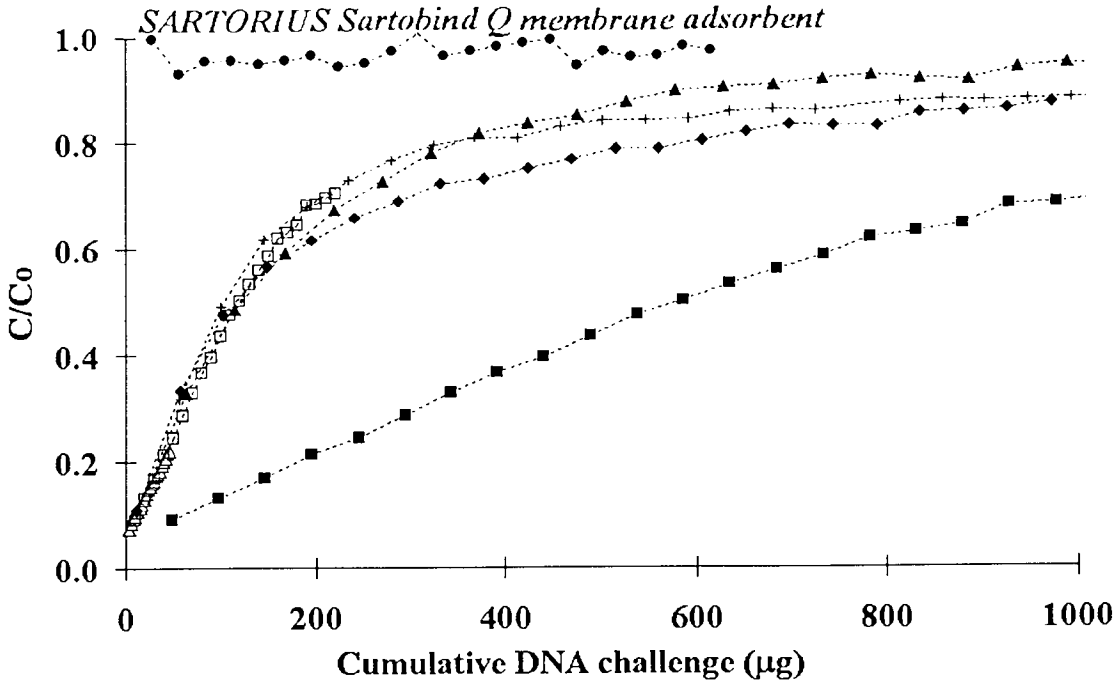

Figure 5-5: Breakthrough curves for Sartobind Q membrane adsorbent challenged with calf thymus DNA. Fractions were collected and assayed for DNA using PicoGreen. Experimental conditions and symbols used: TE was employed as a buffer at pH 7.5, the superficial velocity of challenge material was 23.6 cm s^{-1}, the membrane diameter was 25 mm and the concentration of challenge DNA was approximately 1000 ng ml^{-1} (▲) or as stated below, and in Table 5-1: 47 mm membrane (■); data generated by 47 mm but scaled per unit area for 25 mm membrane (□); 100 mM NaCl in TE pH 7.5 (◆); superficial velocity of 191.3 cm s^{-1}(+); DNA concentration of 184 ng ml^{-1}(△); molar NaCl in TE, pH 7.5(●).

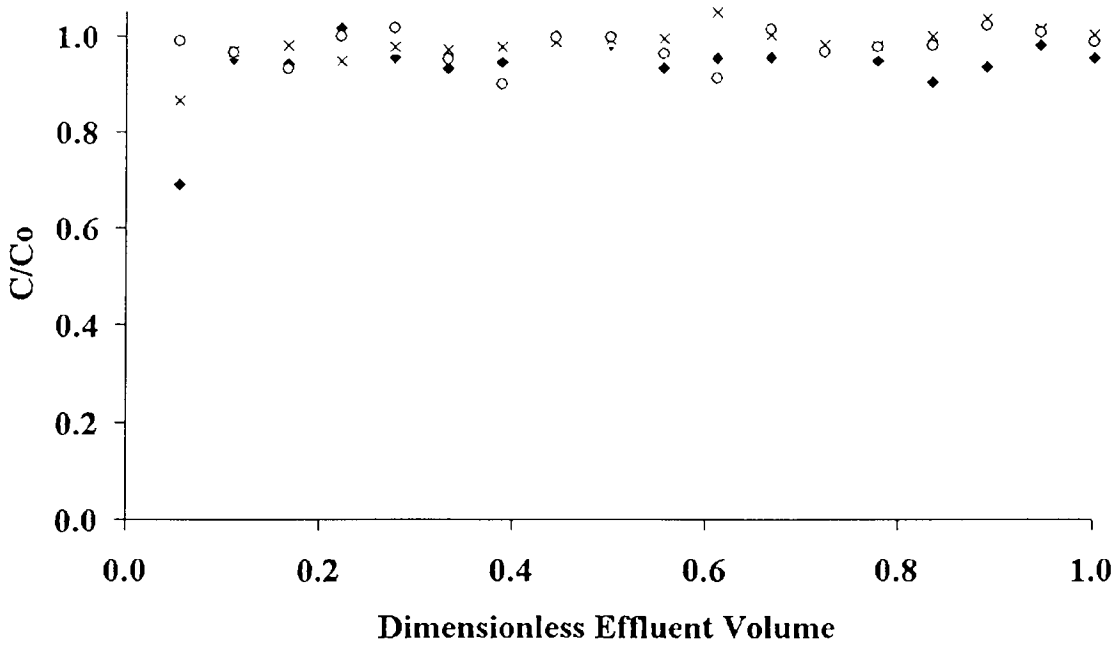

Figure 5-6: Challenge of CUNO 90mm 10SP(×), 47 mm 90SP (◆) and 25mm PALL Posidyne sterilising grade membrane (○) with process material supernatant containing mAb B in a scaled down model as detailed in the Methods section. Material taken from the production vessel at the end of a nine day fed batch fermentation was clarified prior to challenge of the 10SP depth filter by centrifugation (5 minutes 7200g) and 0.2μm filtration (Sartofluor, Sartorius) to remove residual debris that may compete with DNA for binding sites. The concentration of DNA in the debris free material was 16.0 μg ml^{-1}. After challenge of the 90 mm 10SP depth filter with this material 5 ml of each fraction were removed and subsequently digested with RNase prior to assay for DNA with PicoGreen. The remaining effluent was pooled for subsequent challenge of the 47 mm 90SP depth filter and the same exercise was repeated with this material to prepare for challenge of the 25 mm Posidyne membrane.

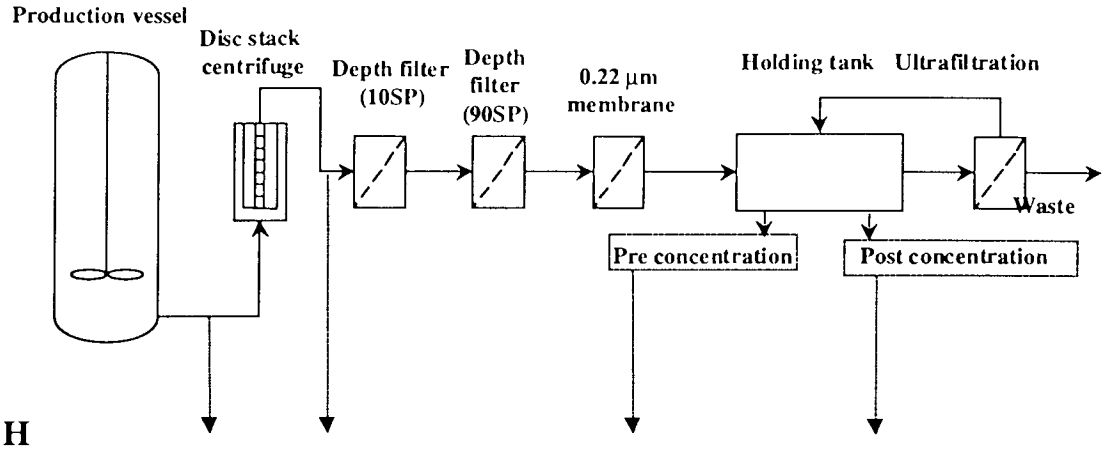

BATCH				
mAb A:1	5.2	6.3	6.0	27.3
mAb B:1	15.5	14.6	14.6	n/a
mAb B:2	17.0	15.0	17.5	n/a
mAb B:3	16.3	16.2	15.4	n/a
mAb B:4	24.9	n/a	20.0	87.8

Figure 5-7: Concentration of DNA (µg ml^{-1}) in process supernatant passing through the initial stages of monoclonal antibody purification as determined by PicoGreen after incubation with RNase A. Material was sampled at the points denoted by the dashed lines. n/a: material was unavailable for sampling.

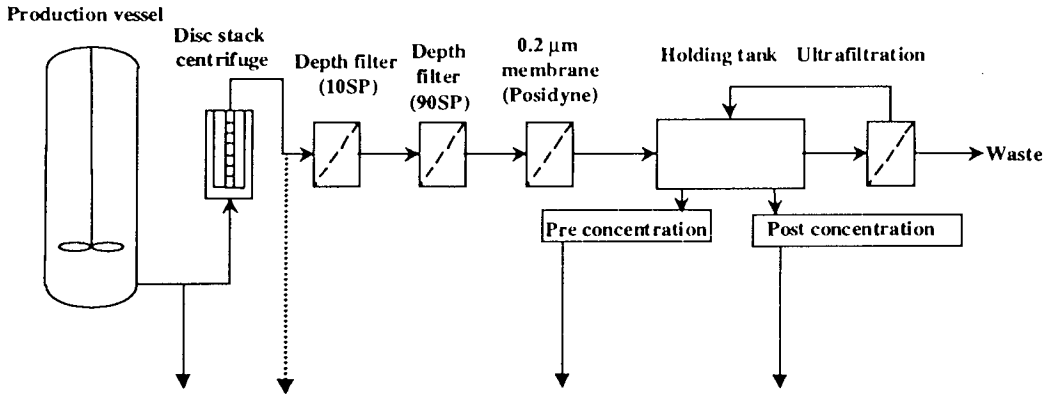

BATCH				
mAb A:1	79.8	9.3	-	-
mAb B:4	107.7	29.7	-	-

Figure 5-8: Total DNA determined (µg ml^{-1}) in process material containing whole cells and debris passing from the production vessel to filtration train. Material was sampled at the points denoted by the dashed lines.

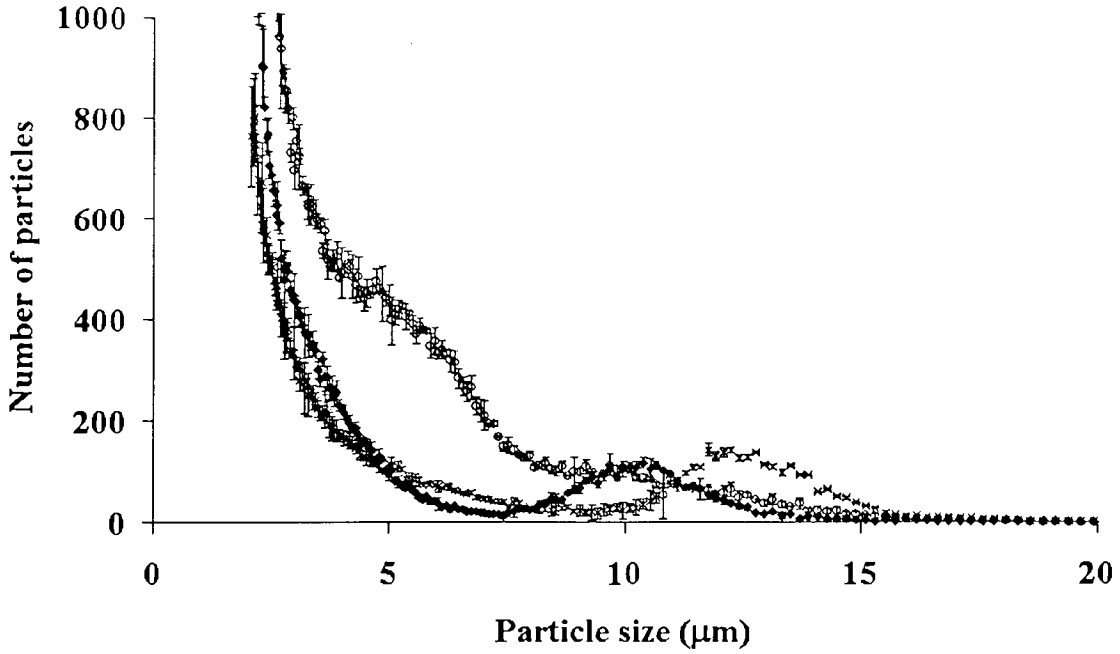

Figure 6-1: Particles counts of viable (x), non-viable apoptotic (○) and non-viable necrotic (◆) cells grown in shake flasks. Samples were diluted 1:200 with PBS and 500 μl of this solution was analysed in triplicate using a Coulter Channelyzer 256. The average of the three replicates was plotted and error bars represent the standard deviation. This plot constitutes the same data shown in figures 6-2, 6-3and 6-4, and has been collated here for comparative purposes.

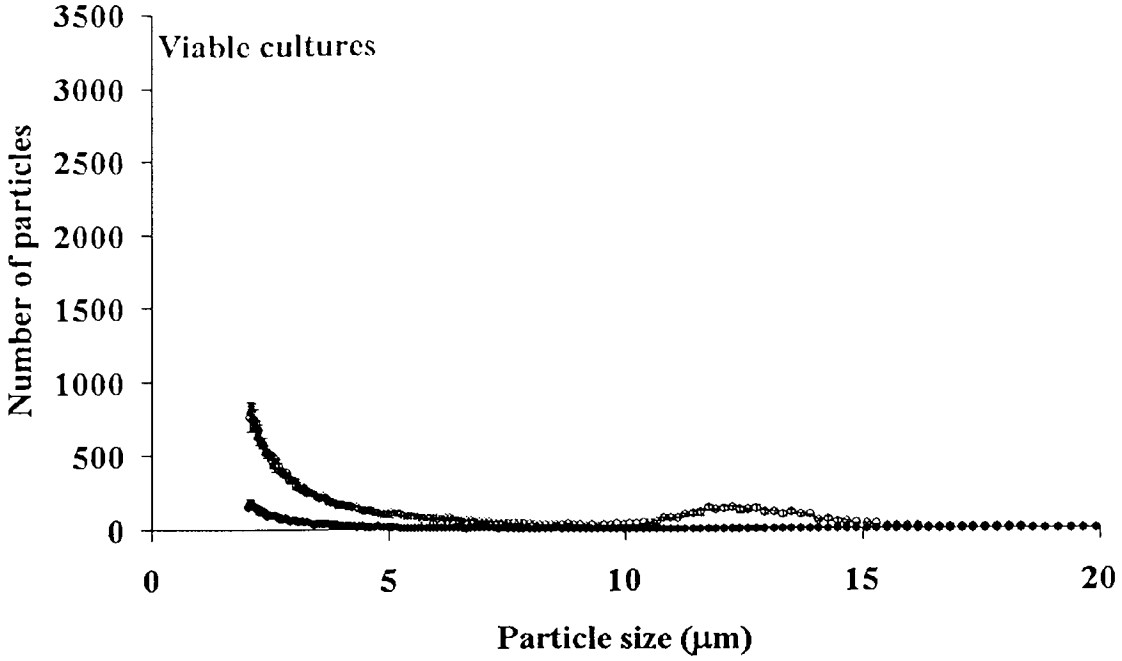

Figure 6-2: Particles counts of viable cells grown for 5 days in shake flasks prior to (○) and following (●) challenge of Cuno Zeta Plus 10SP depth filters. Samples were diluted 1:200 with PBS and 500 µl of this solution was analysed in triplicate using a Coulter Channelyzer 256. The average of the three replicates was plotted and error bars represent the standard deviation.

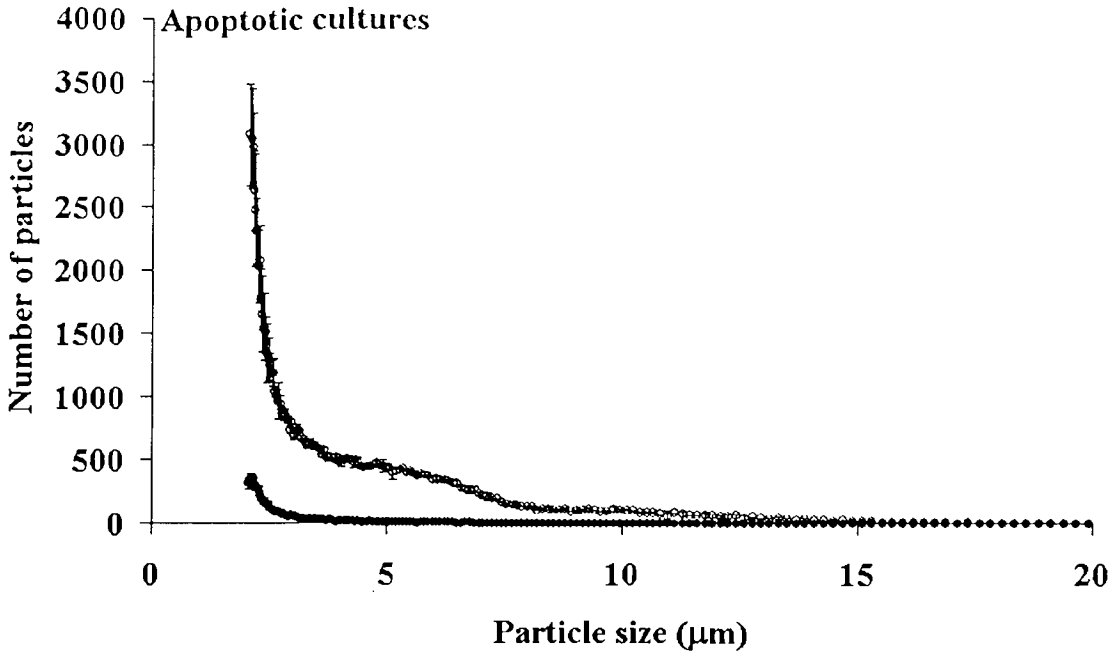

Figure 6-3: Particles counts of non-viable apoptotic cells prior to (○) and following (●) challenge of Cuno Zeta Plus 10SP depth filters. Cells were grown for 5 days in shake flasks before the addition of 70 µm etoposide phosphate to induce apoptotic cell death when the culture was left for a further 48 hours to allow complete cell death to occur. Samples were diluted 1:200 with PBS and 500 µl of this solution was analysed in triplicate using a Coulter Channelyzer 256. The average of the three replicates was plotted and error bars represent the standard deviation.

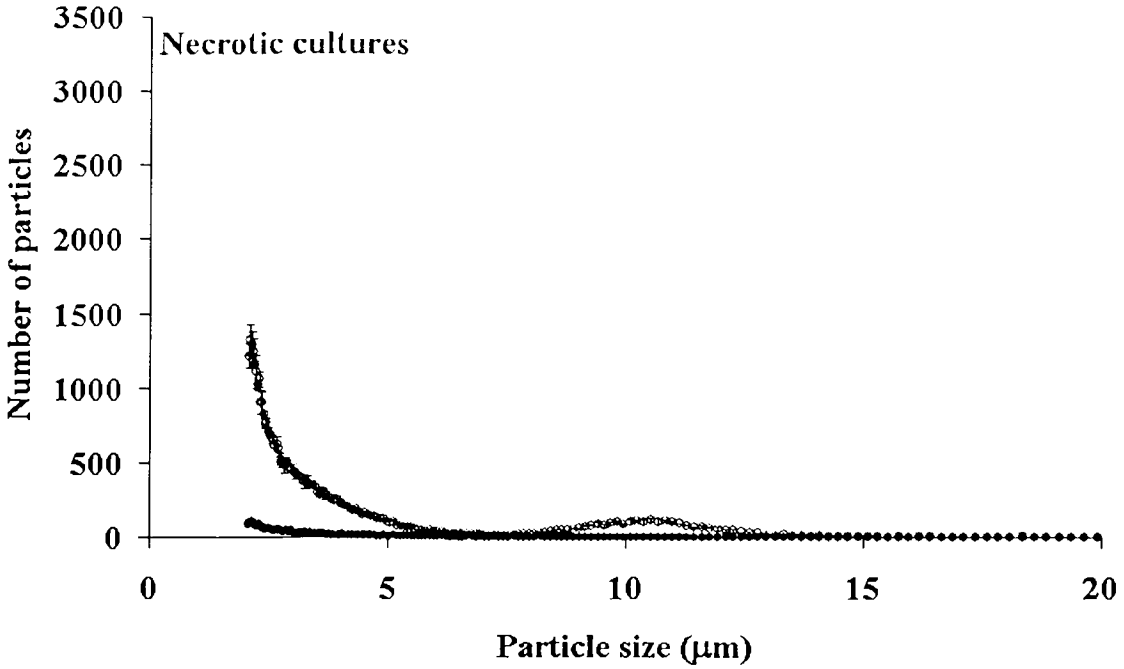

Figure 6-4: Particles counts of non-viable necrotic cells prior to (○) and following (●) challenge of Cuno Zeta Plus 10SP depth filters. Cells were grown for 5 days in shake flasks before the addition of 1.0 % (w/v) sodium azide to induce necrotic cell death when the culture was left for a further 48 hours to allow complete cell death to occur. Samples were diluted 1:200 with PBS and 500 µl of this solution was analysed in triplicate using a Coulter Channelyzer 256. The average of the three replicates was plotted and error bars represent the standard deviation.

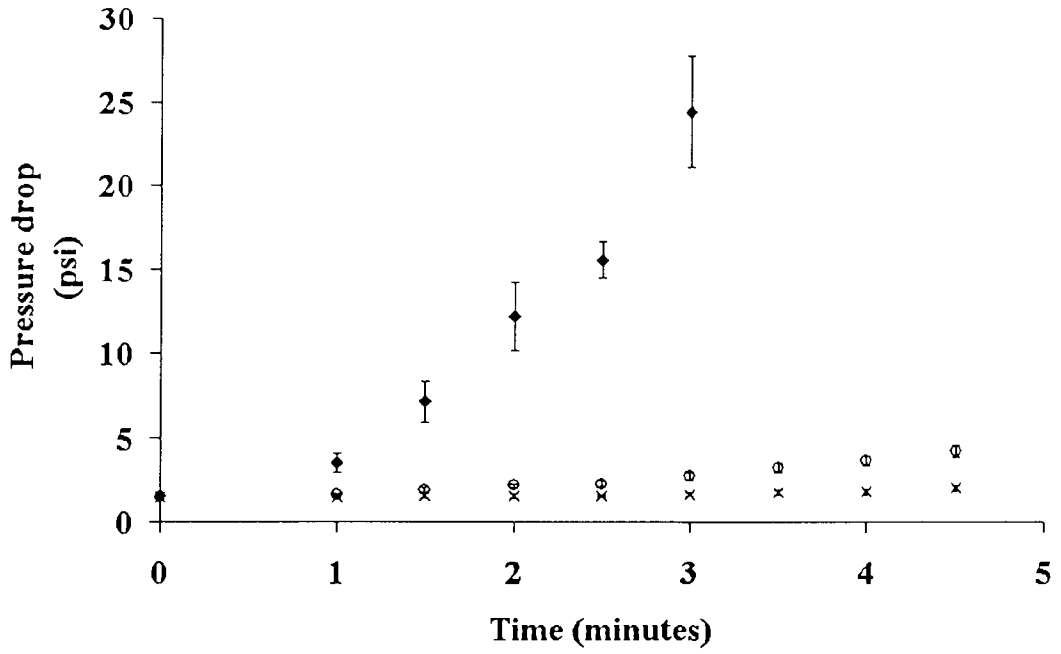

Figure 6-5: Pressure drop generated across Cuno Zeta Plus 10SP 47 mm depth filter as a function of filtration time following challenge of the depth filter with cell culture suspension from viable (x), non-viable apoptotic(o) and non-viable necrotic (◆). Experiments were conducted at a constant flow rate of 24 ml min^{-1}. Filtration experiments were conducted in triplicate and the mean pressure drop for each time point was plotted. Error bars represent the standard deviation.

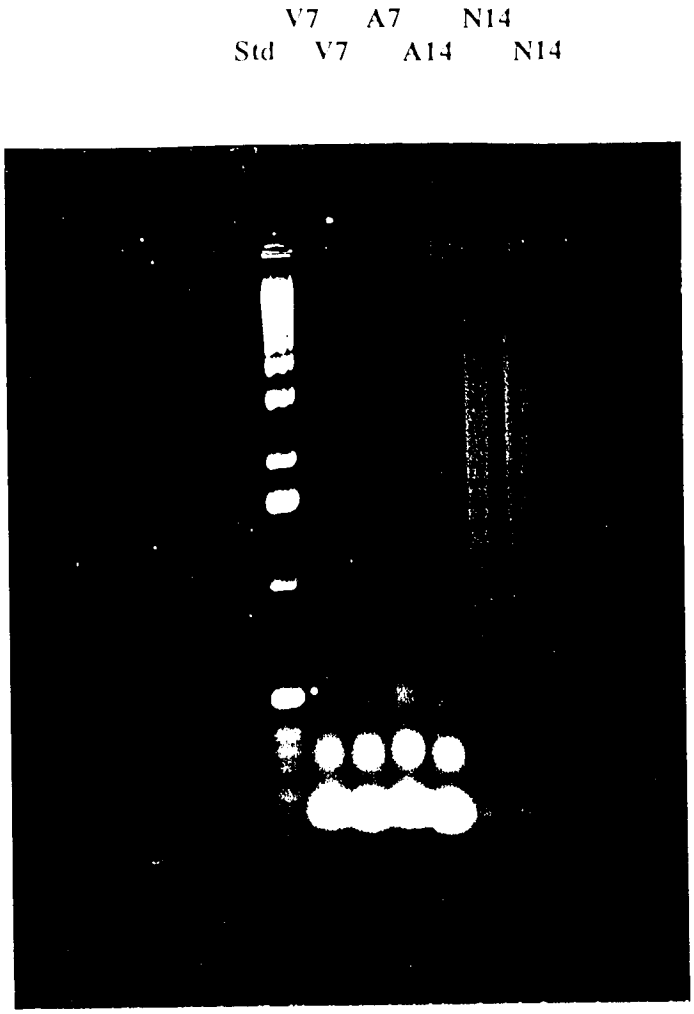

Figure 6-6: Samples were taken from viable (V), apoptotic (A) and necrotic (N) shake flask cultures on days 7 and 14 of culture. Following treatment with Ribonuclease A and Proteinase K, DNA was extracted and 1.0 μg were run on a 1.5% agarose gel and stained with ethidium bromide. The far left hand lane contains a 1 Kb ladder of DNA molecules (Std), 12,216 bp being the largest strand. DNA molecules of strand length 4072 to 506 base pairs were clearly resolved. Lanes have been labelled accordingly.

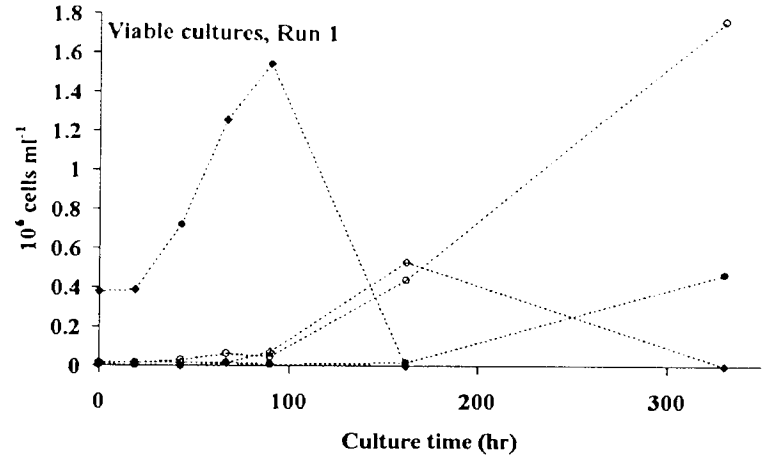

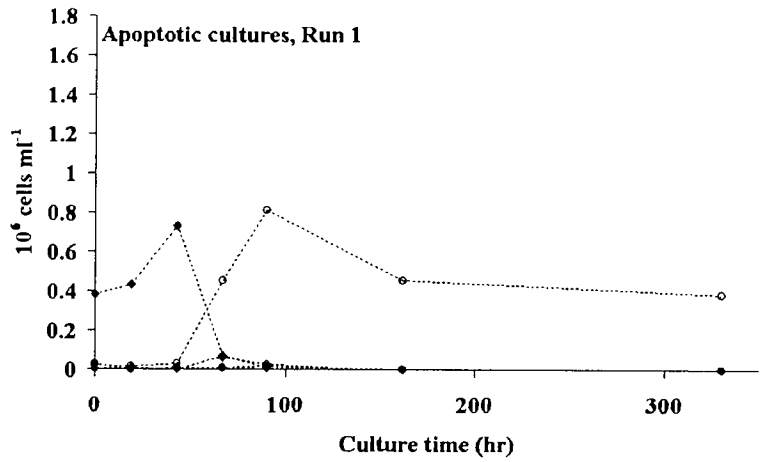

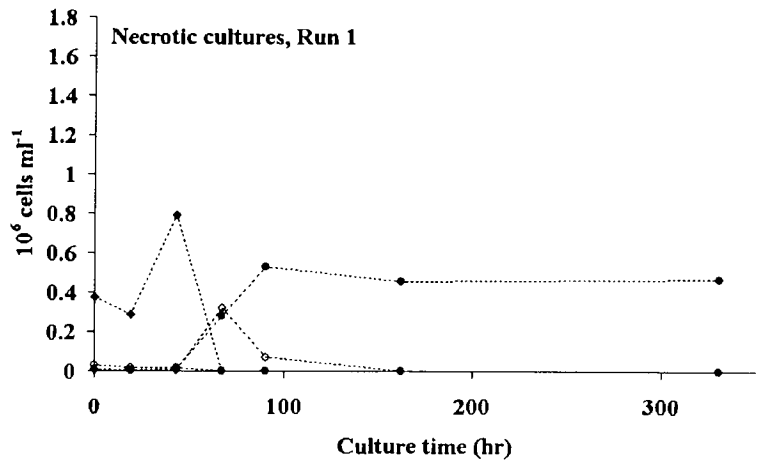

Figure 6-7: Cell counts from shake flask culture of NS0 cells secreting monoclonal antibody A after staining with acridine orange and ethidium bromide as described in the Methods section: healthy viable (◆), non-viable necrotic (●), viable apoptotic (◇), non-viable apoptotic (○). Cells were scored in four squares of a haemacytometer and the average score plotted for each cell type. Cell death was induced 44 hrs after sub-culturing.

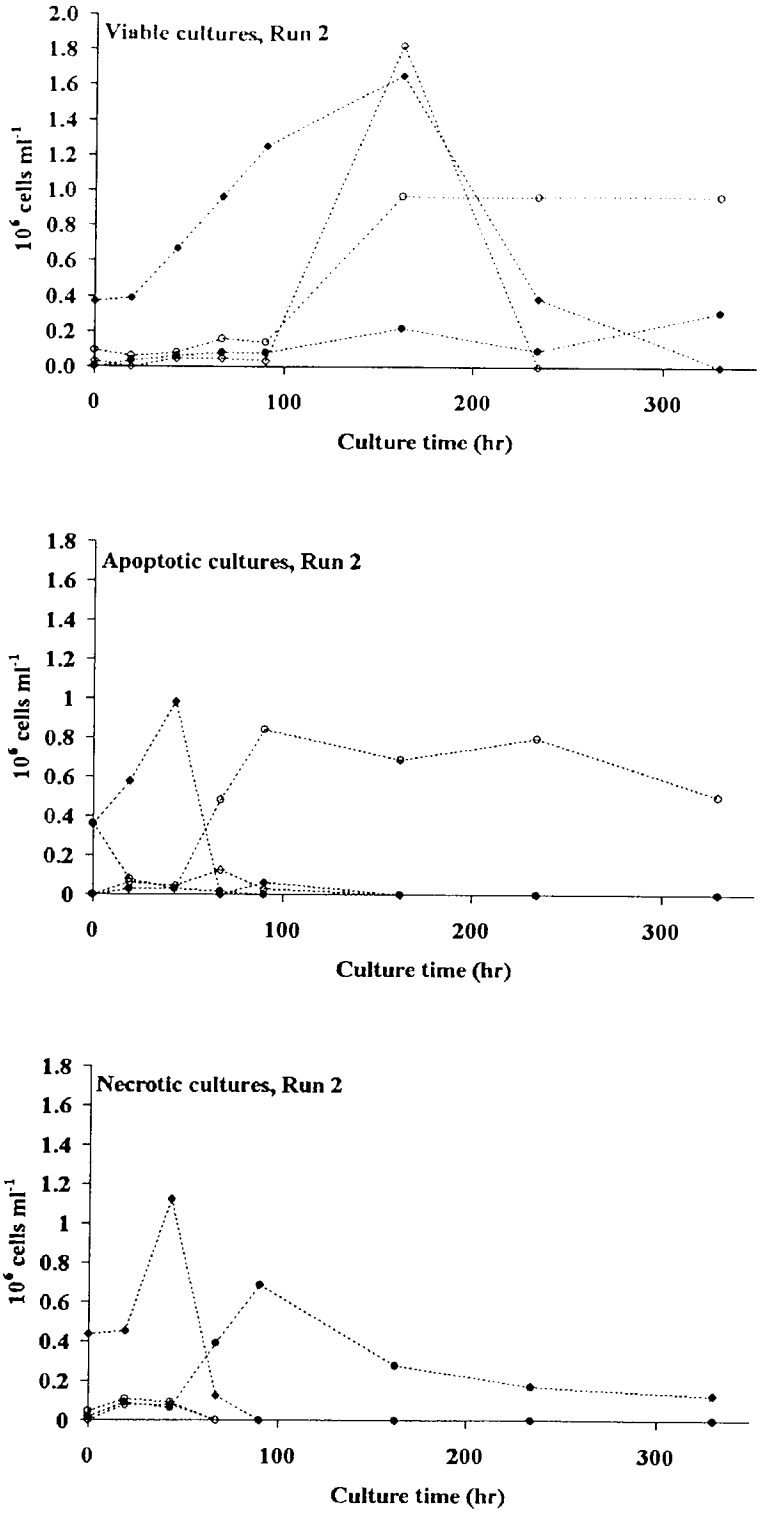

Figure 6-8: Cell counts from shake flask culture of NS0 cells secreting monoclonal antibody A after staining with acridine orange and ethidium bromide as described in the Methods section: healthy viable (◆), non-viable necrotic (●), viable apoptotic (◇), non-viable apoptotic (○). Cells were scored in four squares of a haemacytometer and the average score plotted for each cell type. Cell death was induced 44 hrs after sub-culturing.

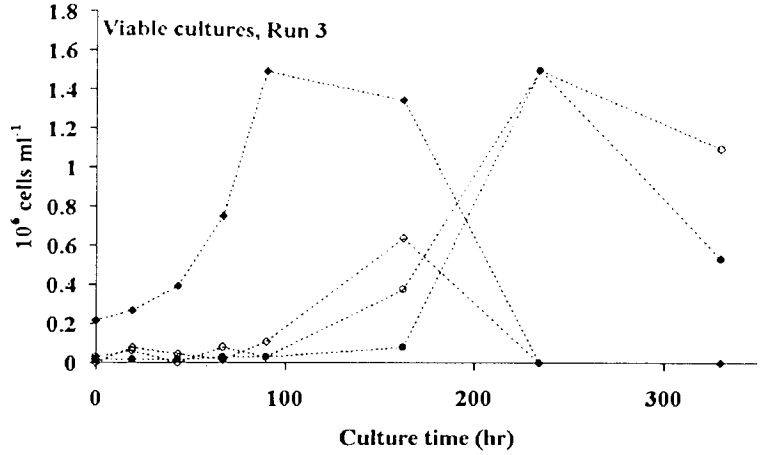

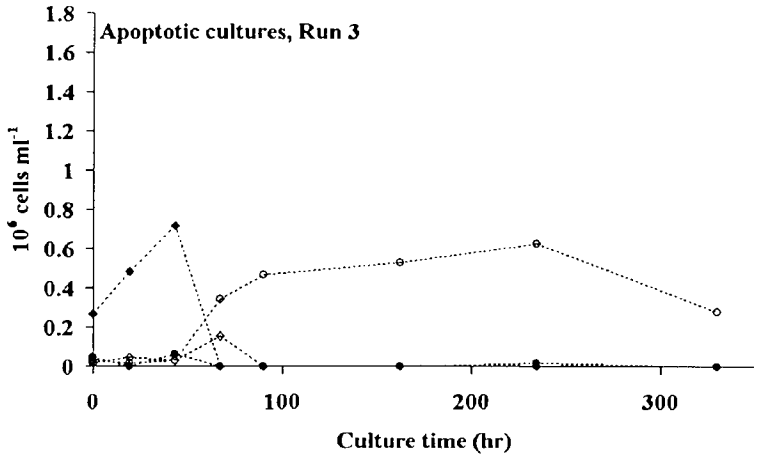

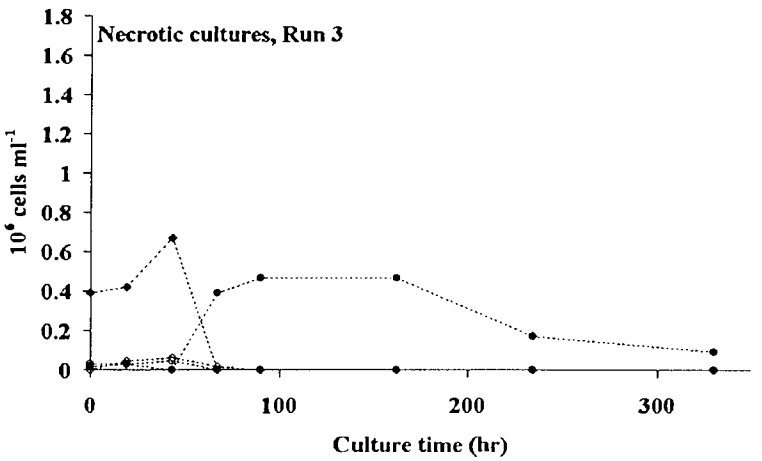

Figure 6-9: Cell counts from shake flask culture of NS0 cells secreting monoclonal antibody A after staining with acridine orange and ethidium bromide as described in the Methods section: healthy viable (◆), non-viable necrotic (●), viable apoptotic (◇), non-viable apoptotic (○). Cells were scored in four squares of a haemacytometer and the average score plotted for each cell type. Cell death was induced 44 hrs after sub-culturing.

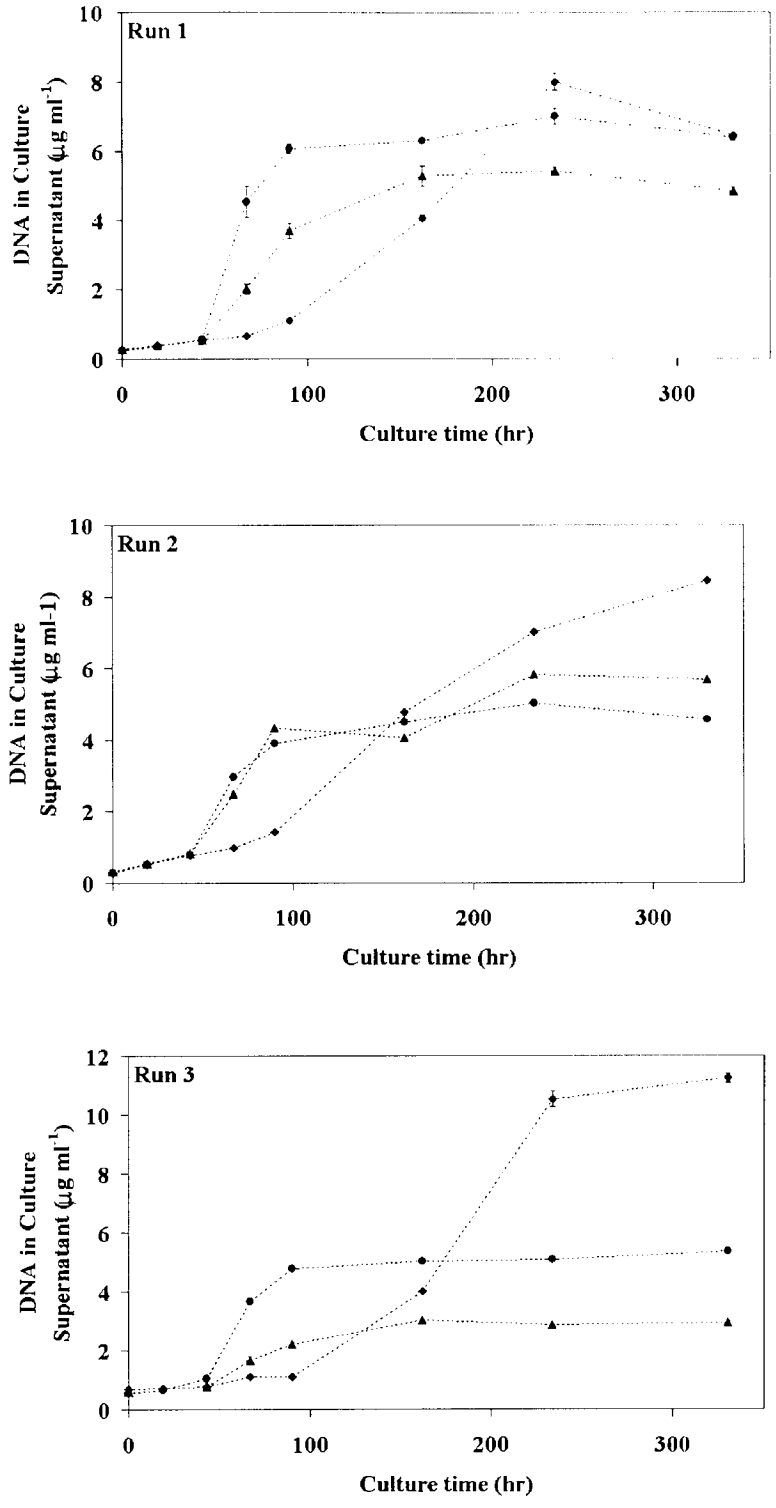

Figure 6-10: Concentration of DNA in supernatants of control (◆), apoptotic (●) and necrotic (▲)cultures over a 14 day culture period as determined by PicoGreen for 3 experimental runs.

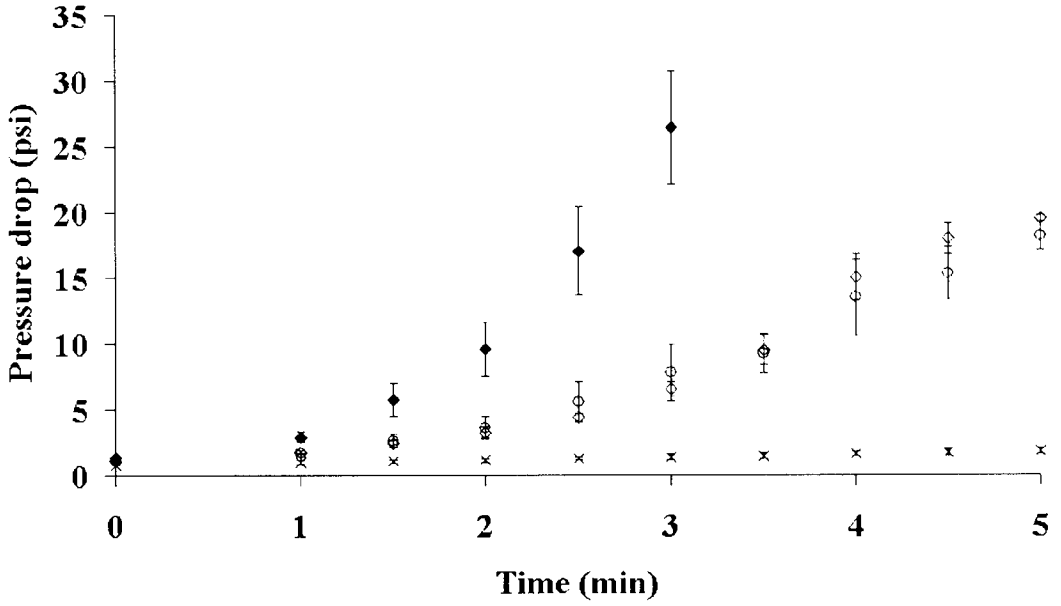

Figure 6-11: Pressure drop generated across Cuno Zeta Plus 10SP 47 mm depth filter as a function of filtration time following challenge of the depth filter with cell suspension from viable cultures (x), non-viable necrotic cultures (◆) non-viable necrotic cultures treated with 20 units ml^{-1} DNase I (○) or non-viable necrotic cultures treated 20 units ml^{-1} benzonase. Where nucleases were employed, the cultures were held at 37 °C for one hour after incorporation of enzyme and 1M MgCl to a final concentration of 10 mM. Experiments were conducted at a constant flow rate of 24 ml min^{-1}. Filtration experiments were conducted in triplicate and the mean pressure drop for each time point was plotted. Error bars represent the standard deviation.